



**Technical University of Crete
School of Environmental Engineering**

**M.Sc. in “Environmental Engineering”
In the “Environmental Management, Sustainable Energy and
Climate Change”**

Dissertation

**Impact assessment of natural ventilation on thermal comfort levels in
sustainable residential buildings**

Αξιολόγηση των επιπτώσεων του φυσικού αερισμού στα επίπεδα θερμικής άνεσης
σε βιώσιμα κτίρια κατοικιών

Tsirintoulaki Elli

3 members Committee:

Prof. Dionysia Kolokotsa (supervisor)

Prof. Theocharis Tsoutsos

Prof. Nikolaos Papamanolis

June 2017

Acknowledgements

I would like to gratefully and sincerely thank my supervisor, Professor Dionysia Kolokotsa for her guidance, collaboration and all the opportunities she gave me.

Furthermore, I would like thank Mr Konstantinos Gompakis (PhD student) and Mr Nikolaos Kampelis (PhD student) for their valuable help, tolerance and patience.

Finally I would like to express my appreciation to my family and friends for their continuous support throughout the years.

Abstract

In the present thesis the impact of natural cross-ventilation on thermal comfort levels in sustainable residential buildings is evaluated. A sustainable dwelling is designed in Crete and is simulated in OpenStudio to assess its energy consumption. For the study of the indoor airflow pattern and the thermal comfort levels the Blender (with CFD plug-in) and the Autodesk CFD are chosen. Various scenarios of different combinations of open windows and doors in the ground floor, the first floor and between the floors are tested in Blender to determine the final scenarios with the best possible airflow movement. Three scenarios with open windows and doors in the ground floor and six (6) between the floors (9 total scenarios) are chosen to be the final scenarios where the impact assessment of natural ventilation on thermal comfort levels is performed. For the study of thermal comfort levels, using the Predicted Mean Vote (PMV) index, the Autodesk CFD software is used for the Computational Fluid Dynamics (CFD) simulations with the 3D steady Reynolds-averaged Navier-Stokes (RANS) approach and the Shear Stress Transport (SST) $k-\omega$ turbulence model. The Scenarios are tested for a typical summer day for four different hours and environmental conditions. The designed building is treated as a stand alone in all the simulations and it is not an existing construction. From the analysis of the results we observe that natural ventilation is an effective way to achieve indoor thermal comfort. In many Scenarios the high values of PMV from the Base Scenario (no windows or doors open) are decreased and in a few cases the values fall into the cold zone of comfort. The layout of the floors also affects the airflow movement in addition with the openings and the environmental conditions and can be used accordingly. According to the author's knowledge in the field of investigating natural ventilation via numerical approach simulation the present study is an original attempt to examine a more elaborate building architectural design and is also concluded that the followed methodology can be applied.

Περίληψη

Στόχος της παρούσας μεταπτυχιακής διπλωματικής εργασίας είναι η αξιολόγηση των επιπτώσεων του φυσικού διαμπερούς αερισμού στα επίπεδα θερμικής άνεσης σε βιώσιμα κτίρια κατοικιών. Μία βιώσιμη κατοικία σχεδιάζεται στην Κρήτη και προσομοιώνεται στο OpenStudio για τον εκτίμηση της ενεργειακής της κατανάλωσης. Η μελέτη της εσωτερικής ροής του αέρα και των επιπέδων της θερμικής άνεσης εξετάζεται με το Blender (με CFD plug-in) και το Autodesk CFD. Διάφορα σενάρια εναλλακτικών συνδυασμών ανοιχτών παραθύρων και θυρών στο ισόγειο, στον όροφο και μεταξύ των ορόφων ελέγχονται στο Blender για να καθοριστούν τα τελικά σενάρια με την καλύτερη δυνατή εσωτερική ροή του αέρα. Τρία σενάρια με ανοιχτά παράθυρα και πόρτες στο ισόγειο και έξι (6) ανάμεσα στους ορόφους (9 σενάρια συνολικά) επιλέγονται ως τελικά σενάρια βάσει των οποίων αξιολογούνται οι επιπτώσεις του φυσικού αερισμού στα επίπεδα θερμικής άνεσης. Για τη μελέτη των επιπέδων της θερμικής άνεσης, με το δείκτη PMV (Predicted Mean Vote), το Autodesk CFD χρησιμοποιείται για την Computational Fluid Dynamics (CFD) ανάλυση με τεχνικές 3D steady Reynolds-averaged Navier-Stokes (RANS) και μοντέλο στροβιλισμού Shear Stress Transport (SST) k- ω . Τα Σενάρια ελέγχονται για μία τυπική μέρα καλοκαιριού για τέσσερις διαφορετικές ώρες και τις αντίστοιχες περιβαλλοντικές συνθήκες. Το σχεδιασμένο κτίριο αντιμετωπίζεται ως απομονωμένο σε όλες τις προσομοιώσεις (δεν είναι υφιστάμενη κατασκευή). Από την ανάλυση των αποτελεσμάτων παρατηρούμε ότι σε πολλές περιπτώσεις και υπό την προϋπόθεση ενός αποτελεσματικού αρχιτεκτονικού σχεδιασμού, ο φυσικός αερισμός είναι ένας αποτελεσματικός τρόπος για την επίτευξη της εσωτερικής θερμικής άνεσης. Στην πλειοψηφία των Σεναρίων που αξιολογήθηκαν σε σχέση με τις υψηλές τιμές του PMV που διαπιστώθηκαν κατά το Βασικό Σενάριο (δεν υπάρχουν ανοιχτά παράθυρα και πόρτες) παρατηρείται ικανοποιητική μείωση στα επίπεδα άνεσης. Παράλληλα συμπεραίνεται ότι η διαρρύθμιση των ορόφων και των ανοιγμάτων επηρεάζει καθοριστικά τη ροή του αέρα στο εσωτερικό της κατοικίας σε συνδυασμό με τις περιβαλλοντικές συνθήκες. Σύμφωνα με τις γνώσεις της συγγραφέα στον τομέα της διερεύνησης του φυσικού αερισμού μέσω προσομοιώσεων, η παρούσα μελέτη αποτελεί μία αρχική προσπάθεια εξέτασης ενός πιο περίπλοκου αρχιτεκτονικού σχεδιασμού κτιρίου και η μεθοδολογία που ακολουθήθηκε είναι εφαρμόσιμη.

Table of Contents

1. Introduction.....	9
1.1. Methodology	9
1.2. Issue layout.....	10
2. Literature review	11
3. Architectural Process.....	16
3.1. Bioclimatic parameters.....	16
3.2. Location	17
3.3. Architectural design.....	18
3.4. Building Constructions.....	25
3.5. Energy Consumption	28
3.6. Lighting study	30
4. Natural ventilation modelling.....	34
4.1. Weather Information.....	34
4.2. Software tools	36
4.3. CFD simulation: computational settings and parameters.....	37
4.4. Presentation of the examined Scenarios.....	41
5. Results Analysis and Discussion.....	44
5.1. Base Scenario: no windows/doors open	44
5.2. Scenario 1: openings in the living room and dining room.....	47
5.3. Scenario 2: openings in the living room and kitchen	52
5.4. Scenario 3: openings in the kitchen and living room	57
5.5. Scenario 4: openings in the living room and bedroom	62
5.6. Scenario 5: openings in the kitchen and bedroom.....	67
5.7. Scenario 6: openings in the living room, kitchen and bedroom.....	72
5.8. Scenario 7: openings in the office and living room	77
5.9. Scenario 8: openings in the living room and office	82
5.10. Scenario 9: openings in the office, living room and kitchen	87
5.11. Comparison between all Scenarios	92
6. Conclusions and Future work	96
6.1. Conclusions.....	96
6.2. Future work	97
7. References	98

List of Figures

Figure 2.1 The relation between PMV and PPD [32].....	14
Figure 2.2 The expanded zone of PMV [33]	14
Figure 3.1 Map of the area [39].....	17
Figure 3.2 Ground floor plan	19
Figure 3.3 1st floor plan.....	20
Figure 3.4 Views of the building	21
Figure 3.5 Views of the building	22
Figure 3.6 Position of the building in the area	23
Figure 3.7 Position of the building in the area	24
Figure 3.8 Roof construction	25
Figure 3.9 Construction of floor/Ceiling with tile/wood	25
Figure 3.10 Construction of floor with outside boundary.....	25
Figure 3.11 Construction of ground floor with tile/wood.....	26
Figure 3.12 Construction of exterior wall.....	26
Figure 3.13 Construction of interior wall	26
Figure 3.14 Lighting analysis for March 21 st	30
Figure 3.15 Lighting analysis for June 21 st	31
Figure 3.16 Lighting analysis for September 23 rd	32
Figure 3.17 Lighting analysis for December 22 nd	33
Figure 4.1 The climate areas of Greece [44]	34
Figure 4.2 Prevailing winds per month.....	35
Figure 4.3 Prevailing winds throughout the year	35
Figure 4.4 Prevailing winds for the period 1 st June-31 st Aug.....	35
Figure 4.5 Computational Domain	38
Figure 4.6 Examined Scenarios.....	42
Figure 4.7 Position of the Avatars in the building	43
Figure 5.1 PMV results for the four examined hours of the day.....	44
Figure 5.2 Detailed PMV results of the Avatars inside the building (A-G: position, S-E-N-W: orientation).....	45
Figure 5.3 Detailed PMV results of the Avatars inside the building (A-G: position, S-E-N-W: orientation).....	46
Figure 5.4 Airflow movement inside the building	47
Figure 5.5 Velocity results for the four examined hours of the day	48
Figure 5.6 PMV results for the four examined hours of the day.....	49
Figure 5.7 Detailed PMV results of the Avatars inside the building (A-G: position, S-E-N-W: orientation).....	50
Figure 5.8 Detailed PMV results of the Avatars inside the building (A-G: position, S-E-N-W: orientation).....	51
Figure 5.9 Airflow movement inside the building	52
Figure 5.10 Velocity results for the four examined hours of the day	53
Figure 5.11 PMV results for the four examined hours of the day.....	54
Figure 5.12 Detailed PMV results of the Avatars inside the building (A-G: position, S-E-N-W: orientation)....	55
Figure 5.13 Detailed PMV results of the Avatars inside the building (A-G: position, S-E-N-W: orientation)....	56
Figure 5.14 Airflow movement inside the building	57
Figure 5.15 Velocity results for the four examined hours of the day	58
Figure 5.16 PMV results for the four examined hours of the day.....	59
Figure 5.17 Detailed PMV results of the Avatars inside the building (A-G: position, S-E-N-W: orientation)....	60
Figure 5.18 Detailed PMV results of the Avatars inside the building (A-G: position, S-E-N-W: orientation)....	61

Figure 5.19 Airflow movement inside the building	62
Figure 5.20 Velocity results for the four examined hours of the day	63
Figure 5.21 PMV results for the four examined hours of the day.....	64
Figure 5.22 Detailed PMV results of the Avatars inside the building (A-G: position, S-E-N-W: orientation)....	65
Figure 5.23 Detailed PMV results of the Avatars inside the building (A-G: position, S-E-N-W: orientation)....	66
Figure 5.24 Airflow movement inside the building	67
Figure 5.25 Velocity results for the four examined hours of the day	68
Figure 5.26 PMV results for the four examined hours of the day.....	69
Figure 5.27 Detailed PMV results of the Avatars inside the building (A-G: position, S-E-N-W: orientation)....	70
Figure 5.28 Detailed PMV results of the Avatars inside the building (A-G: position, S-E-N-W: orientation)....	71
Figure 5.29 Airflow movement inside the building	72
Figure 5.30 Velocity results for the four examined hours of the day	73
Figure 5.31 PMV results for the four examined hours of the day.....	74
Figure 5.32 Detailed PMV results of the Avatars inside the building (A-G: position, S-E-N-W: orientation)....	75
Figure 5.33 Detailed PMV results of the Avatars inside the building (A-G: position, S-E-N-W: orientation)....	76
Figure 5.34 Airflow movement inside the building	77
Figure 5.35 Velocity results for the four examined hours of the day	78
Figure 5.36 PMV results for the four examined hours of the day.....	79
Figure 5.37 Detailed PMV results of the Avatars inside the building (A-G: position, S-E-N-W: orientation)....	80
Figure 5.38 Detailed PMV results of the Avatars inside the building (A-G: position, S-E-N-W: orientation)....	81
Figure 5.39 Airflow movement inside the building	82
Figure 5.40 Velocity results for the four examined hours of the day	83
Figure 5.41 PMV results for the four examined hours of the day.....	84
Figure 5.42 Detailed PMV results of the Avatars inside the building (A-G: position, S-E-N-W: orientation)....	85
Figure 5.43 Detailed PMV results of the Avatars inside the building (A-G: position, S-E-N-W: orientation)....	86
Figure 5.44 Airflow movement inside the building	87
Figure 5.45 Velocity results for the four examined hours of the day	88
Figure 5.46 PMV results for the four examined hours of the day.....	89
Figure 5.47 Detailed PMV results of the Avatars inside the building (A-G: position, S-E-N-W: orientation)....	90
Figure 5.48 Detailed PMV results of the Avatars inside the building (A-G: position, S-E-N-W: orientation)....	91
Figure 6.1 The physical model of the residence with the implementation of the control system	97

List of Tables

Table 3.1 The required building layout	18
Table 3.2 Roof construction	25
Table 3.3 Construction of floor/Ceiling with tile/wood	25
Table 3.4 Construction of floor with outside boundary	25
Table 3.5 Construction of ground floor with tile/wood	26
Table 3.6 Construction of exterior wall	26
Table 3.7 Construction of interior wall.....	26
Table 3.8 Construction of windows/glass doors	26
Table 3.9 Thermal characteristics of the selected buildings materials [40].....	27
Table 3.10 Building energy consumption	28
Table 3.11 Comparison of the heating and cooling primal energy consumption	29
Table 3.12 Luminance levels per space type of a residence	30
Table 4.1 The examined outdoor conditions for the selected hours	36
Table 6.1 Legend of the PMV range	93
Table 6.2 PMV results of the Avatars at 2:00 o'clock of all the Scenarios	93
Table 6.3 PMV results of the Avatars at 8:00 o'clock of all the Scenarios	93
Table 6.4 PMV results of the Avatars at 14:00 o'clock of all the Scenarios	94
Table 6.5 PMV results of the Avatars at 20:00 o'clock of all the Scenarios	94

List of Diagrams

Diagram 3.1 Percentage of the building energy consumption.....	28
Diagram 3.2 Heating and cooling energy consumption per month	29

1. Introduction

Natural ventilation is an alternative way to achieve indoor thermal comfort and healthy environmental conditions. It is linked to Indoor Air Quality (IAQ) and the comfort of the occupants as well as to the potential of reducing building energy consumption. Natural ventilation can be effectively used during the day for the improvement of thermal comfort levels and during the night for cooling the thermal mass of the building [1]–[5].

The objective of the present study is to assess the impact of natural cross-ventilation on thermal comfort levels in sustainable residential buildings. Alternative strategies were explored for the study of natural ventilation and the effect of a complex building geometry on indoor airflow patterns and thermal comfort levels. Various software packages are included in this research for the required simulations.

According to the author's knowledge in the field of investigating natural ventilation via numerical approach simulation the present study is an original attempt to examine a more elaborate building architectural design.

In this framework, the impact of natural cross-ventilation on thermal comfort levels in a complex two storey building geometry, with its inner layout is investigated. Moreover, the thermal comfort is studied on seven human figures (Avatars) located in various spaces of the residence, and not just on some points in a specific height or plane of the building volume. In all the simulations the building is isolated modelled.

The dwelling is designed for the needs of 4 people (family or cohabitation of students) and can be treated as a Live Lab. For that reason the location of the dwelling is chosen to be in the Campus of the Technical University of Crete.

1.1. Methodology

The applied methodology in this research consists of the following main steps:

- Literature review of evaluating thermal comfort in a building with natural ventilation
- Design of the dwelling with bioclimatic parameters
- Energy consumption of the building with the OpenStudio software
- Study of indoor lighting levels using the Ecotect
- Selection of the programs for the CFD simulations
- Study of the natural ventilation inside the dwelling with the Blender program using the CFD analysis
- Study of the indoor thermal comfort (PMV index) of the dwelling using the Autodesk CFD program

1.2. Issue layout

- In the 1st section, the objective and the applied methodology are presented,
- In the 2nd section, the literature review of previous works on the field of naturally ventilated buildings is analysed,
- In the 3rd section, the architectural design process of the residence is presented,
- In the 4th section, the applied methodology for the natural ventilation modelling and simulation is introduced
- In the 5th section, the indoor airflow and thermal comfort results per Scenario are analysed,
- In the 6th section, a comparison of the results from all the Scenarios is made and some future steps or changes are suggested
- In the 7th section, the above results are summarised
- In the 8th section, the references of this research are displayed.

2. Literature review

Over the years a lot of works study the impact of natural ventilation inside the buildings. For their study, some works [4]–[12] used field/experimental measurements or examined the natural ventilation in an existing building. **Stavrakakis et al [4]** used field measurements to validate the numerical results from their simulation for the study of indoor conditions and thermal comfort levels. **Evola et al [5]** and **Nikas et al [11]** used experimental data of previous works on the same building geometrical configuration to validate their simulation results. **Su et al [6]** used an existing building in China as a study case where measurements and tests are performed and in combination with the use of the adaptive model an evaluation method of natural ventilation system base on thermal comfort is established. **Wong et al [7]** conducted a field survey in naturally ventilated building in Singapore to evaluate the thermal comfort perception of the occupants. The occupants voted on thermal sensation (TS), comfort perception (TC) and air movement sensation (wind sensation, five-point scale). **Cui et al [8]** used field measurements to validate the CFD models of their study case. **Chu et al [9]** used wind tunnel experiments to examine the impact of natural ventilation in a building with two openings on the same external wall while **Karava et al [10]** conducted a wind tunnel experiment in a cross-ventilated space and they highlighted the importance of inlet-to-outlet ratio and related location of the openings on the sides of the building. **Kolokotsa et al [12]** experimented on a naturally ventilated chamber for the testing and optimization of an advanced EIB system on its effect on the indoor environment.

In other works they preferred to use various software packages to model the study case and simulate the airflow pattern inside a space. Some used Flow Networks for their simulations [2], [13]–[15] while others used CFD analysis [1], [4], [5], [8], [11], [16]–[27]. **Schulze et al [2]** used the coupled approach of airflow network and dynamic building simulations (EnergyPlus software) to determine the annual thermal comfort and energy savings in a naturally ventilated space. **Pisello et al [13]** investigated the impact of natural ventilation on building primary energy requirement for heating and cooling using the Design Builder and EnergyPlus software. **Good et al [14]** used the IES Virtual Environment to model the proposed building and simulate the natural ventilation based on their proposed process on designing buildings for natural ventilation. **Kinnane et al [15]** evaluated the passive ventilation provision inside a building using an advanced airflow network and the EnergyPlus in conjunction with DesignBuilder for the transient simulations. **Castillo et al [16]** used a numerical simulation of a cross ventilated building by the ANSYS Fluent 14 program for the development of a methodology for the evaluation of thermal comfort in naturally ventilated spaces. **Menchaca-Brandan et al [17]** used the Fluent (part of ANSYS 14.5) to perform CFD simulation to analyze the radiative effects on the indoor air temperature in a naturally ventilated space. A typical office space was modelled with several heat sources and it was found that the indoor air temperature was lower when the radiation was not considered and that the air velocity inside the space was higher when the radiation factor was included in the simulations. **Bastide et al [18]** performed CFD analysis (without mentioning the software package that they used) and the velocity coefficient (C_v) to examine the behaviour of the indoor airflow of a naturally ventilated

space. **Prianto et al [19]** used the N3S software to study the airflow pattern inside a building as a result of the balcony configuration, the opening design and the internal division. **Liping et al [20]** investigated the impact of various ventilation strategies and facade designs for naturally ventilated buildings on indoor thermal environment using the TAS, ESP-r and ANSYS Fluent 15 software packages for the simulations. **Faizal et al [21]** examined the effect of the porches on the indoor flow field modification by simulating a typical one-storey terraced house, in Malaysia, using the Open FOAM software. **Gilani et al [22]** used the ANSYS Fluent 12.1 software to perform a CFD analysis in a naturally ventilated room (cross ventilation) with a heat source. The purpose was to predict the indoor temperature stratification. **Perén et al [23]** used ANSYS Fluent 12 to perform CFD simulations to analyse the indoor natural ventilation flow, in a wind-driven cross-ventilated space with different roof inclination angles. **Cui et al [8]** used ANSYS Fluent 14 for the CFD analysis to examine the effects of a loggia and window opening size on cross-flow ventilation rates in a low-rise building on the seaside in Corsica, France. **Daemei et al [24]** used Design Builder to model an existing building in Rasht in Iran, in order to assess natural ventilation based on CFD analysis. Airflow and indoor air velocity was explored to investigate the effect of single-sided and cross ventilation. **Ayata et al [1]** used the ANSYS Fluent 6.2 program to investigate, by CFD, the potential of natural ventilation as a passive cooling system in new building in Kayseri, Turkey. **Perén et al [25]** used the ANSYS Fluent 12 program to perform CFD simulations in order to study the impact of different roof geometries (single-span and double-span leeward sawtooth roof) on the wind-driven cross-ventilation flow inside a building. **T. van Hooff et al [26]** focused on the accuracy of CFD simulations and the most known models used for the examination of cross-ventilation flow patterns in a generic isolated building. **Stavrakakis et al [4]** and **Nikas et al [11]** used the Fluent 6.3 for their numerical simulation of a naturally cross-ventilated building. **Hawendi et al [27]** examined the effect of an external boundary wall on the indoor airflow pattern with the Fluent R16.3 software for the CFD simulations.

In the works that use a CFD approach for the simulation of natural ventilation, the selection of a turbulence model is required. Six works found in literature **[4], [5], [8], [17], [18], [21]** choose the RNG (Re-Normalisation Group) $k-\epsilon$ turbulence model, which is the most commonly used for indoor airflow simulations, as it is also referred from **Perén et al [23]** in their literature research. **Cui et al [8]** tested the RNG $k-\epsilon$ and the Reynolds Stress Model (RSM) where they resulted that the second seems a bit more accurate than the first, but for their study they choose the RNG $k-\epsilon$ turbulence model because of its shorter convergence time. **Stavrakakis et al [4]** and **Evola et al [5]** tested the turbulence models $Sk-\epsilon$, $Rk-\epsilon$ and RNG $k-\epsilon$, and $Sk-\epsilon$ and RNG $k-\epsilon$ respectively and both works concluded that the RNG $k-\epsilon$ model presented slightly better results. Other works **[11], [16], [22], [23], [25], [26]** choose the SST (Shear-Stress Transport) $k-\omega$ turbulence model for their simulations. Four of them **[16], [22], [23], [26]** tested some of the turbulence models: (1) Standard $k-\epsilon$ model ($Sk-\epsilon$), (2) realizable $k-\epsilon$ model ($Rk-\epsilon$), (3) renormalization group $k-\epsilon$ model (RNG $k-\epsilon$), (4) standard $k-\omega$ model ($Sk-\omega$), (5) shear-stress transport $k-\omega$ model (SST $k-\omega$) and (6) low-Re stress-omega RSM model, and the first 3 concluded that for their work the SST $k-\omega$ turbulence model had more

accurate results. **Perén et al [25]** choose that model because it was resulted in their previous work **[23]** that it had a slightly better performance than the other turbulence models.

The most common method for the evaluation of thermal comfort is the Predicted Mean Vote (PMV) with the Predicted Percentage Dissatisfied (PPD). PMV (Predicted Mean Vote) is a thermal comfort index. It was developed for the prediction of the human mean vote of thermal sensation from a large sample of people that was exposed to a given indoor environment. PMV has a 7 scale range from -3 to +3 (-3=cold, -2=cool, -1=slightly cool, 0=neutral, 1=slightly warm, 2=warm, 3=hot). The ideal value of PMV is 0, with a comfortable range from -0.5 to +0.5, but even in the comfortable zone some people will not be satisfied with the indoor temperature **[28], [29]**.

That could be due to other factors that the human consider or do in order get to a comfortable state in the exposed environmental conditions (adaptation model). From the literature **[6], [30], [31]**, three primary modes exist:

- Behavioural adaptation. In this mode are all the actions that people do to themselves to adapt in the environment conditions (change of clothing or their position, drinking cold beverages, ect) or the adjustments that do to the environment in order to meet their needs (adjusting the shading system, the air velocity, etc).
- Physiological adaptation. The physiological reaction of long term/repeatedly exposure to a thermal environment, which leads to adjustment of thermal sensation of the occupant in the conditions of the exposed environment.
- Psychological adaptation. This mode is depended from many factors that are different from person to person and are important for the human thermal sensation. Such factors are:
 - The natural environment
 - The expectations that the environment should be different
 - The exposure time
 - The previous experiences, etc

All these factors can affect the human perception of the environmental conditions and thus, their thermal comfort and satisfaction.

To predict the percentage of dissatisfaction of the occupants in the given thermal conditions the PPD index (Predicted Percentage of Dissatisfaction) was developed and is a function of PMV. **Figure 2.1** shows the relation between PMV and PPD. For an acceptable thermal environment the PPD is defined as $PPD > 10\%$ **[28], [29]**.

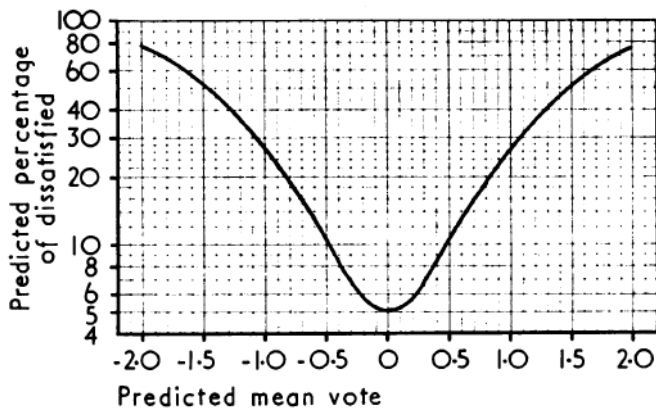


Figure 2.1 The relation between PMV and PPD [32]

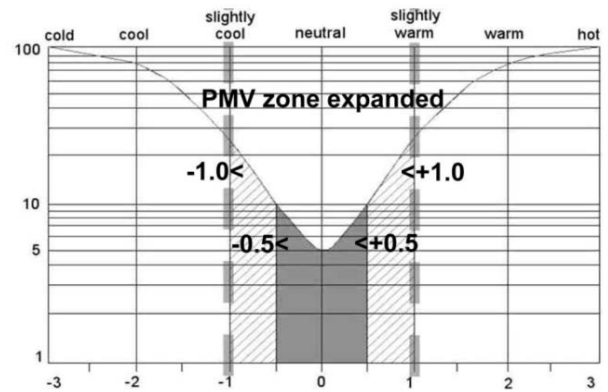


Figure 2.2 The expanded zone of PMV [33]

Pitt et al [33] examined the extended limits of the PMV comfort zone (Figure 2.2) and concluded that the extended limits of PMV can be applied in many cases.

From the literature four works [5], [12], [16], [20] used the PMV index for the thermal comfort evaluation of the CFD simulations of a naturally ventilated space. Castillo et al [16] used the Heat Balance Index (HBI) and the Predicted Mean Value (PMV) to study the indoor thermal comfort of a naturally ventilated space in hot climate. Liping et al [20] used the PMV index to evaluate the impact of various ventilation strategies for naturally ventilated buildings on the indoor thermal environment; and Stavrakakis et al [4] for the thermal comfort evaluation in naturally cross-ventilated buildings under high-temperature experimental conditions. Kolokotsa et al [12] used the PMV index to estimate the effects of an advanced EIB system on the indoor environment in a naturally ventilated test chamber. Castillo et al [16] and Luo et al [34], from their literature research, concluded that PMV was invalid when it was applied to naturally ventilated buildings since it ignores the psychological criteria that are significant for the thermal sensation of the occupants in these cases. The first, mentioned the SET approach (Standard Effective Temperature) that is used to correct the PMV and is applied for outdoor, semi-outdoor and interior spaces. In their study, they used a correlation between the PMV and HBI to estimate the comfort evaporation. The latest used the ACS (Adapted Comfort Standard) method to evaluate the indoor thermal comfort in their study case of a naturally ventilated space.

Four works [4], [6], [34], [35] used the Adaptation Model/Adaptive Comfort Standard (ACS) to evaluate the thermal comfort of the occupants. Luo et al [34] used it to assess the thermal comfort and the Infiltration Air Quality (IAQ) in a naturally ventilated space in four cities in China. Emmerich et al [35] used it to assess indoor thermal comfort regarding the humidity factor in four US cities while Su et al [6] used the Adaptive model to evaluate the natural ventilation system of an existing building based on indoor thermal comfort. Stavrakakis et al [4] except from the PMV, PPD and PD indexes used also the Adaptive model to evaluate the impact of natural cross ventilation on the indoor thermal comfort in their work.

Two works [17], [22] used other factors to evaluate the indoor thermal comfort in a naturally ventilated space. Menchaca-Brandan et al [17] examined the influence of radiation heat transfer

on indoor temperature and velocity and thus the influence on indoor thermal comfort. **Gilani et al [22]** performed a CFD analysis in a naturally ventilated room (cross ventilation) with a heat source to predict the indoor temperature stratification which is an important factor for the occupants' thermal comfort.

A few works [1]–[3], [5], [13], [15], [18], [36] have investigated the impact of natural ventilation in buildings on their energy consumption. **Pisello et al [13]** studied the role and effect of natural ventilation through building openings on building energy demand for heating and cooling. **Bastide et al [18]** aimed to optimise the building energy efficiency by reducing the air-conditioning period due to the use of natural ventilation and the better study of the bioclimatic design. **Ayata et al [1]** concluded that the design of a city, where the location of the buildings is based on wind data, can benefit the affect of natural ventilation and can significantly reduce the energy consumption. **Schulze et al [2]** determined the annual thermal comfort and energy savings in a naturally ventilated space in three different locations. **Kinnane et al [15]** evaluated the passive ventilation provision inside a building after housing energy-efficiency retrofits. **Santamouris et al [3]** concluded that night ventilation may increase the next day peak of the indoor temperature and a significant energy reduction can be achieved. With the use of natural ventilation a better indoor air quality conjoint with the reduction of the energy consumption can be achieved as is reported in the work of **Evola et al [5]**. According to **Papamanolis [45]** natural ventilation systems in Greece can have better performance over the mechanical ones, especially regarding to the energy efficiency of the buildings.

Few works [2], [18], [36] address the results of their research to the architects and the necessity of taking into account natural ventilation systems from the early stage of architectural design. **Bastide et al [18]** studied the reduction of the energy consumption by natural ventilation and better bioclimatic design of the building and noted that the followed method is useful for an architect. **Schulze et al [2]** concluded that the method used, for their work, for the study of indoor airflow by natural ventilation can be used in the architectural design phase. **Papamanolis [36]** highlighted the importance of natural ventilation strategies, especially in Greece, as a design factor which is often ignored by the designers.

In most of the research works, the examined space, where the simulations were performed, had a simple geometry, except from three works [21], [24], [27] where the effects of natural ventilation were examined in simple low-rise house geometry. In the work of **Nikas et al [11]** a simple cell is used but the impact of indoor layout on the indoor flow patterns from natural ventilation is examined. In the present study, the impact of natural cross ventilation on thermal comfort levels in an isolated residential building with complex geometry is examined.

From literature we find that natural ventilation in buildings is still a concern and is studied with various software packages and field measurements. A numerical approach, mostly CFD, is used but there is no specific method in which provides best results, more accuracy and meets the computational demands. So far, the majority of the simulations are performed in a simple geometry and only one factor is investigated each time.

3. Architectural Process

3.1. Bioclimatic parameters

The design process of this dwelling is done with consideration of the bioclimatic design principles that apply in Greece. As noted in the work of **Karkanias et al [37]**, bioclimatic architecture needs to be further studied and implemented and is a key factor for the energy efficiency in the building sector. The bioclimatic design aims to integrate buildings into the natural environment and the utilisation of the local climate, for the optimal comfort conditions of the users in combination with the reduction of energy consumption. The bioclimatic parameters become important in the architectural design, and the management of natural lighting and ventilation is directly related to the layout of the floor and the sitting of the building.

The orientation and the sizing of the openings are a key element of the building orientation. The shading of the openings is based on their orientation and is preferable the application of external shadings, which prevent the penetration of unwanted sunlight and the overheating of the interior space. Generally, the following can be applied **[38]**:

- in south orientation is recommended the use of suitable horizontal fixed or operable shading systems,
- in east or west orientation vertical fixed or operable shading systems are more appropriate,
- in SE and SW orientation the combination of horizontal and vertical shading systems is recommended, and
- in north orientation a shading system is not required.

The use of natural ventilation for the means of cooling the building has plenty benefits. The indoor air is recirculated and has better quality, which directly affects the health of the occupants, better thermal comfort conditions can be achieved as well as the feeling of wellness in the spaces of the building. Some factors that affect the indoor air movement and conditions from natural ventilation are **[38]**:

- the environmental conditions and specially the direction of the cold winds of the area,
- the orientation, the size and the position of the openings on the sides of the building,
- the type of the building and the occupants activity,
- the colour and texture of the outside surfaces,
- the creation of ventilation currents through water evaporation,
- the environment around the building, existence of vegetation, trees, bushes, fences, etc.

3.2. Location

The selected lot is located in the Campus of the Technical University of Crete, in the area of Kounoupidiana, a seaside suburb in the northern part of the prefecture of Chania, Crete (**Figure 3.1**). The area, being outside of the centre, is characterised as residential area and has few commercial shops, cafe houses, supermarkets, etc. It is located close to several beaches, the airport and the Old Harbour of Chania.

The access in the lot is from the NE side where a small road ends. Close to the lot, from the east side, there are three low-rise green houses and far in the north side, are the buildings of the Architectural Engineering and Environmental Engineering School (**Figure 3.1**).

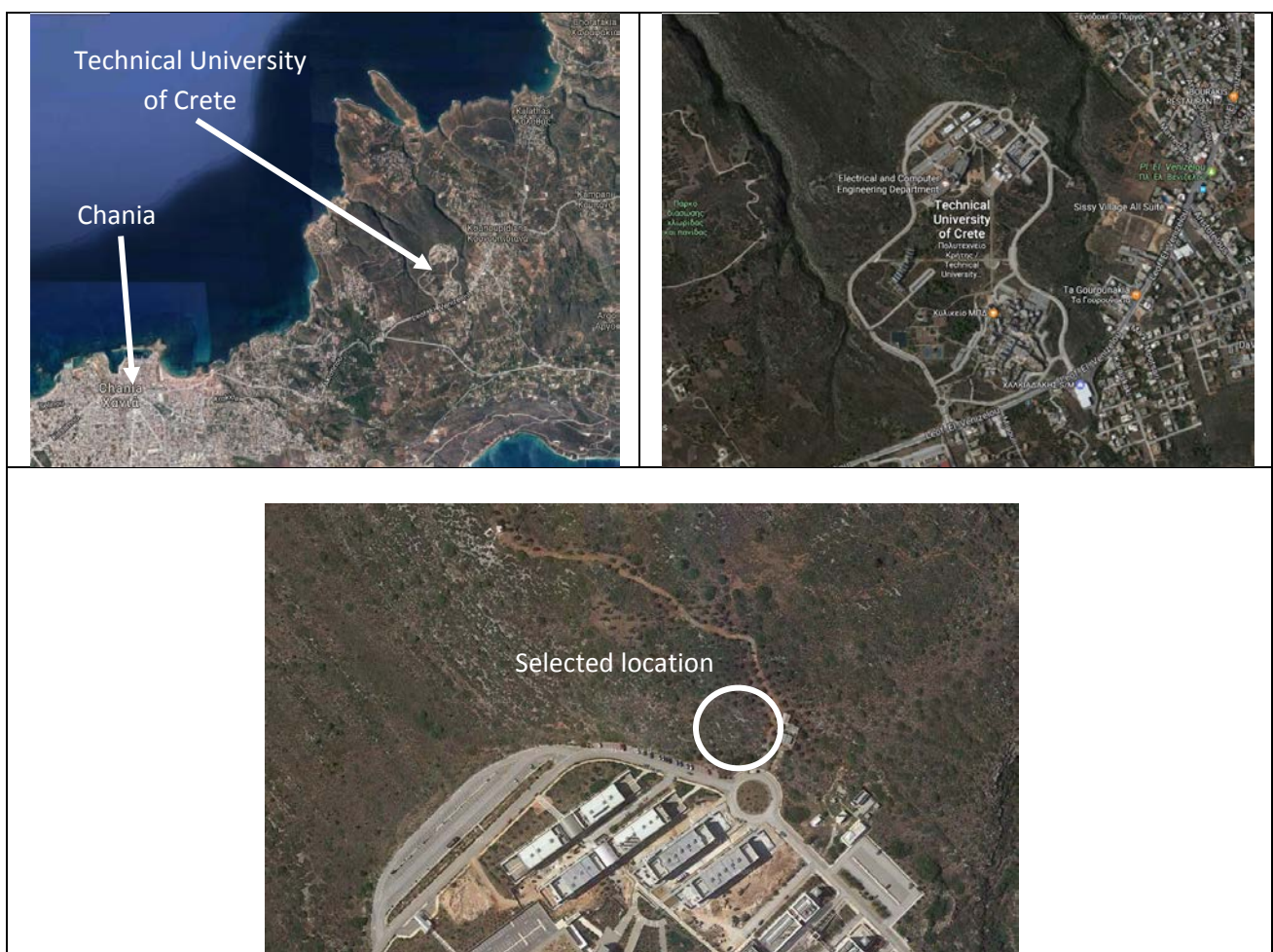


Figure 3.1 Map of the area [39]

3.3. Architectural design

After the study of the selected location the designing process of the building began. The lot does not have specific dimensions and the required area of the building is not boundary. The originally defined building space requirements are presented in the **Table 3.1** below.

Building layout	
Ground floor	First floor
Living room	2 Bedrooms
Kitchen	Office
Dining room	2 WC
Laundry room	
WC	

Table 3.1 The required building layout

The dwelling is designed for the needs of 4 people (family or cohabitation of students) and can be treated as a Live Lab. For that reason the design is not binding further changes or additions on the envelope or the inside of the building or its surrounded environment (shading systems/constructions, alternation of the size and location of the openings, etc).

The building has openings in the North, East and South directions, avoiding completely the West. The floor plan of the house is elongated with the long sides facing the north-south direction. In the ground floor an open space of the Living room-Kitchen-Dining room is created and on the first floor the two bedrooms and the office are placed. The living room has N and S orientation, the kitchen E and N and the dining room S, but the open space layout of the ground floor allows the diffusion of light in the various areas. In the living room there is a two-storey open space which allows communication with the hallway on the first floor and a two-storey northern opening that creates a sense of unity. The office has N and E openings and the two bedrooms have E and S openings. The laundry and the 3 bathrooms are located in the western area of the residence with N and S windows. The floor plans (**Figure 3.2, Figure 3.3**), sides (**Figures 3.4 and 3.5**) and position (**Figures 3.6, 3.7**) of the building are presented below.

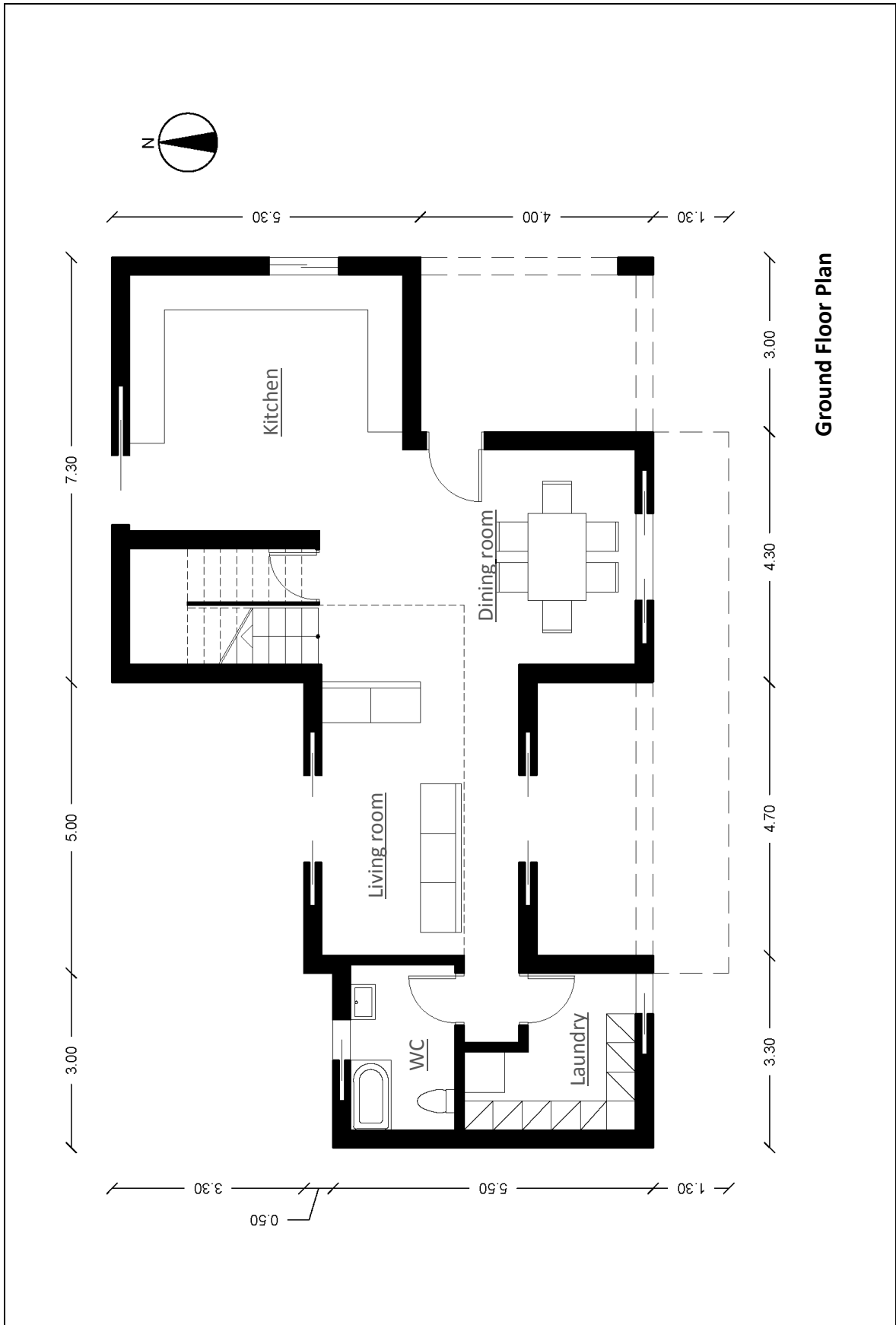


Figure 3.2 Ground floor plan

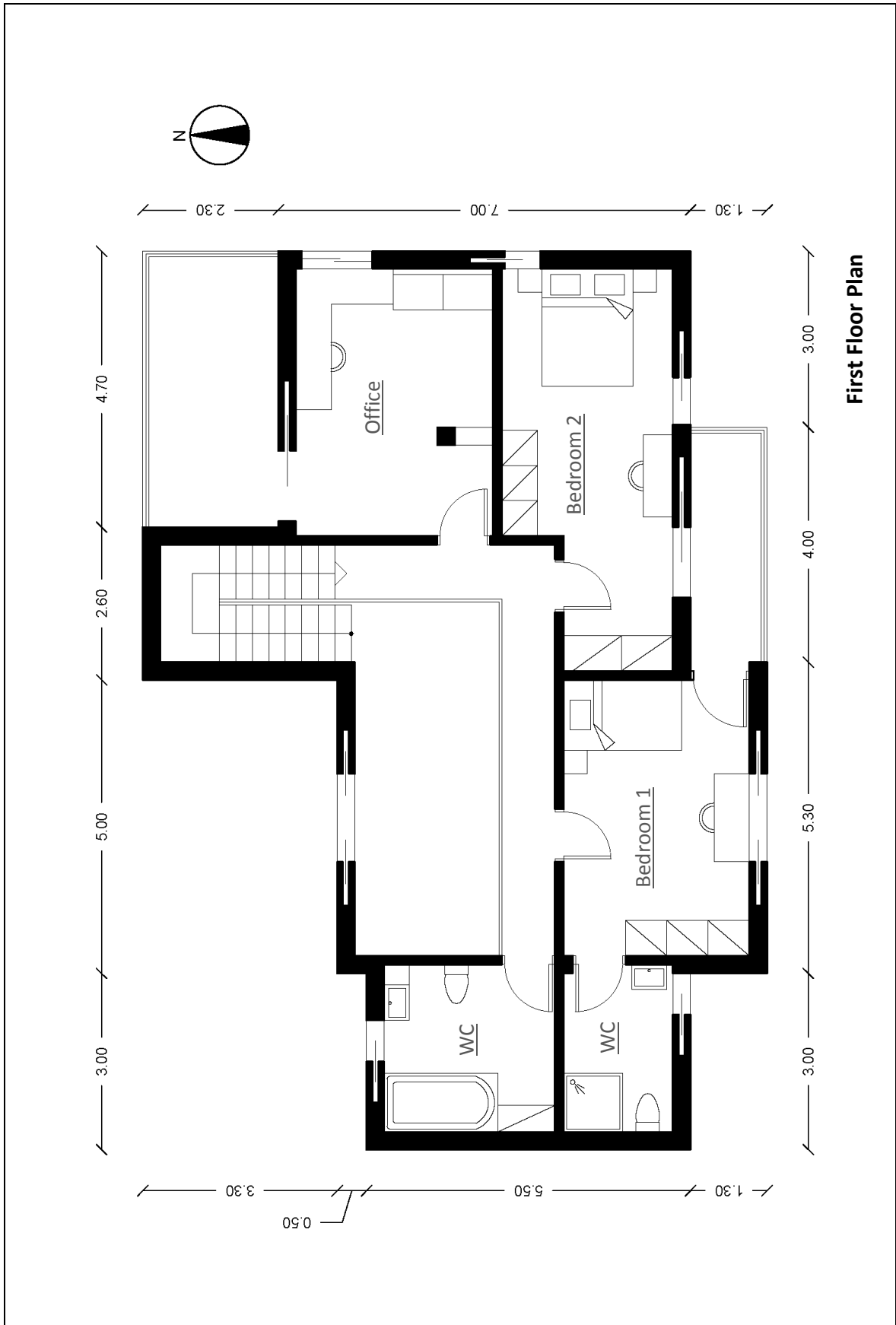


Figure 3.3 1st floor plan



South view



East view



North view

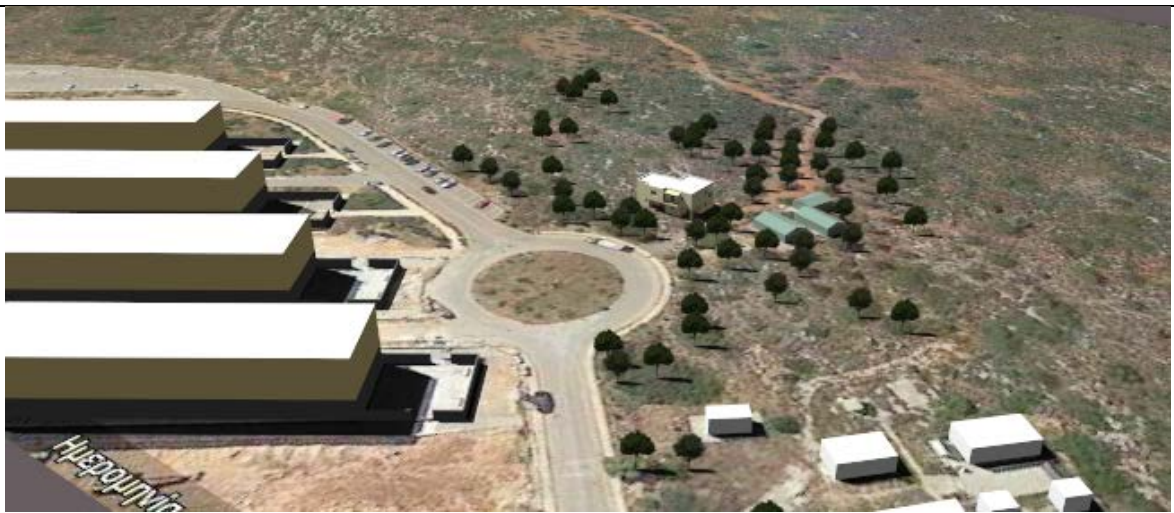
Figure 3.4 Views of the building



Figure 3.5 Views of the building

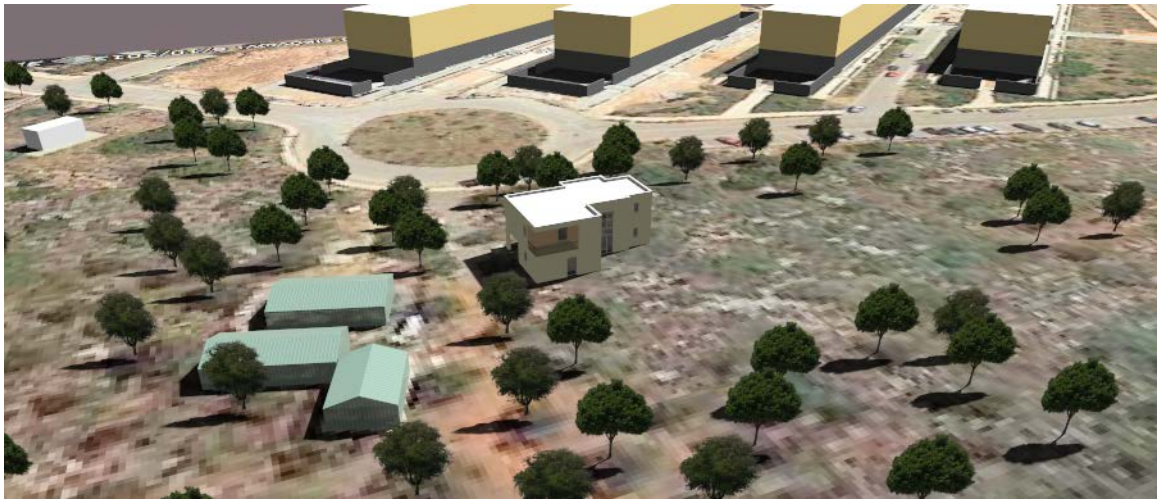


Top view of the area



SE view of the area

Figure 3.6 Position of the building in the area



NE view of the area



NW view of the area

Figure 3.7 Position of the building in the area

3.4. Building Constructions

In this section the detailed construction of the building is presented in the **Tables 3.2-3.8** and **Figures 3.8- 3.13** below as well as the thermal characteristics of the selected materials in **Table 3.9**.

Roof		
1	Gravel	0.05m
2	Polyethylene membrane	
3	Extruded polystyrene (insulation XPS)	0.05m
4	Asphalt membrane	
5	Reinforced concrete	0.15m
6	Air	0.15m
7	Gypsum Board	0.015m
	Total	0.415m

Table 3.2 Roof construction

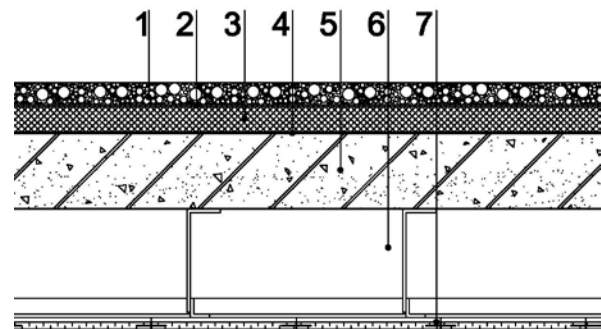


Figure 3.8 Roof construction

Floor/Ceiling with tile/wood		
1	Ceramic tiles/ Wood floor	0.01m/0.03m
2	Tile adhesive	0.03m
3	Screed concrete	0.07m/0.05m
4	Extruded polystyrene (insulation XPS)	0.05m
5	Polyethylene membrane	
6	Reinforced concrete	0.15m
7	Air	0.15m
8	Gypsum Board	0.015m
	Total	0.475m

Table 3.3 Construction of floor/Ceiling with tile/wood

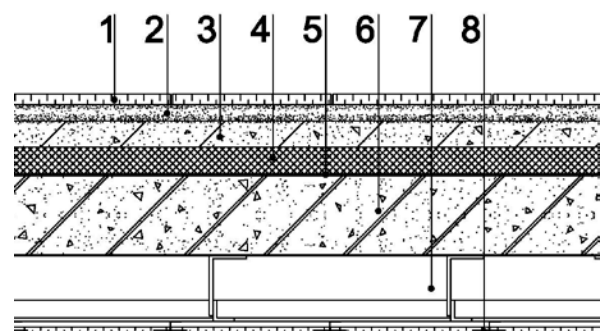


Figure 3.9 Construction of floor/Ceiling with tile/wood

Floor with outside boundary		
1	Wood floor	0.03m
2	Tile adhesive	0.03m
3	Screed concrete	0.05m
4	Extruded polystyrene (insulation XPS)	0.05m
5	Polyethylene membrane	
6	Reinforced concrete	0.15m
7	Plaster	0.03m
	Total	0.34m

Table 3.4 Construction of floor with outside boundary

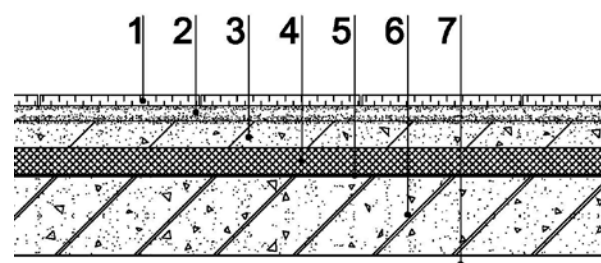


Figure 3.10 Construction of floor with outside boundary

Ground Floor with tile/wood		
1	Ceramic tiles/ Wood floor	0.01m/0.03m
2	Tile adhesive	0.03m
3	Screed concrete	0.07m/0.05m
4	Polyethylene membrane	
5	Extruded polystyrene (insulation XPS)	0.05m
6	Asphalt membrane	
7	Cement mortar	0.02m
8	Reinforced concrete	0.15m
	Total	0.33m

Table 3.5 Construction of ground floor with tile/wood

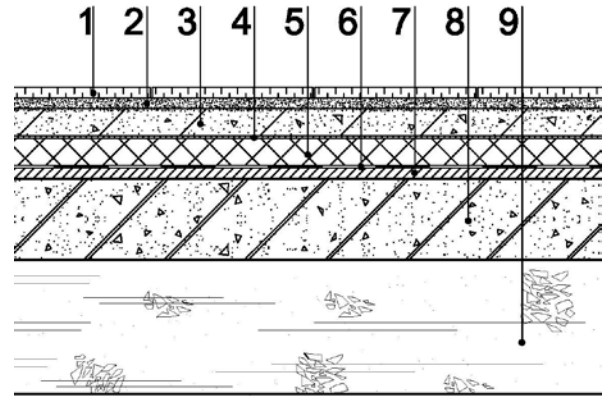


Figure 3.11 Construction of ground floor with tile/wood

Exterior Wall		
1	Plaster	0.035m
2	Brick	0.09m
3	Extruded polystyrene (insulation XPS)	0.05m
4	Brick	0.09m
5	Plaster	0.035m
	Total	0.30m

Table 3.6 Construction of exterior wall

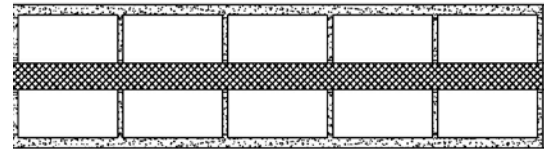


Figure 3.12 Construction of exterior wall

Interior Wall		
1	Plaster	0.03m
2	Brick	0.09m
3	Plaster	0.03m
	Total	0.15m

Table 3.7 Construction of interior wall

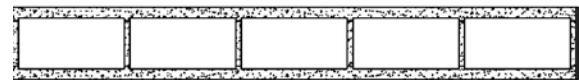


Figure 3.13 Construction of interior wall

Windows/Glass Doors		
1	Glass	5mm
2	Air	18mm
3	Glass	5mm
	Total	28mm (0.028m)

Table 3.8 Construction of windows/glass doors

Thermal characteristics of the building materials				
	Materials	Density Kg/m³	Conductivity W/m K	Specific Heat J/kg K
1	Air	1.23	0.26	1008
2	Asphalt membrane	1100	0.23	1000
3	Brick	1200	0.45	1000
4	Cement mortar	1800	0.87	1000
5	Ceramic tiles	2000	1.84	840
6	Extruded polystyrene (insulation XPS)	35	0.031	1450
7	Glass		1	
8	Gravel	2200	2	1000
9	Gypsum Board	700	0.21	1000
10	Plaster	1800	0.87	1000
11	Polyethylene membrane	980	0.50	1800
12	Reinforced concrete	2400	2.50	1000
13	Screed concrete	1500	0.64	1000
14	Tile adhesive	1800	0.87	1000
15	Wood floor	700	0.21	1600

Table 3.9 Thermal characteristics of the selected buildings materials [40]

3.5. Energy Consumption

After completion of the architectural design and the selection of the materials for the building construction the residence is modelled in OpenStudio (with the SketchUp plug in) for the assessment of its energy consumption. The building geometry is created using the SketchUp interface. The chosen materials, constructions and the schedules for the operation of the building and its systems are created in OpenStudio. The setpoints for heating and cooling in a typical HVAC system (in Greece) are 20°C and 26°C respectively, as they are recommended from [41] for new residential buildings.

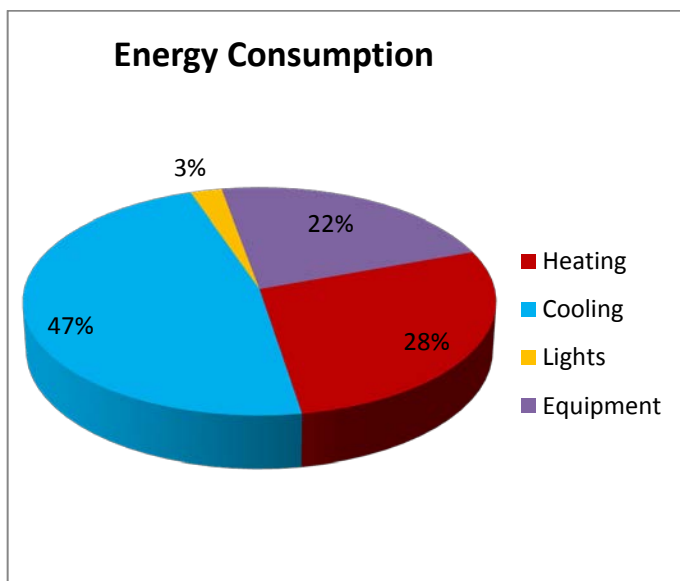


Diagram 3.1 Percentage of the building energy consumption

	kWh	kWh/m ²
Heating	2755.59	14.67
Cooling	4660.63	24.81
Lighting	234.55	1.25
Equipment	2197.3	11.69
Total	9848.07	52.41

Table 3.10 Building energy consumption

Diagram 3.1 depicts the allocation of the building energy consumption where we observe that the required energy for cooling is 47%, almost the half percentage of the total energy consumption. The energy for heating and the electric equipment of the building is 28% and 22% respectively, while lighting has the lowest percentage, 3%.

Table 3.10 shows the energy consumption for heating, cooling, the lighting and the electric equipment of the modelled building.

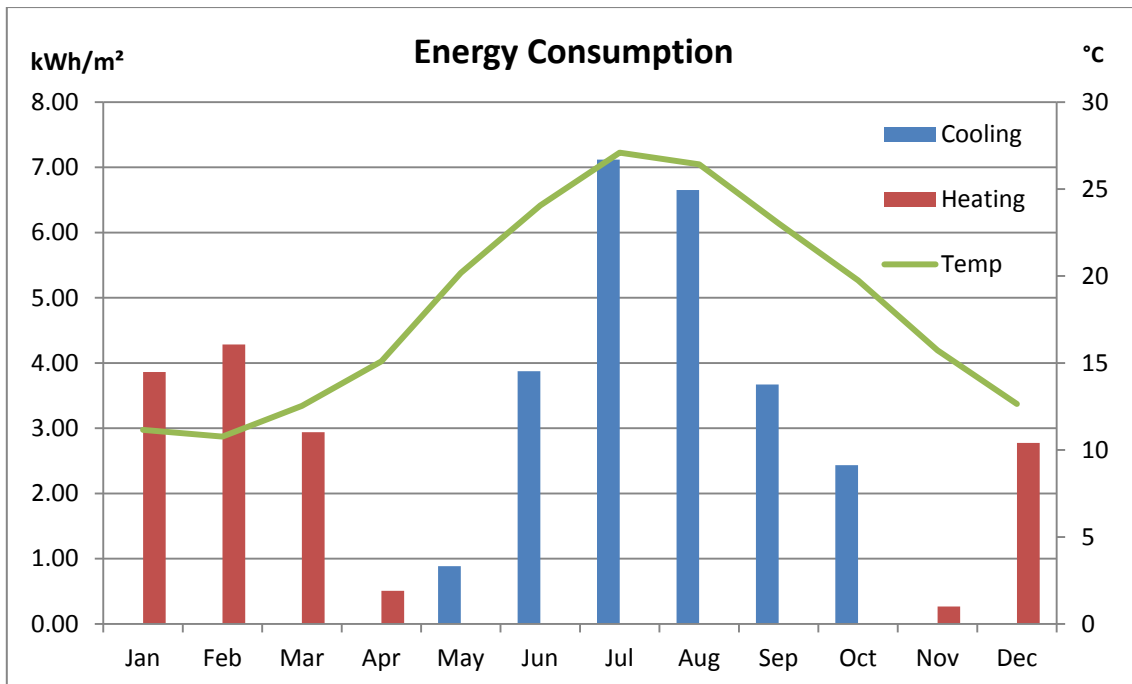


Diagram 3.2 Heating and cooling energy consumption per month

Diagram 3.2 shows the energy consumption of the modelled building for heating and cooling needs per month in comparison with the mean outdoor air temperature. The need for cooling is appeared more for July and August, when the outdoor temperature is at its highest. On January and February is the highest need for heating, when the outdoor temperature is around 10°C.

The energy consumption for heating and cooling of the modelled building is converted into the Primal Energy Consumption, using the guidelines of [42]. They are then compared with the mean heating and cooling primal energy consumption of residential buildings for the year 2015 as they were resulted from [43] and are presented in **Table 3.11**. We observe that the modelled building requires a lot less energy for heating purposes (24.85%) but a lot more for cooling, more than double. This can be explained by the fact that the designed building is located in the A climatic zone of Greece where the need for cooling is more while the compared data are the mean values from all the climatic zones.

	Heating Primary Energy Consumption (kWh/m ²)	Cooling Primary Energy Consumption (kWh/m ²)
Mean Value for 2015	171.18	31.04
Examined building	42.53	71.93

Table 3.11 Comparison of the heating and cooling primal energy consumption

3.6. Lighting study

During the stage of architectural process and design of the residential building the indoor lighting levels are also studied. The aim is to see if the luminance levels in the spaces are adequate and if any further study is required for the implementation of shading systems or other changes in the envelope, the openings or the surrounding environment of the building. The required lighting levels for the various space types of a residence are presented in **Table 3.12 [41]**.

Spaces	Luminance levels (lux)
Living room	200-250
Kitchen-Dining room	250-300
Bedroom	200
Office	300-500

Table 3.12 Luminance levels per space type of a residence

The lighting analysis, using the Ecotect software, for March 21st, June 21st, September 23rd and December 22nd (summer and winter equinox and solstice) for the hours 9:30, 13:00 and 16:30 is presented below. The building is modelled and simulated as an isolated building without taking into account its surroundings.

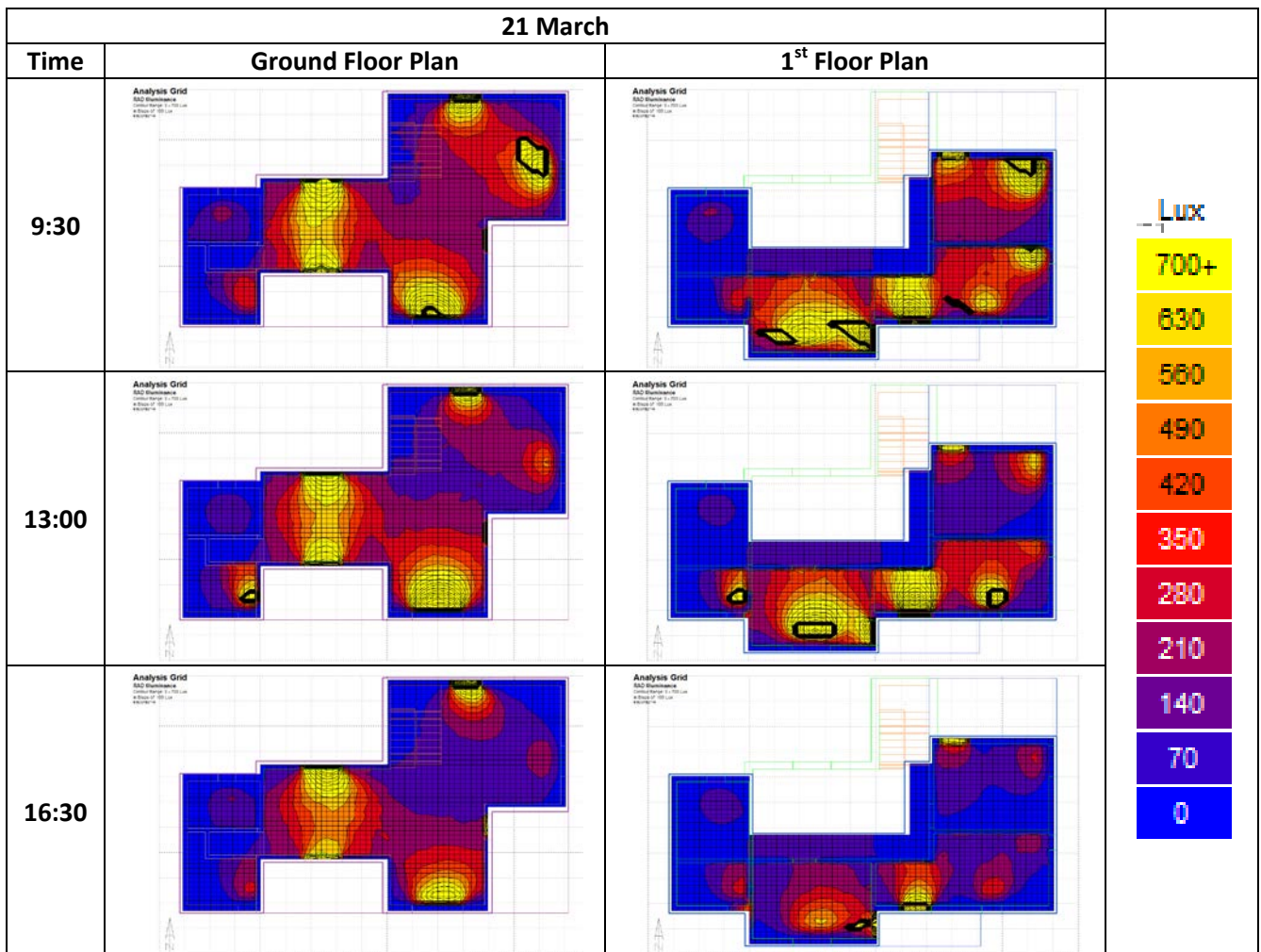


Figure 3.14 Lighting analysis for March 21st

From the above analysis (**Figure 3.14**) we observe high lighting levels in the living and dining room in all the three examined hours. In the first floor high levels appears in the two bedrooms at 9:30 and 13:00 o'clock.

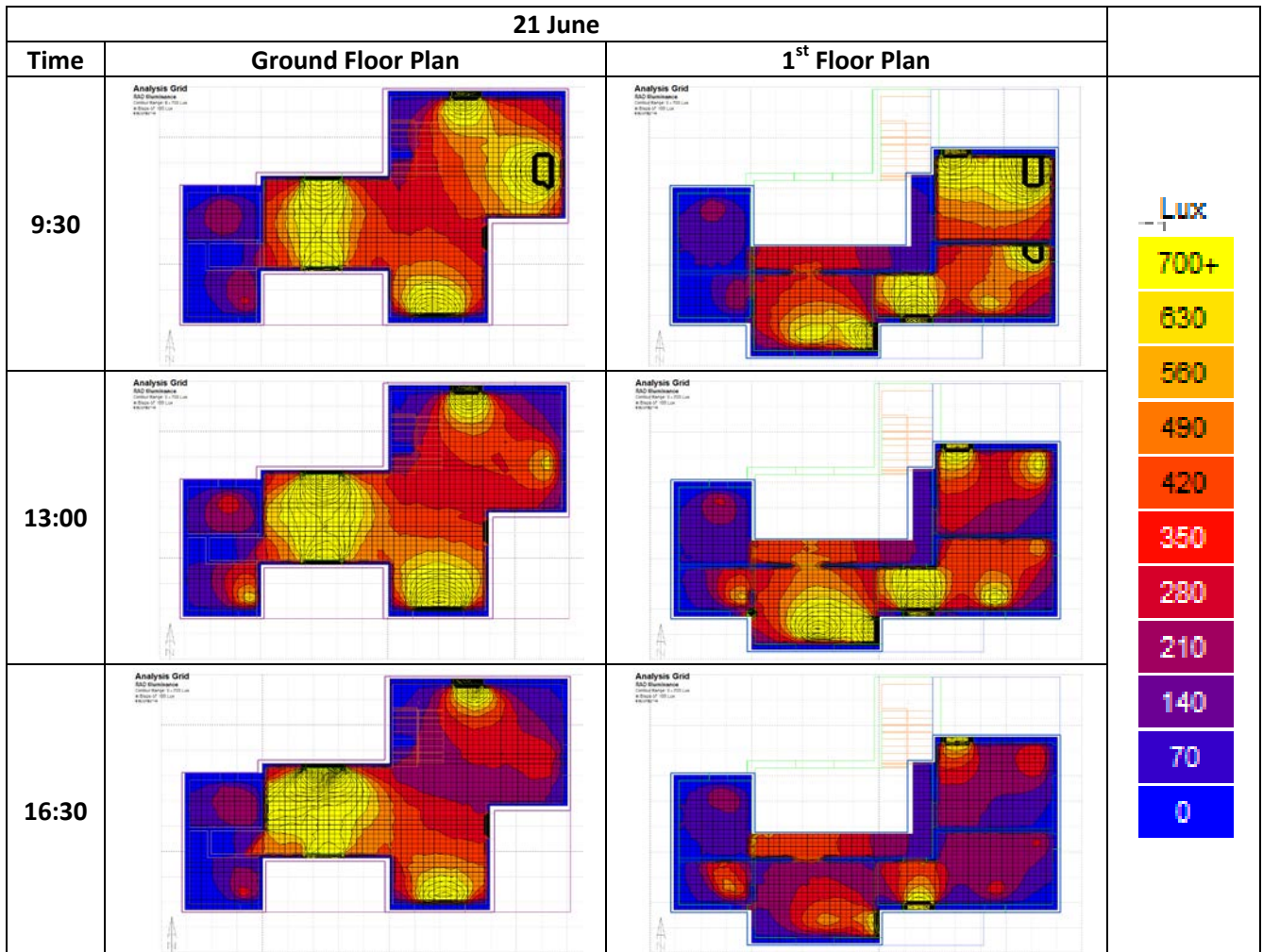


Figure 3.15 Lighting analysis for June 21st

At June 21st (**Figure 3.15**) high lighting levels (more than 700 lux) appears in all the spaces of the ground floor (except in the WCs) for all the examined hours. Similar results are presented in the first floor at 9:30 and 13:00 o'clock. At 16:30 the luminance levels drop under 500lux in all the spaces.

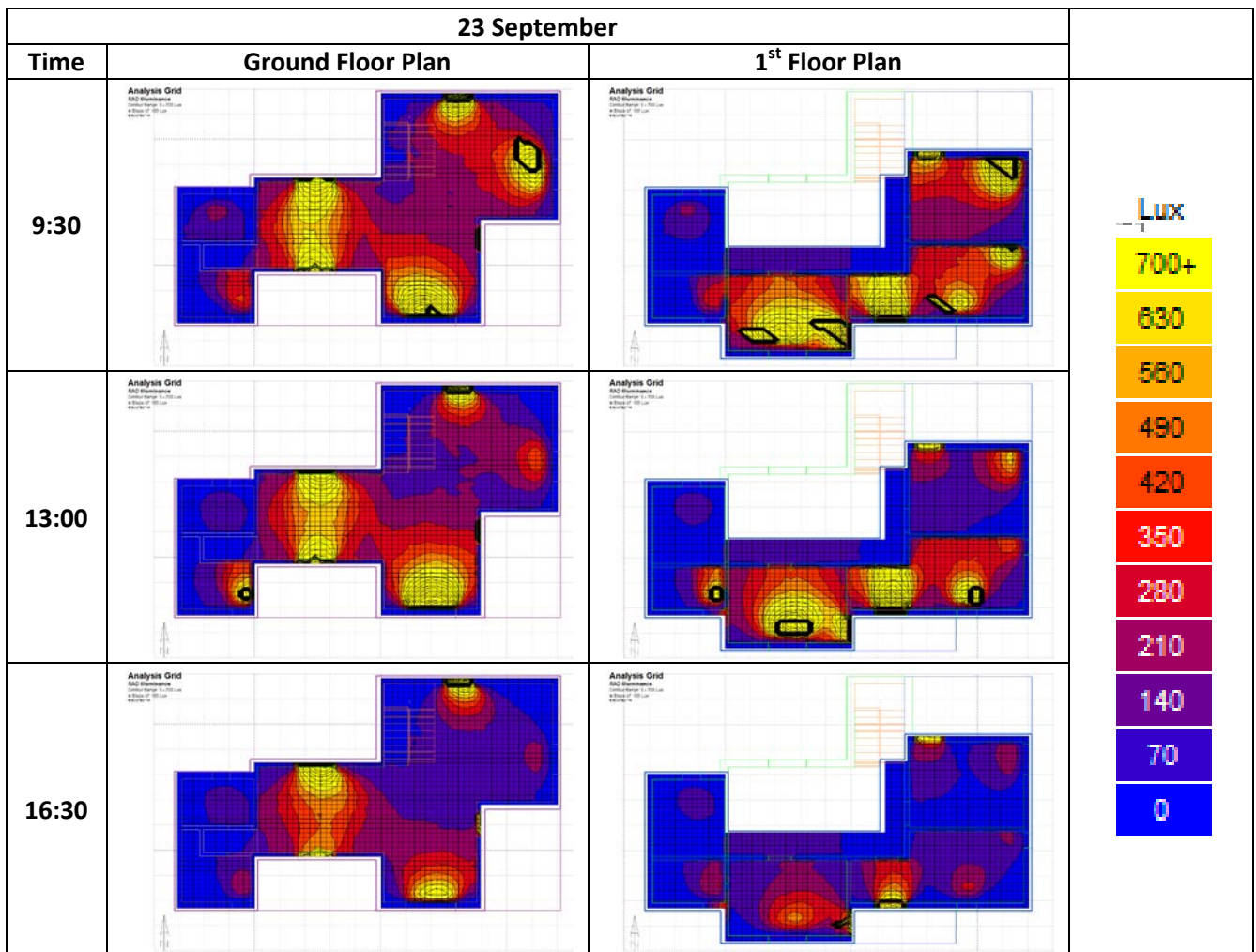


Figure 3.16 Lighting analysis for September 23rd

In **Figure 3.16** high lighting levels appear mostly in living and dining room, Bedroom 1 and partially in Bedroom 2 at 9:30 and 13:00 o'clock. At 16:30 the luminance levels present a significant drop, especially in the kitchen and the spaces on the first floor.

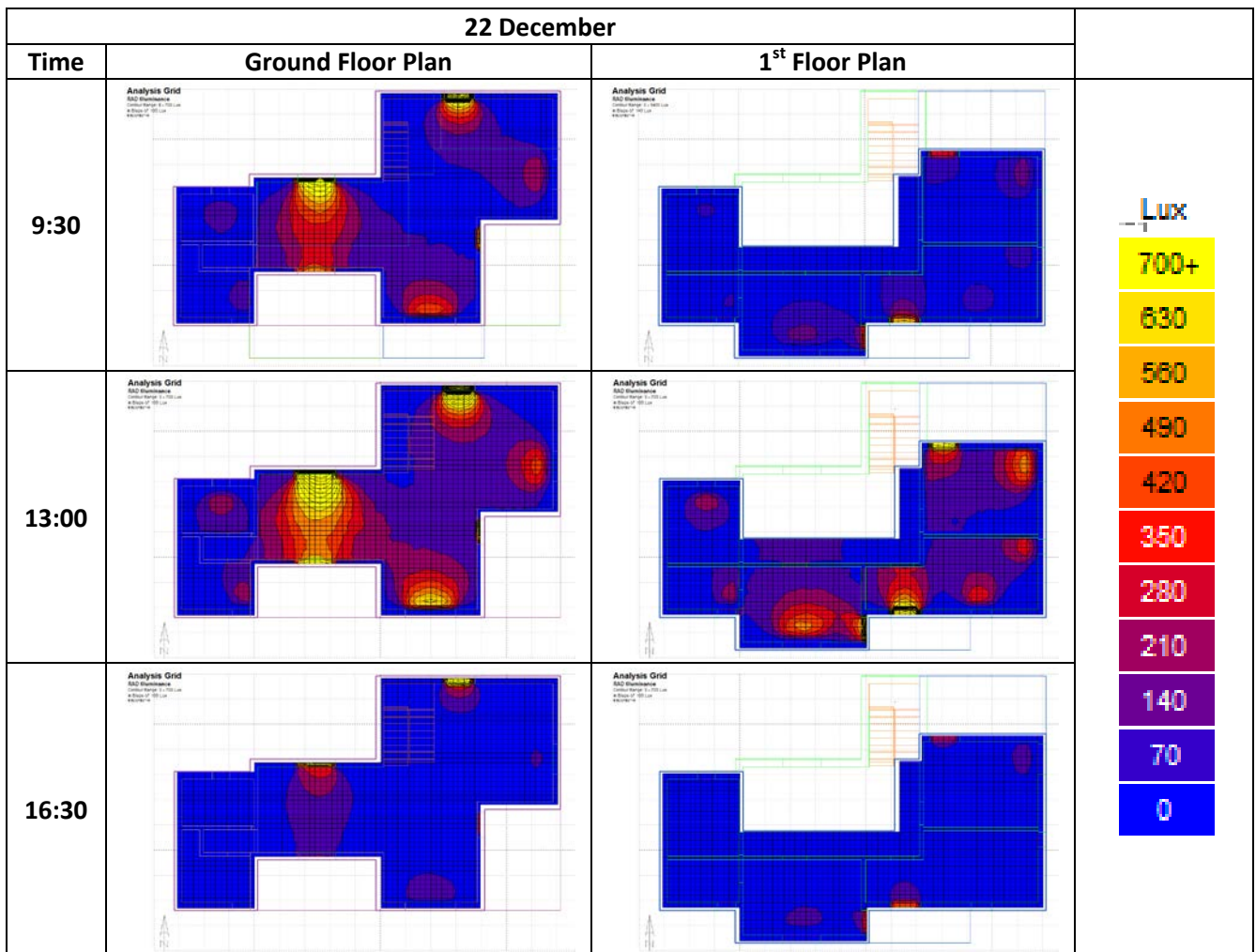


Figure 3.17 Lighting analysis for December 22nd

From the analysis above (**Figure 3.17**) almost sufficient luminance levels appear in the living room at 9:30 and 13:00 o'clock and in bedroom 1 at 13:00 o'clock. Overall, the lighting levels seem to not meet the required in most of the spaces for the examined hours at 22 December.

A study for the lighting levels inside the dwelling is performed, in the stages of the architectural design, but needs further work due to the need of shadings' implementation or other changes in the outdoor environment (trees, shading constructions, etc). The impact of these interventions on the indoor airflow pattern and the indoor conditions need to be further studied and are not inside the framework of this research.

4. Natural ventilation modelling

4.1. Weather Information

Greece is characterised by the Mediterranean type of temperate climate and has mild moist winters and hot dry summers, with long sunshine periods nearly all year round. In individual areas of the country we find great variety of climate types, with common feature the high summer temperatures especially in closed valleys and highlands of the country.

Crete's climate is characterised as temperate Mediterranean and we find long sunshine periods in almost all months of the year. Winter is generally mild and the summer season extends from April to October. The warmest period is detected during July and August, with the temperature range from 29°C to 35°C, but is tempered by the sea breeze and the northern winds (**Figure 4.1**).

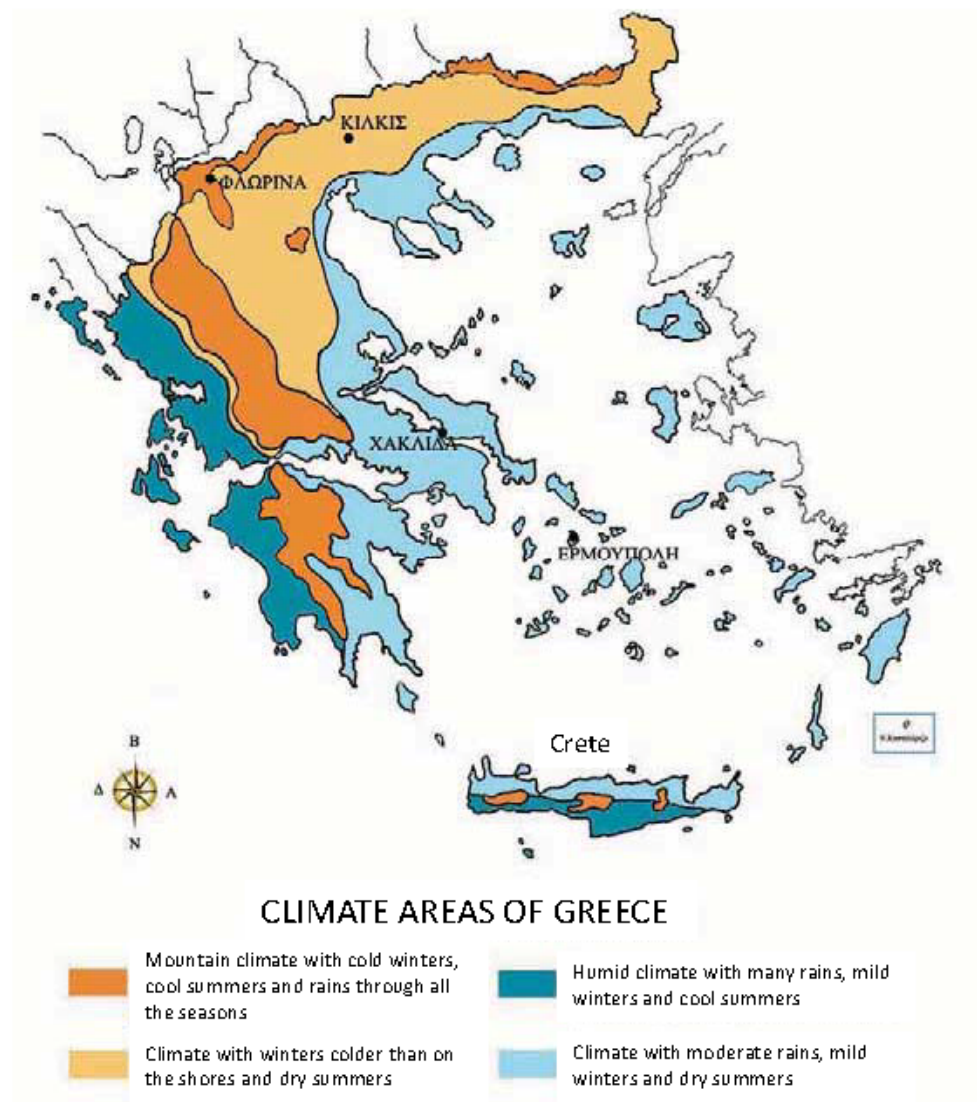


Figure 4.1 The climate areas of Greece [44]

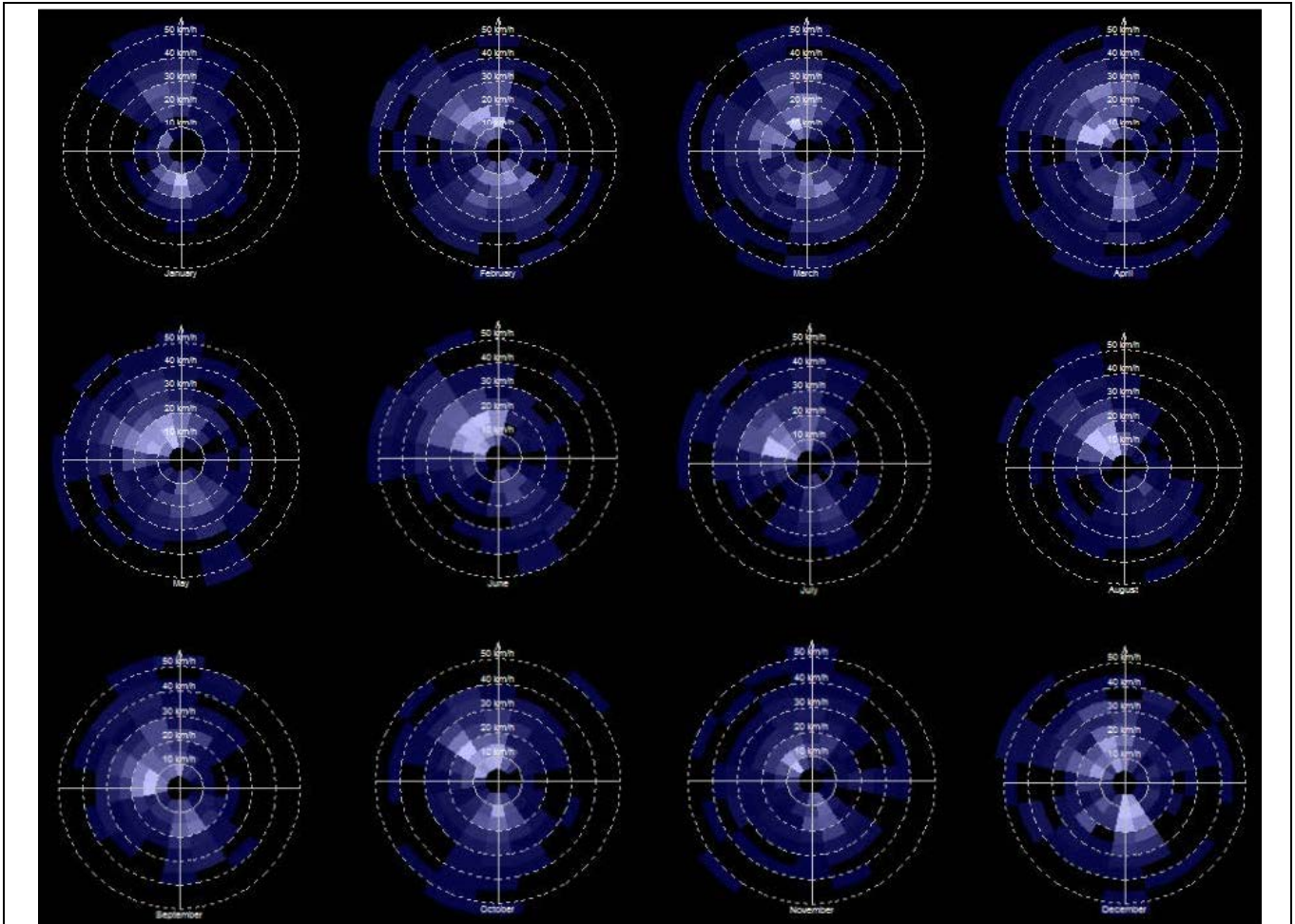


Figure 4.2 Prevailing winds per month

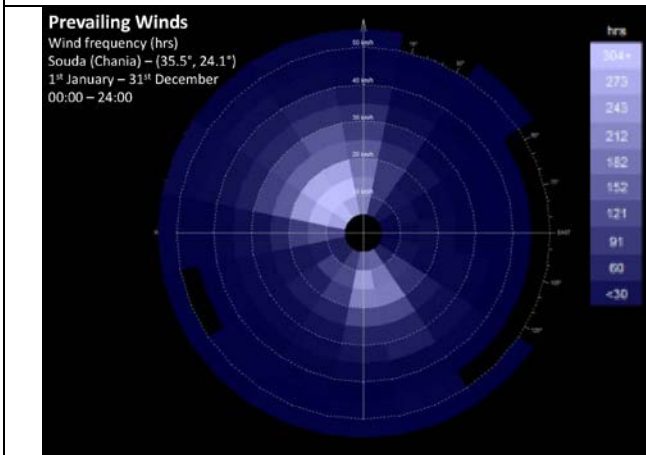


Figure 4.3 Prevailing winds throughout the year

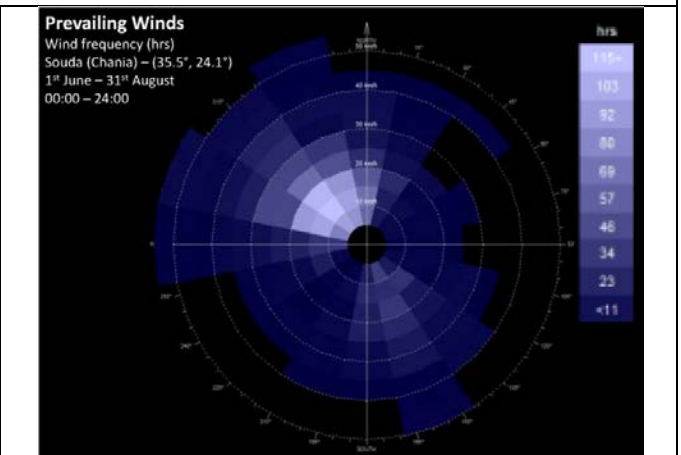


Figure 4.4 Prevailing winds for the period 1st June-31st Aug

From **Figures 4.2** and **4.3** we observe that the direction of the wind throughout the year is mostly NW and S. In **Figure 4.4**, for the summer season, the NW direction of the wind prevails.

The weather conditions of a typical summer day are 26°C, 55%RH and 3.5m/s velocity, therefore a day with these values is picked as the study day (30th of July). The climate data of four hours of this day (2:00, 8:00, 14:00 and 20:00) are chosen, as they are recorded from the meteorological station, to be the input of the external conditions, as shown in **Table 4.1**. The initial indoor temperature is

decided to be constant, same as the clothing level [28], [45]–[47], the metabolic rate [28], [45]–[47] and the human activity, so the only changes in the simulations are the outdoor conditions.

Time	Temperature (°C)	Relative Humidity (%)	Wind speed (m/s)
2:00	25	65	2
8:00	25	65	1
14:00	30	40	7
20:00	27	50	5.5

Table 4.1 The examined outdoor conditions for the selected hours

4.2. Software tools

The criteria for the choice of the software that is going to be used for the simulation of the natural ventilation inside the building for this dissertation are:

- A software with the potential of 3D view mode of the results
- A free/open source software
- A software with friendly environment for someone with architectural background while providing the required features.

After research, the Blender program with the CFD plug-in is chosen for the preliminary results of the airflow inside the building. The results can be seen in 3D mode, so it is easy to understand the movement of the wind inside the building and the computational time of every scenario is less than 10 minutes. The software uses simple solve for the run, the pro version had some issues and it is not possible to set the ambient temperature and the environmental conditions that are necessary for the simulation. The geometry of the building is designed in SketchUp and then is imported in Blender. Scenarios with alternative combinations of open windows and doors in the ground floor, the first floor and between the floors are tested to determine the final scenarios with the best possible airflow movement. For the tests, the wind velocity is set at 1m/s and 5m/s and the wind has S, N and NW direction. Three scenarios with open windows in the ground floor and six between the floors (9 total scenarios) are chosen to be the final scenarios where the impact assessment of natural ventilation on thermal comfort levels is performed.

For the study of thermal comfort levels, using the PMV index, the Autodesk CFD software is chosen. The geometry of the building and the nine scenarios are designed in Revit and then exported in Autodesk CFD. Every time the materials, boundary conditions, environmental conditions and all the other parameters are assigned from the beginning. The internal conditions of the building and the human activity are in all cases constants so that the results could be compared on how the external environmental conditions affect the indoor environment. The effect of solar radiation in the simulations is considered, and the location and time of the day are also inputs in every case.

4.3. CFD simulation: computational settings and parameters

Regarding the creation of the model in Autodesk CFD [47] for the simulation of natural ventilation inside a building and its impact on thermal comfort levels, there are no specific instructions. From research, tutorials and documentation of the Autodesk Knowledge Network the following methodology is created. In this work, the building is treated as stand alone case for the CFD analysis. The steps for the model creation are:

- Creation of the building geometry in Revit
- Set of the orientation of the building, so that the domain in Autodesk CFD is on the x&y axes and the wind direction (NW) is on the y axis (it was observed that the software responded a little better if the domain was aligned to the axis)
- Hide, in the 3D view, the selected windows/doors that will be open in the simulation
- Launch in Autodesk CFD
- Use the Geometry Tools to:
 - Merge edges
 - Fill Void, to create the air volume inside the building since there are some windows/doors open
 - Create the Domain, the air volume of the environment around the building (**Figure 4.5**)
- Assign the Materials in the imported geometry
- Assign the Boundary Conditions, velocity and temperature for inlet and pressure=0 for outlet for the domain and 70W heat generation for the human figures
- Set initial conditions, 26°C for the inside air volumes
- Create the Mesh of the model
- From the Solve dialog:
 - Set the Thermal Comfort Factors, Metabolic rate 60W/m², Clothing 0.36clo and Relative Humidity (different values)
 - The location of the building, the study time and day and the orientation
 - For the turbulence the SST k- ω model is chosen
 - The PMV index is used for the thermal comfort assessment
- Run the Scenario

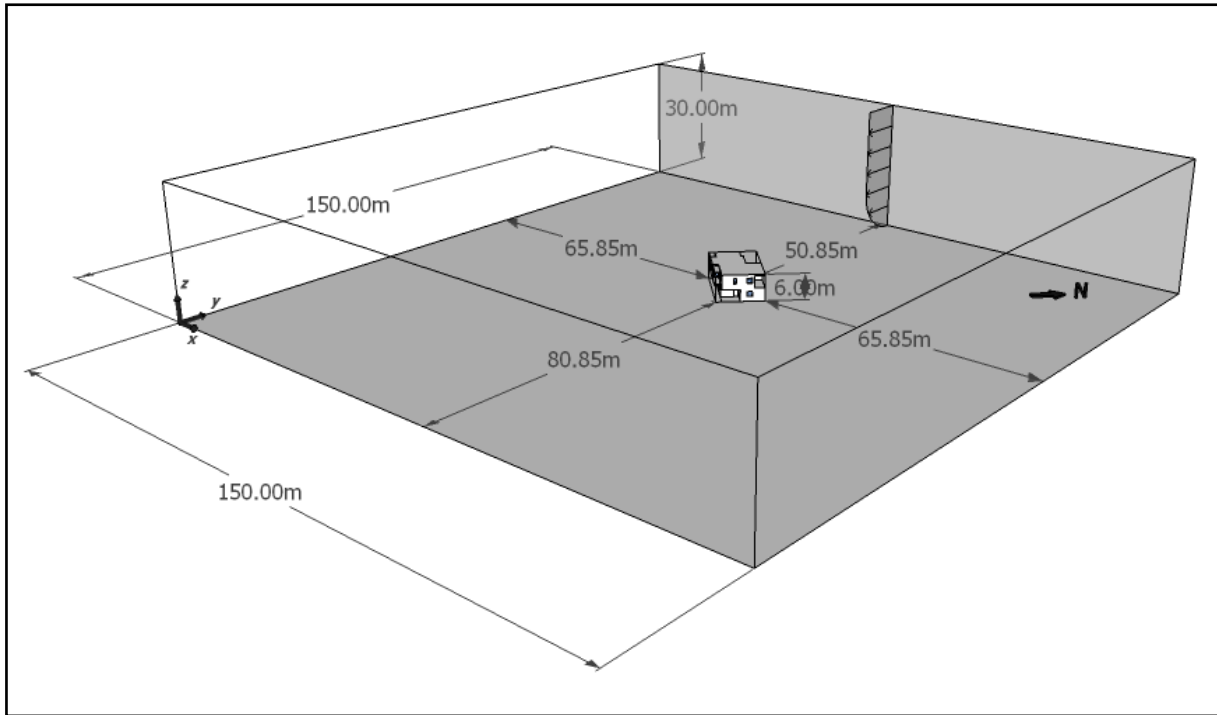


Figure 4.5 Computational Domain

The equations (1-12) for the PMV index and the turbulence model that the selected software uses are presented below [47]:

PMV equation

$$\begin{aligned}
 PMV = & [0.303e^{-0.036M} + 0.028]\{(M - W) - 3.96E^{-8}f_{cl}[(t_{cl} + 273)^4 - (t_r + 273)^4] \\
 & - f_{cl}h_c(t_{cl} - t_a) - 3.05[5.73 - 0.007(M - W) - p_a] - 0.42[(M - W) \\
 & - 58.15] - 0.0173M(5.87 - p_a) - 0.0014M(34 - t_a)\}
 \end{aligned} \tag{1}$$

With:

$$f_{cl} = \frac{1.0 + 0.2I_{cl}}{1.05 + 0.1I_{cl}} \tag{2}$$

$$\begin{aligned}
 t_{cl} = & 35.7 - 0.0275(M - W) - R_{cl}\{(M - W) - 3.05[5.73 - 0.007(M - W) - p_a] \\
 & - 0.42[(M - W) - 58.15] - 0.0173M(5.87 - p_a) - 0.0014M(34 - t_a)\}
 \end{aligned} \tag{3}$$

$$R_{cl} = 0.155I_{cl} \tag{4}$$

$$h_c = 12.1(V)^{1/2} \tag{5}$$

Where:

- e: Euler's number (2.718)
- fcl: clothing factor
- hc: convective heat transfer coefficient
- lcl: clothing insulation [clo]
- M: metabolic rate [W/m²] 115 for all scenarios
- pa: vapour pressure of air [kPa]
- Rcl: clothing thermal insulation
- ta: air temperature [°C]
- tcl: surface temperature of clothing [°C]
- tr: Mean radiant temperature [°C]
- V: air velocity [m/s]
- W: external work (assumed=0)

SST k-omega Governing Equations

Turbulence Kinetic Energy:

$$\frac{\partial k}{\partial t} + U_j \frac{\partial k}{\partial x_j} = P_k - \beta^* k \omega + \frac{\partial}{\partial x_j} \left[(\nu + \sigma_k \nu_T) \frac{\partial k}{\partial x_j} \right] \quad (6)$$

Specific Dissipation Rate:

$$\frac{\partial \omega}{\partial t} + U_j \frac{\partial \omega}{\partial x_j} = \alpha S^2 - \beta \omega^2 + \frac{\partial}{\partial x_j} \left[(\nu + \sigma_\omega \nu_T) \frac{\partial \omega}{\partial x_j} \right] + 2(1 - F_1) \sigma_\omega \frac{1}{\omega} \frac{\partial k}{\partial x_i} \frac{\partial \omega}{\partial x_i} \quad (7)$$

F_1 :

$$F_1 = \tanh \left\{ \left\{ \min \left[\max \left(\frac{\sqrt{k}}{\beta^* \omega y}, \frac{500 \nu}{y^2 \omega} \right), \frac{4 \sigma_\omega k}{CD_{kw} y^2} \right] \right\}^4 \right\} \quad (8)$$

CD_{kw} :

$$CD_{kw} = \max \left(2 \rho \sigma_\omega \frac{1}{\omega} \frac{\partial k}{\partial x_i} \frac{\partial \omega}{\partial x_i}, 10^{-10} \right) \quad (9)$$

Kinematic eddy viscosity:

$$\nu_T = \frac{a_1 k}{\max(a_1 \omega, SF_2)} \quad (10)$$

F₂:

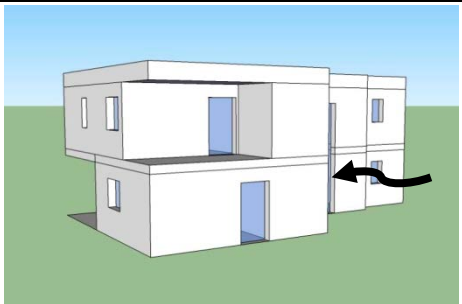
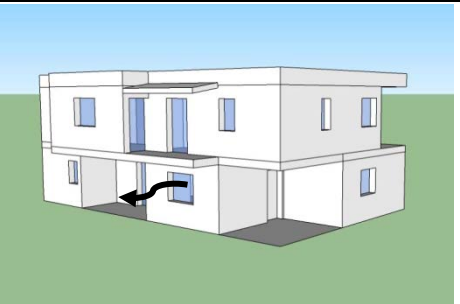
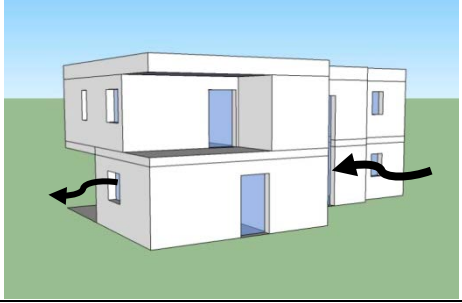
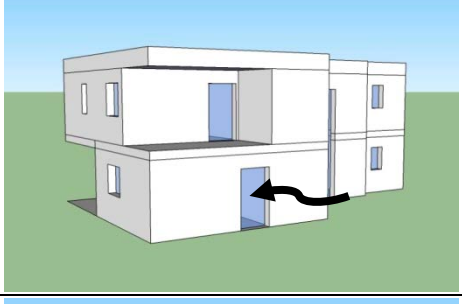
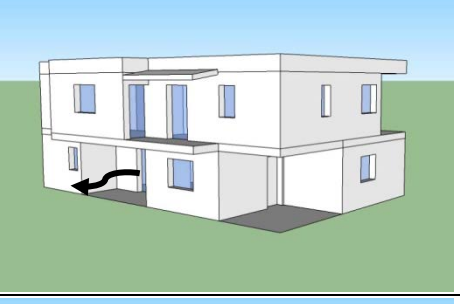
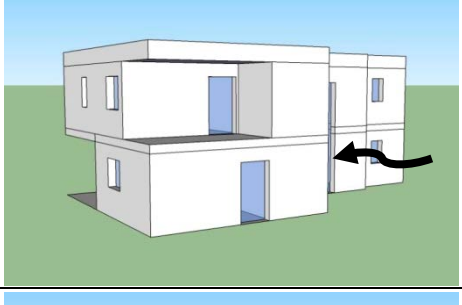
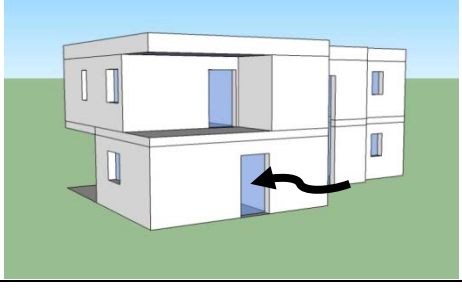
$$F_2 = \tanh \left[\left[\max \left(\frac{2\sqrt{k}}{\beta^* \omega y}, \frac{500\nu}{y^2 \omega} \right) \right]^2 \right] \quad (11)$$

P_k (Production limiter):

$$P_k = \min \left(\tau_{ij} \frac{\partial U_i}{\partial x_j}, 10\beta^* k \omega \right) \quad (12)$$

4.4. Presentation of the examined Scenarios

For the airflow movement inside the dwelling various scenarios were simulated in Blender software with the basic CFD plug-in and in Autodesk CFD. The examined Scenarios are presented in the Figure 4.6 below.

Scenario	NE Perspective view	SE Perspective view	Openings
1			<u>Inlet:</u> N glass door of the living room <u>Outlet:</u> S window of the dining room
2			<u>Inlet:</u> N glass door of the living room <u>Outlet:</u> E kitchen window
3			<u>Inlet:</u> N glass door of the kitchen <u>Outlet:</u> S glass door of the living room
4			<u>Inlet:</u> N glass door of the living room <u>Outlet:</u> S window of the bedroom 1
5			<u>Inlet:</u> N glass door of the kitchen <u>Outlet:</u> S window of the bedroom 1

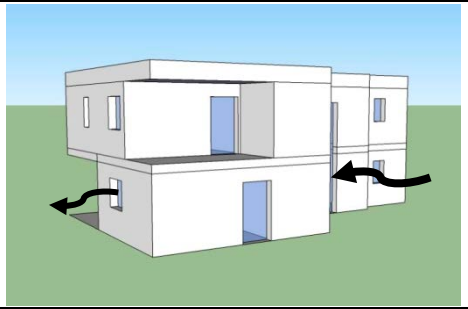
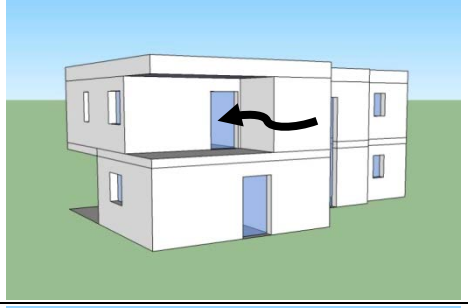
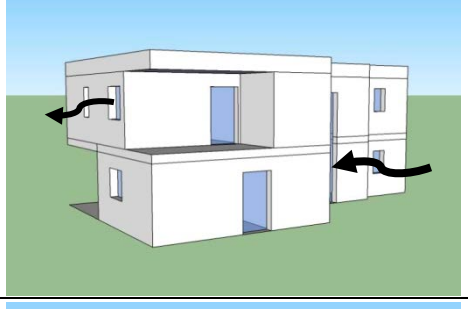
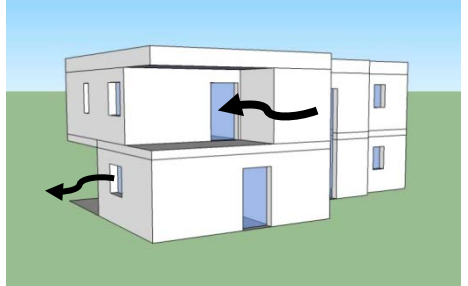
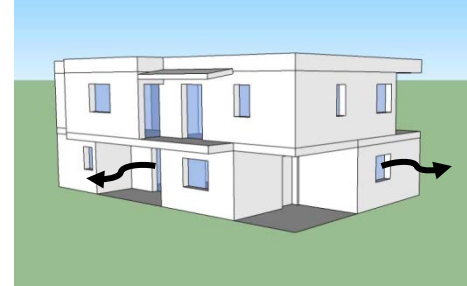
6			<p><u>Inlet:</u> N glass door of the living room <u>Outlet:</u> S window of the bedroom 1 and E kitchen window</p>
7			<p><u>Inlet:</u> N glass door of the office <u>Outlet:</u> S glass door of the living room</p>
8			<p><u>Inlet:</u> N glass door of the living room <u>Outlet:</u> E window of the office</p>
9			<p><u>Inlet:</u> N glass door of the office <u>Outlet:</u> S glass door of the living room and E kitchen window</p>

Figure 4.6 Examined Scenarios

For the evaluation of the thermal comfort levels, seven (7) human figures (Avatars) are placed in the examined spaces of the building as they are depicted in **Figure 4.7**. One Avatar is placed in a room that is not examined to see if the changed conditions in the other spaces will affect it.

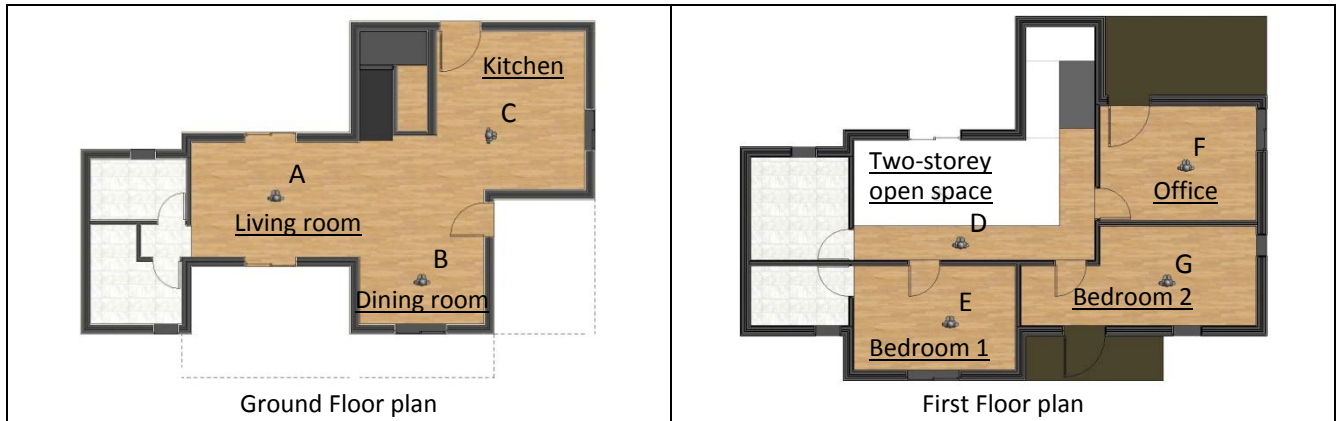


Figure 4.7 Position of the Avatars in the building

5. Results Analysis and Discussion

5.1. Base Scenario: no windows/doors open

From the SE perspective view of the building (**Figure 5.1**) we have a general image of the PMV on the Avatars' body for the four examined hours of the day. At 2:00 o'clock the PMV seems to be inside the comfort zone, at 8:00 the Avatars C, G and F record high values, in the hot zone, at 14:00 the PMV of all Avatars is located inside the hot zone and at 20:00 the values are in the warm zone.

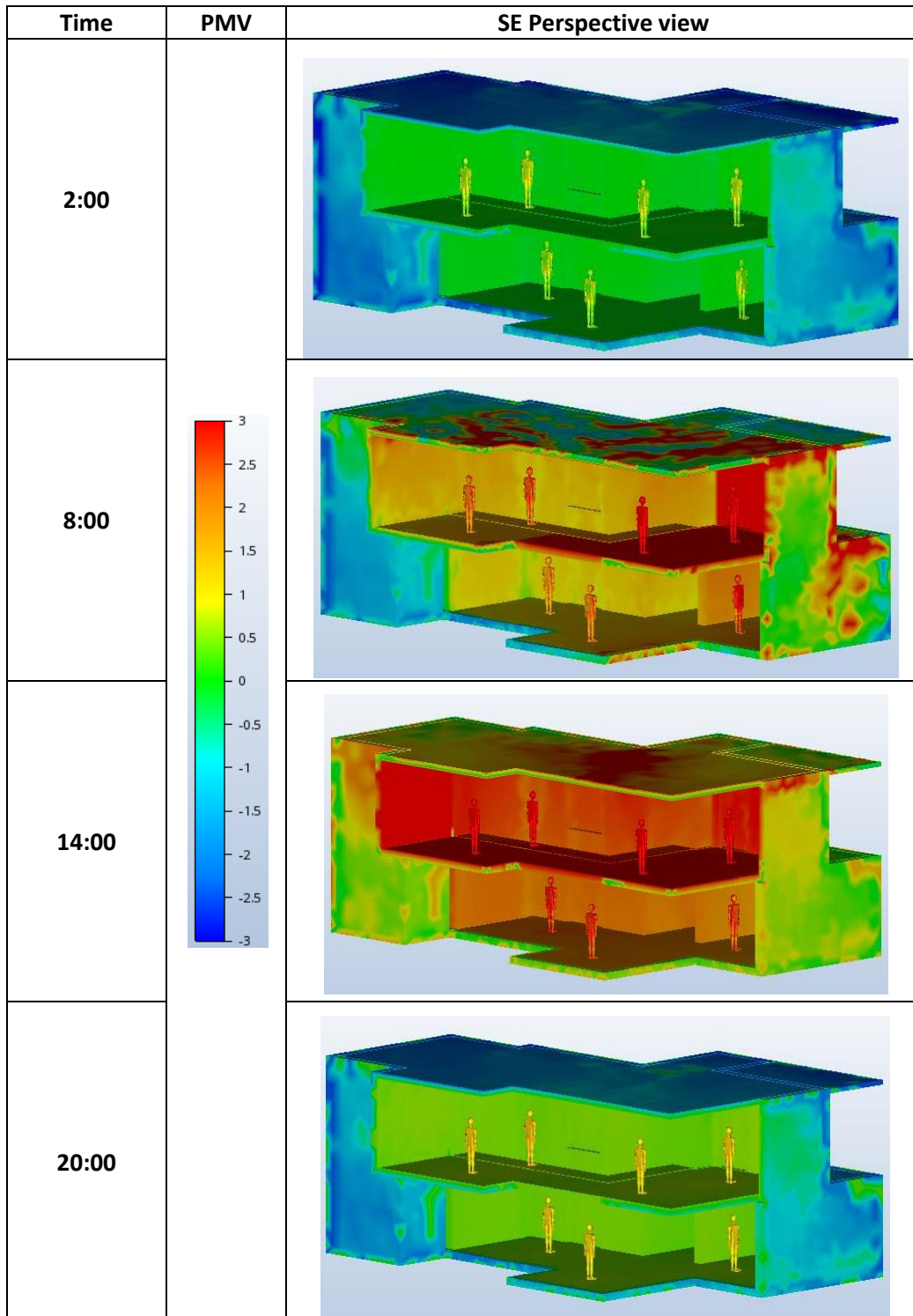


Figure 5.1 PMV results for the four examined hours of the day

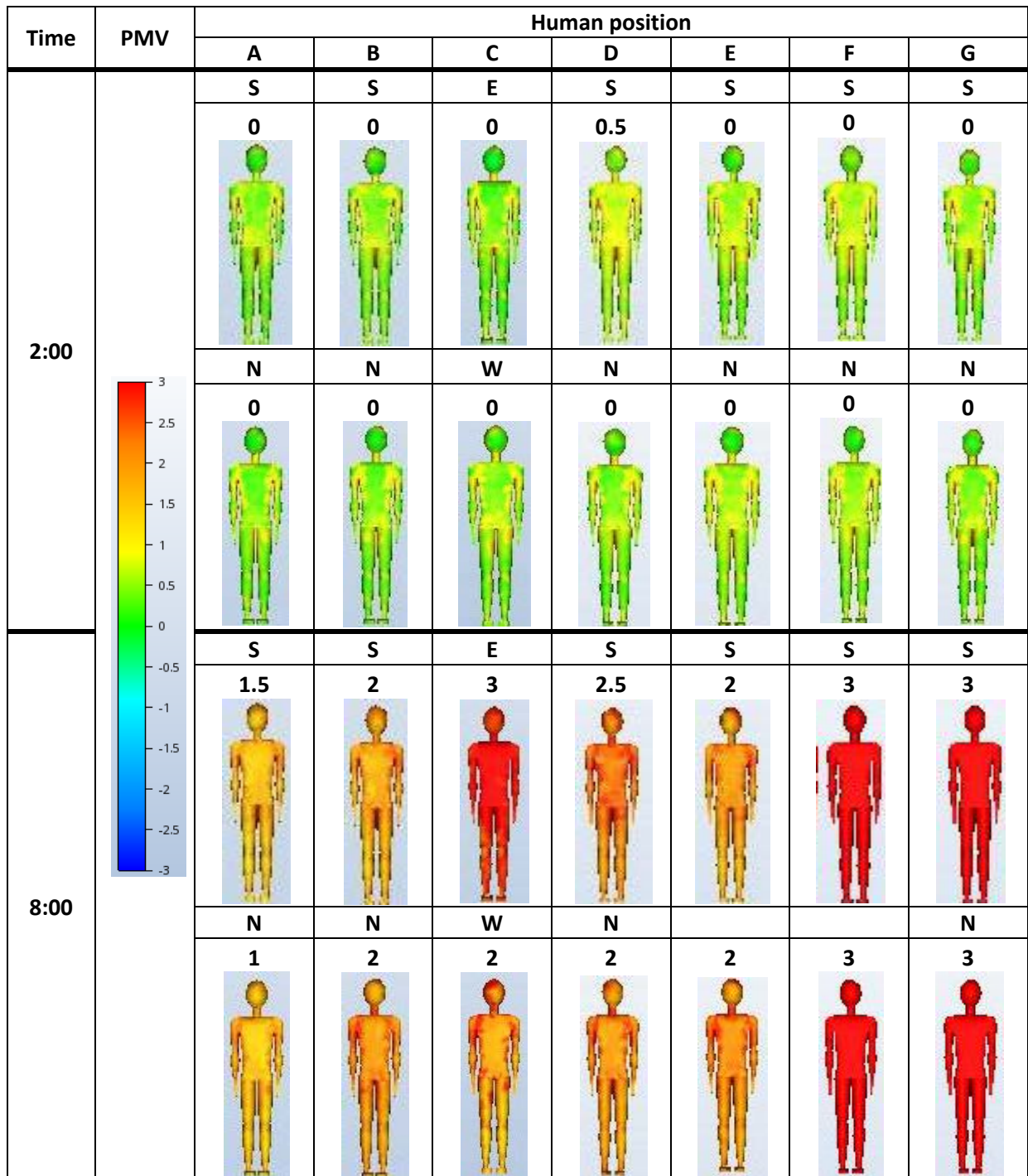


Figure 5.2 Detailed PMV results of the Avatars inside the building (A-G: position, S-E-N-W: orientation)

From the thermal comfort results, PMV values appear on the body of the Avatars. In this study the PMV value on the heads of the Avatars is measured but not without leaving uncommented the thermal comfort levels on the rest of the body.

At 2:00 o'clock (Figure 5.2) the PMV of all the Avatars is located inside the comfort zone. In the case of 8:00 o'clock we observe that the eastern side of the body of Avatar C has higher values, probably because of its position and the incoming sunlight the examined hour. The PMV values of all the Avatars are recorded in the warm and hot zone.

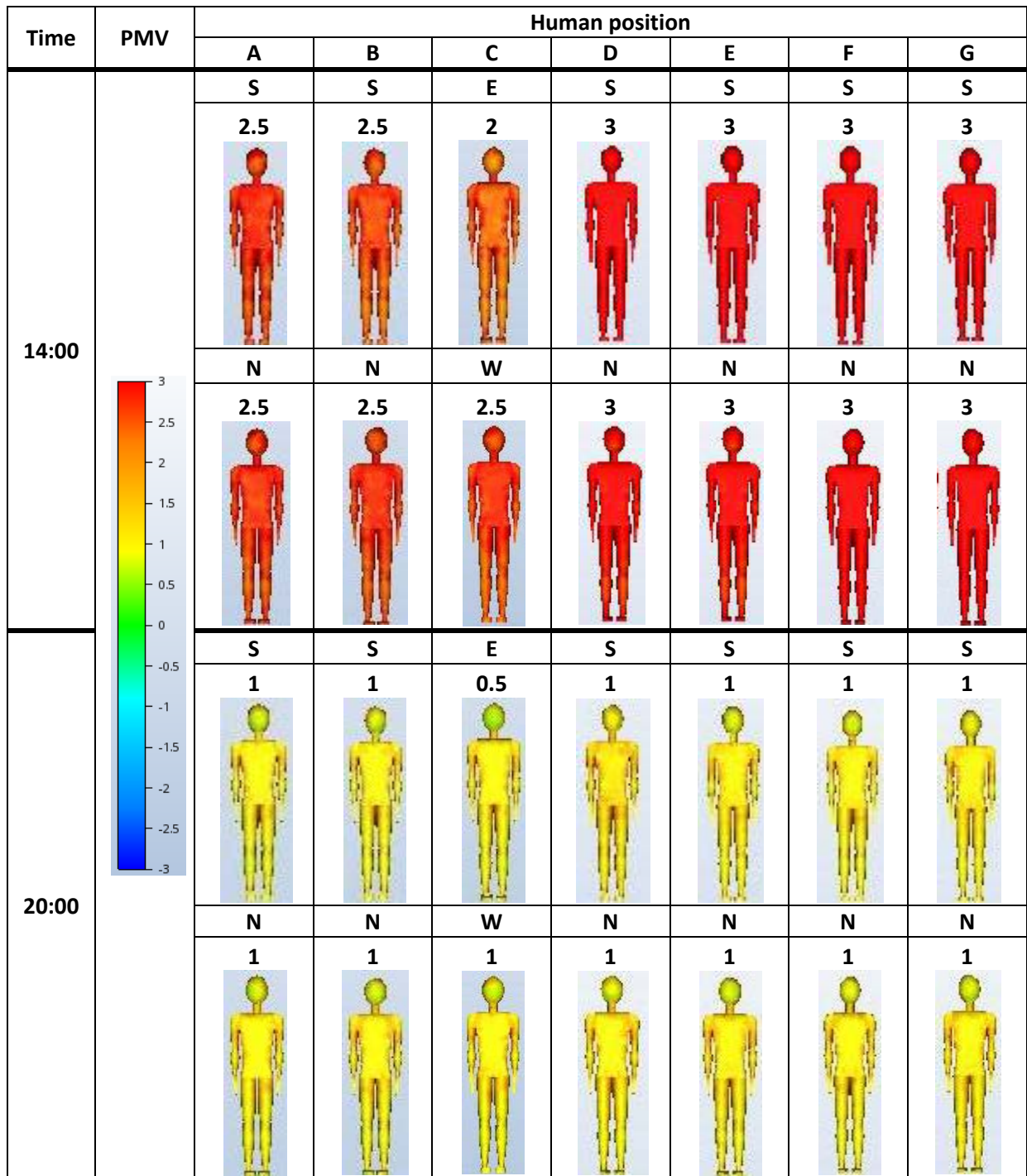


Figure 5.3 Detailed PMV results of the Avatars inside the building (A-G: position, S-E-N-W: orientation)

At 14:00 o'clock (Figure 5.3) the PMV of all the Avatars is located in the hot zone and in the last case (20:00 o'clock) all the values are in the warm zone.

5.2. Scenario 1: openings in the living room and dining room

Figure 5.4 presents the airflow movement of Scenario 1 where the northern glass door (inlet) of the living room and the window (outlet) of the dining room are open. The air is moving with low speed inside the building but gets higher when reaches the outlet opening. The airflow does not appear in the kitchen area but we observe movement in all the height of the two-storey open space of the living room. This is probably caused by the geometry of the building and the stack effect, where the different pressures that exist that moment inside and around the building make the air move upwards and in other areas.

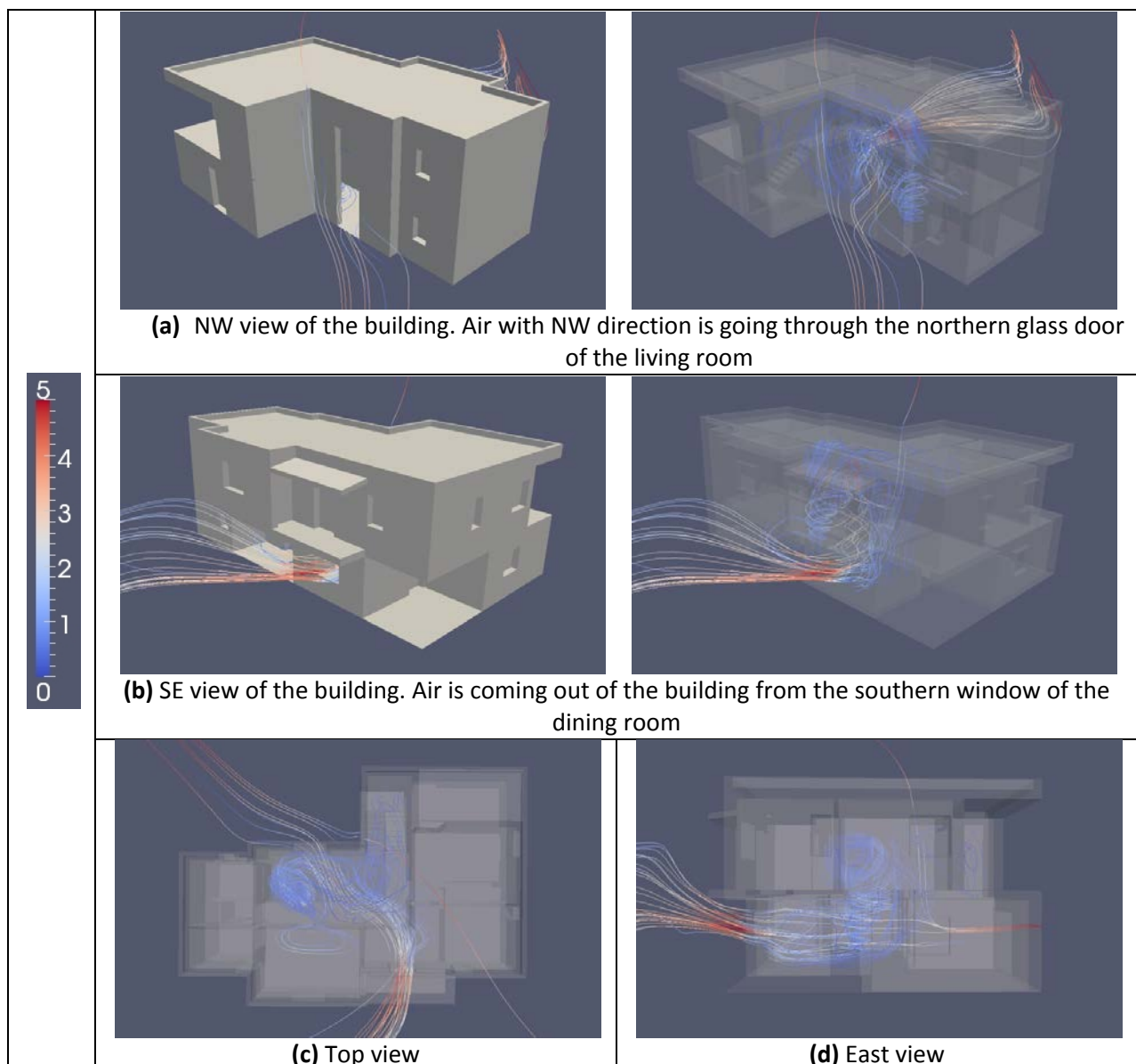


Figure 5.4 Airflow movement inside the building

Figure 5.5 shows the measurement planes a (inlet) and b (outlet). From the planes we confirm that air is moving in the two-storey space of the living room and that the wind speed is higher closer to

the openings. For the cases of 2:00 and 8:00 o'clock the maximum speed is recorded around 1m/s and for the 14:00 and 20:00 o'clock around 3m/s.

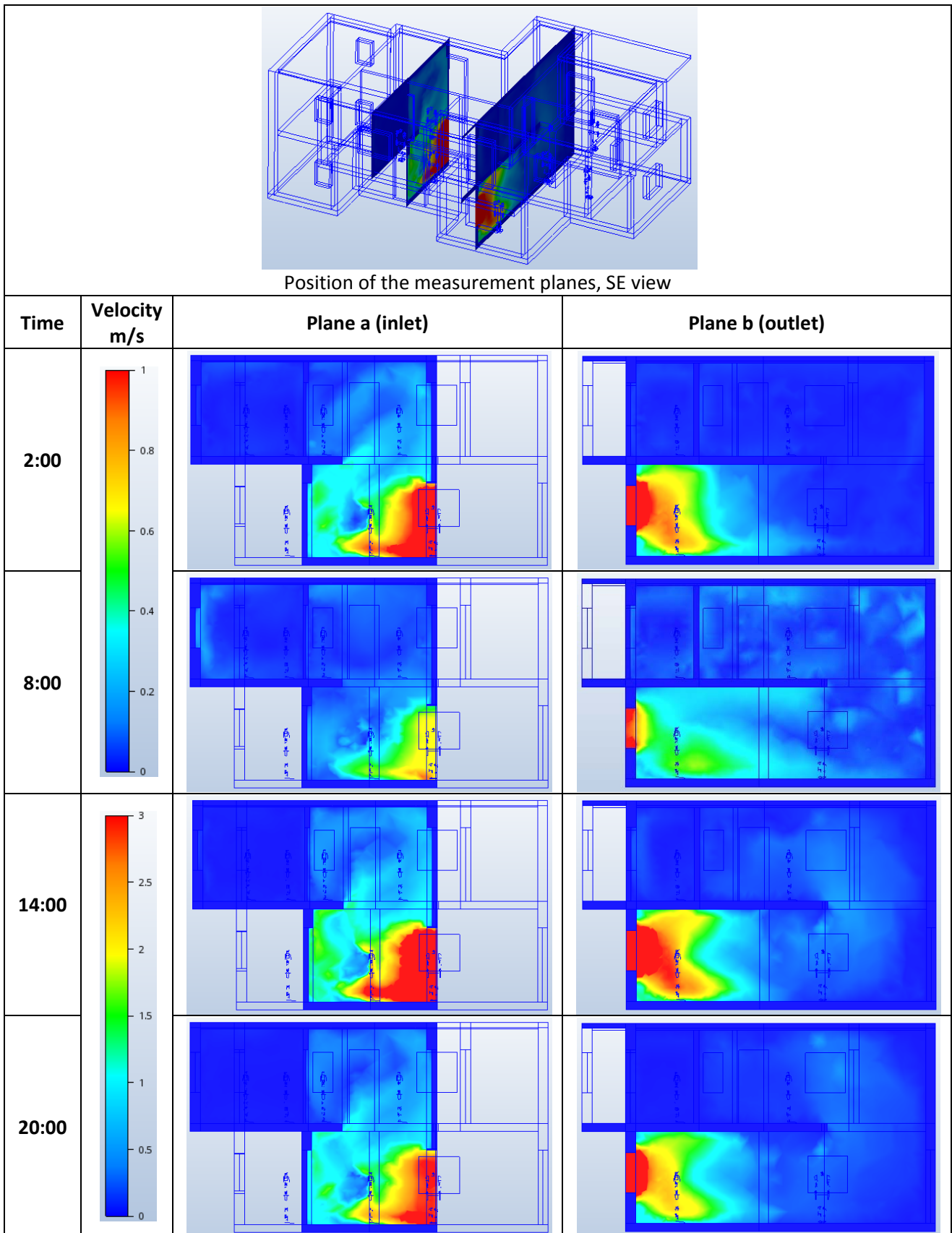


Figure 5.5 Velocity results for the four examined hours of the day

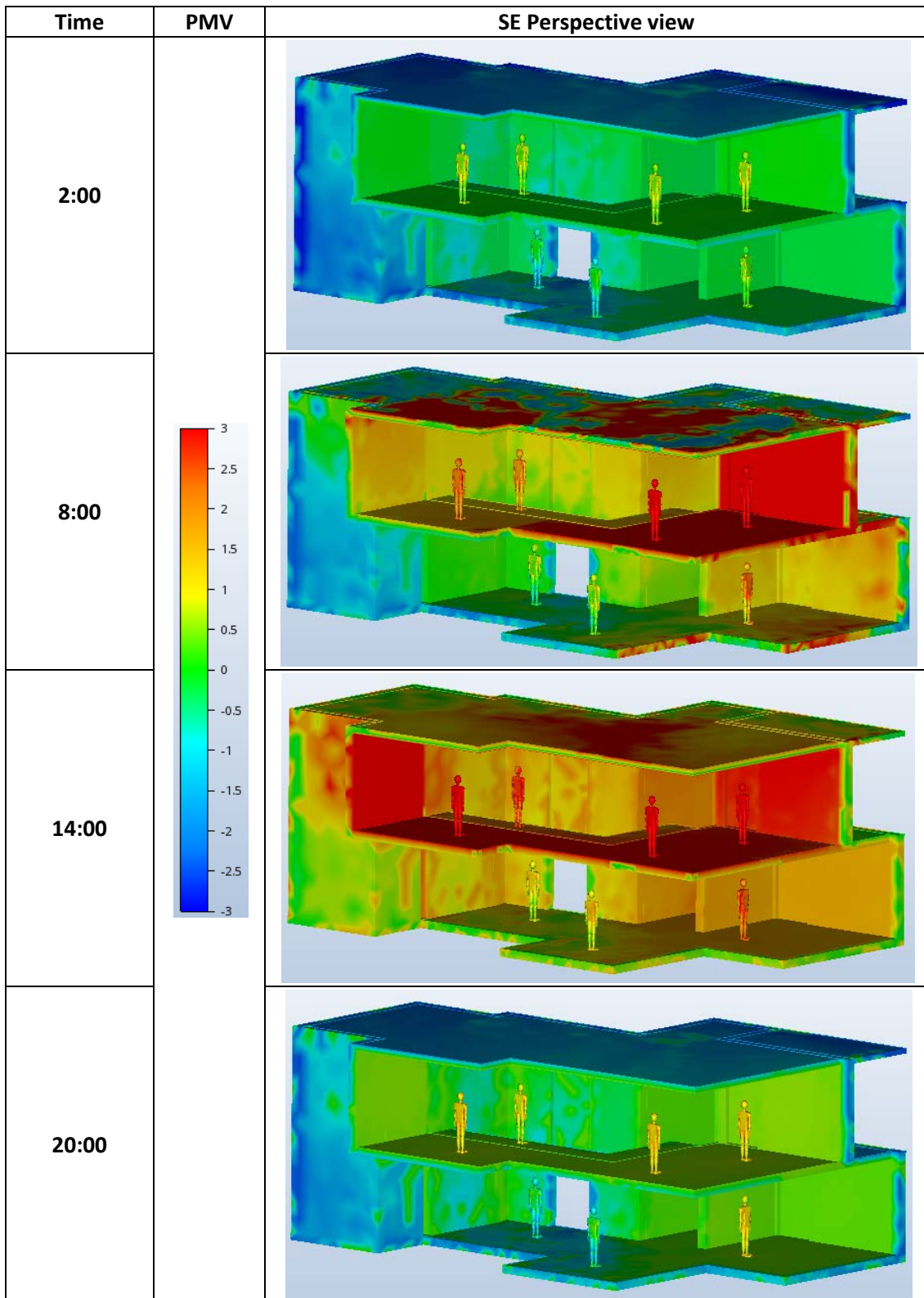


Figure 5.6 PMV results for the four examined hours of the day

PMV results for the different hours of the day

From **Figure 5.6** we observe that the thermal comfort levels of the Avatars (A&B) that are in the direct path of the wind, going in and out of the building, are lower than the others.

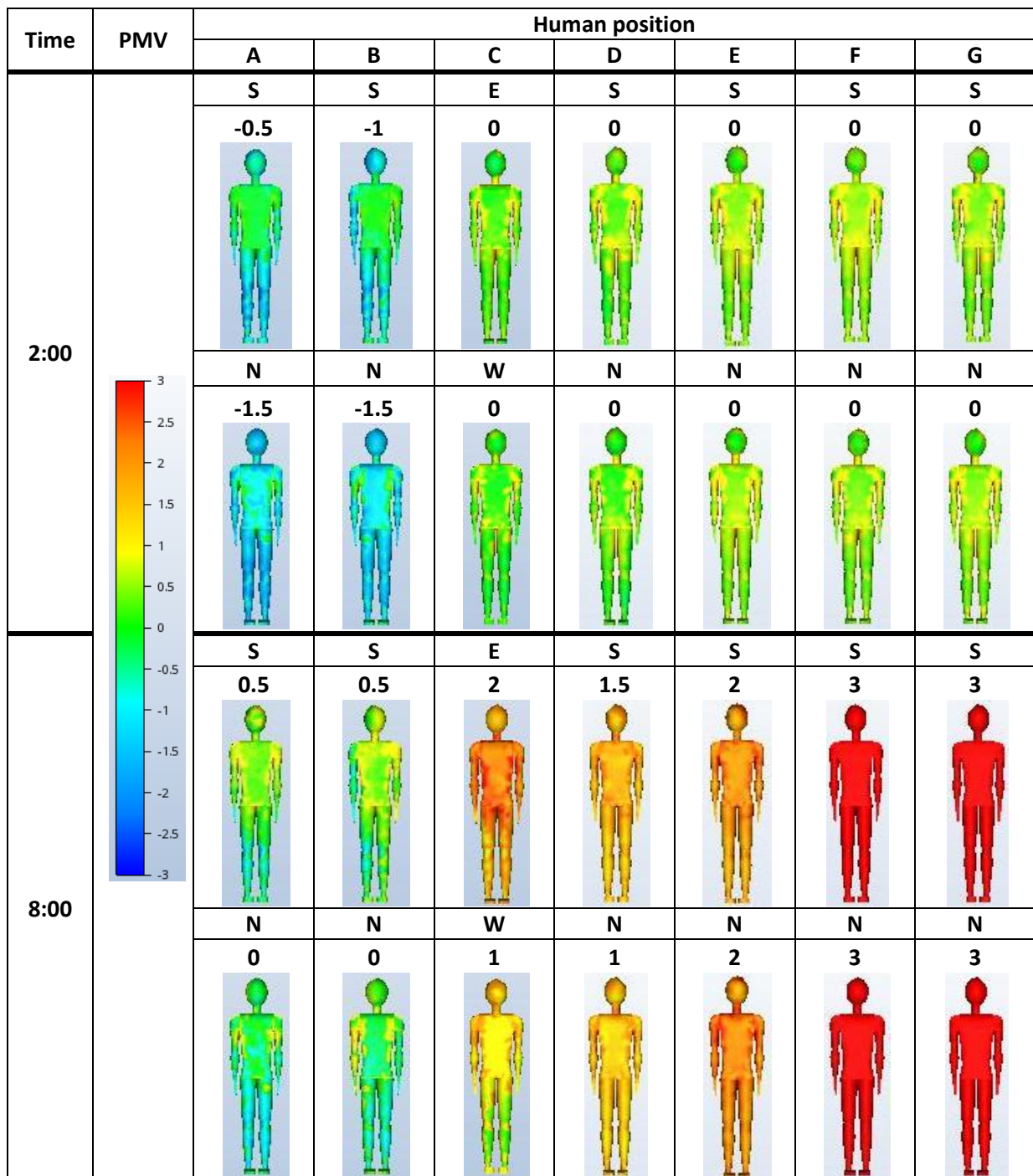


Figure 5.7 Detailed PMV results of the Avatars inside the building (A-G: position, S-E-N-W: orientation)

For the case of 2:00 o'clock (**Figure 5.7**) the Avatars C-G are in the comfort zone with 0 PMV value. Avatar A and B are located in the direct wind path and their PMV has negative values, especially from the side where the air is entering the building, even though the velocity is around 1m/s. In the next case (8:00 o'clock, **Figure 5.7**) Avatars A and B are in the comfort zone (PMV=0.25) but we can see different values on their body, some of 1 on the upper body and -1 on the legs probably because the airflow has higher speed in the leg height. Avatar C presents lower PMV values on its west side which means that the air conditions in the kitchen have been affected although no particular air movement is recorded. The air movement in the two-storey space has affected Avatar D and records lower value on the northern side of its body.

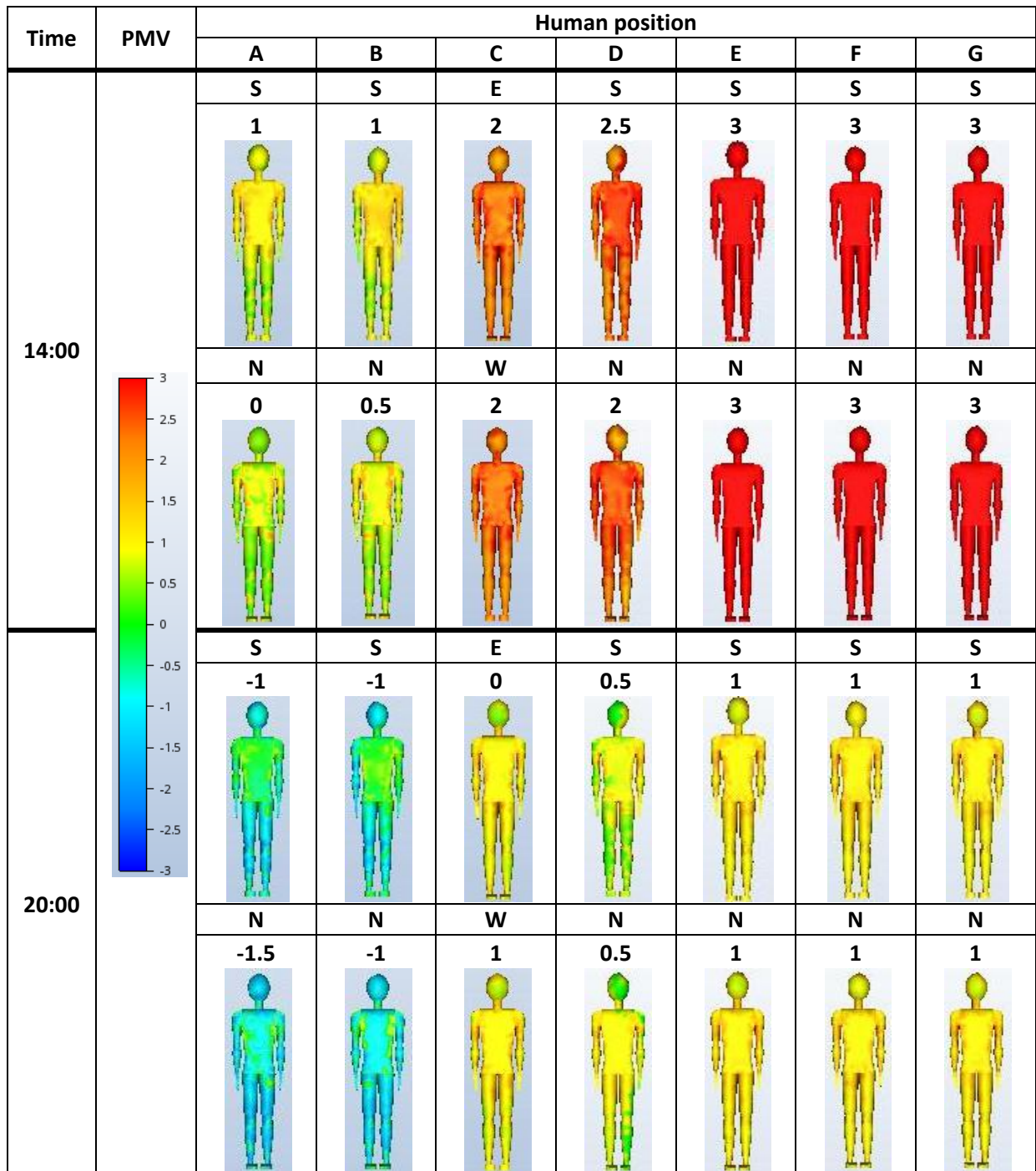


Figure 5.8 Detailed PMV results of the Avatars inside the building (A-G: position, S-E-N-W: orientation)

In the case of 14:00 o'clock (**Figure 5.8**) the Avatars A and B have significantly lower PMV values than Avatars C and D with the A being in the comfort zone and B just outside with a value of 0.75. For the last case (20:00 o'clock, **Figure 5.8**) the Avatars A and B present negative values and are in the cold zone while Avatars C and D are in the comfort zone.

Avatars E, F and G are in spaces that the air cannot reach, therefore they do not record any difference in the PMV values in any case of this Scenario.

5.3. Scenario 2: openings in the living room and kitchen

In Scenario 2 the building with the northern glass door of the living room (inlet) and the eastern kitchen window (outlet) open is simulated. The air is moving with low velocity in the areas of the building but gets higher in the kitchen on the way out. In this Scenario also, there is air movement in the first floor of the open space of the living room and some in the dining area (**Figure 5.9**).

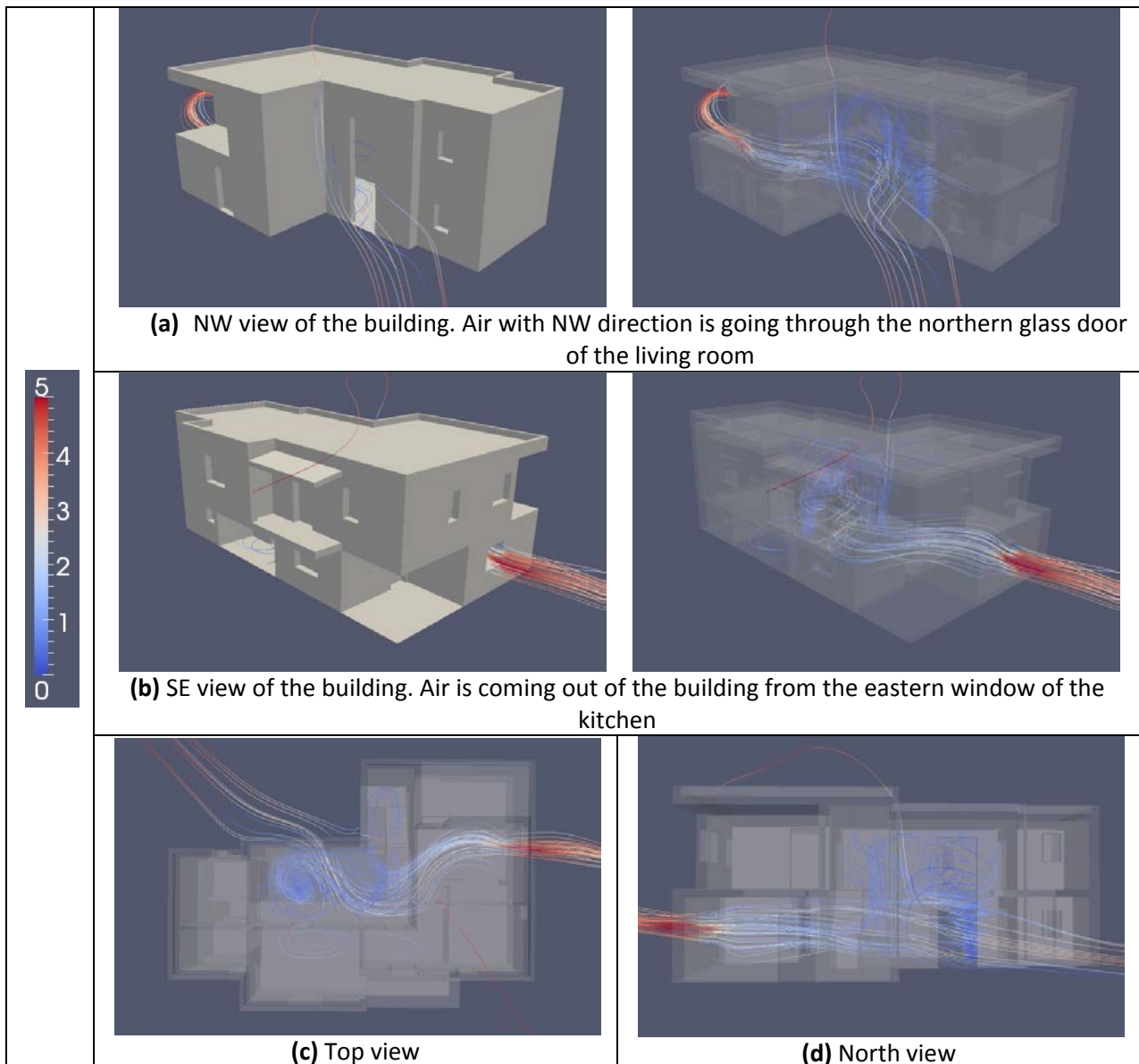
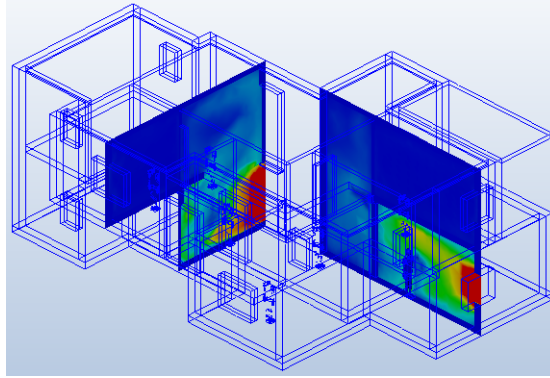


Figure 5.9 Airflow movement inside the building

Figure 5.10 presents the measurement planes a (inlet) and b (outlet). From the planes of the four cases we observe higher air speed in the openings and air movement in the two-storey spaces. For the cases of 2:00 and 8:00 o'clock the maximum speed is around 2m/s and for the 14:00 and 20:00 o'clock around 3m/s.



Position of the measurement planes, SE view

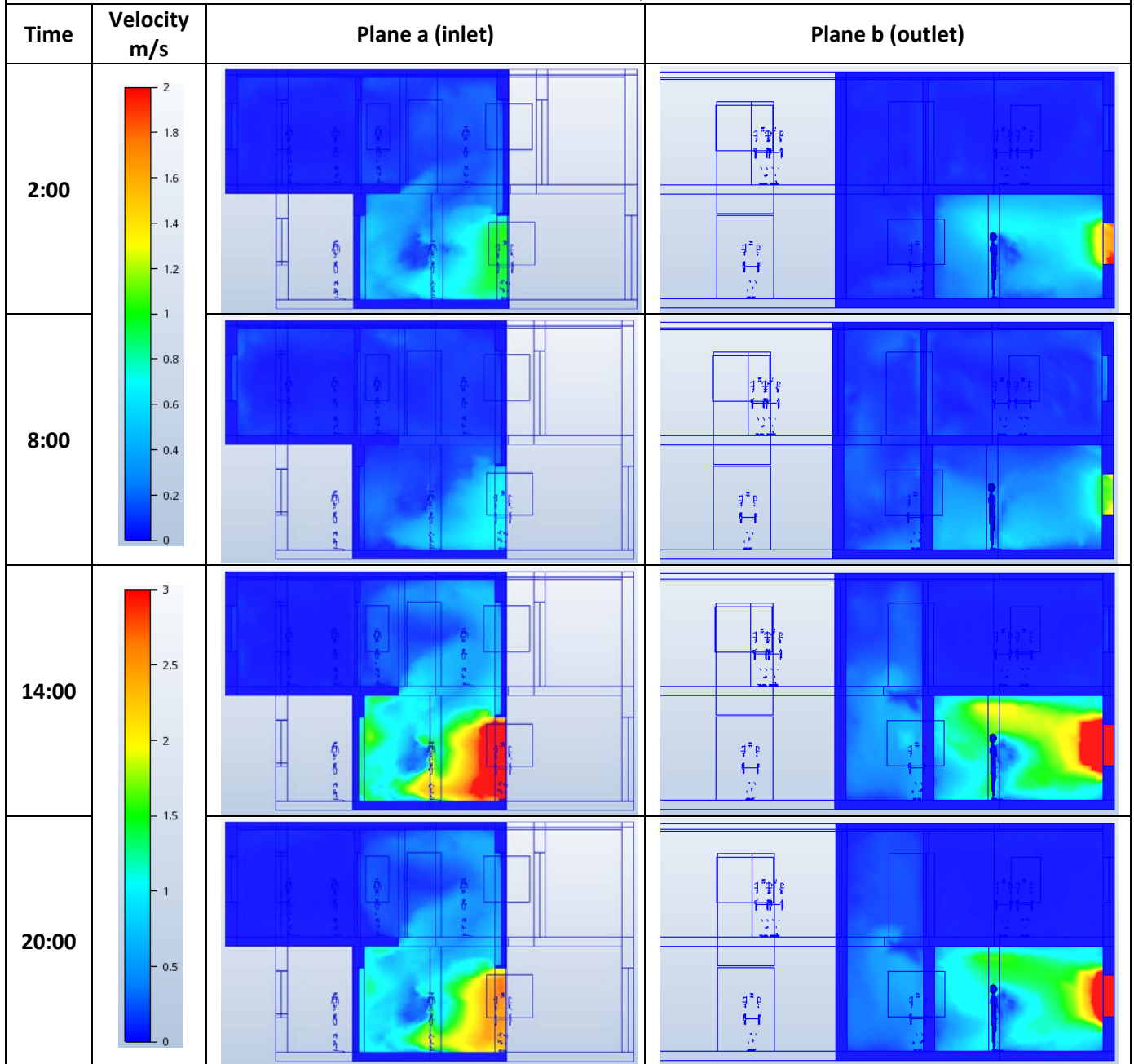


Figure 5.10 Velocity results for the four examined hours of the day

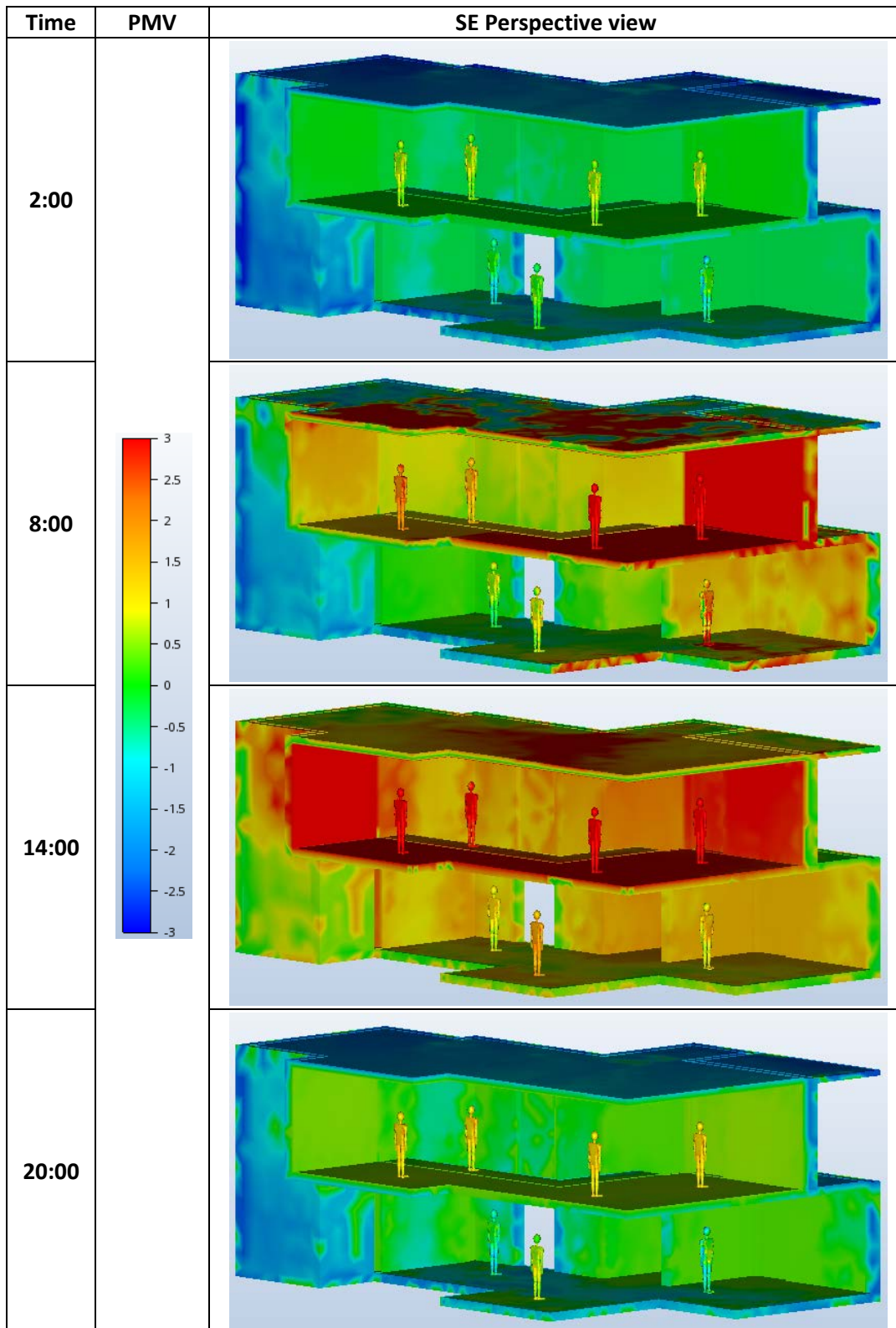


Figure 5.11 PMV results for the four examined hours of the day

From **Figure 5.11** we observe that the thermal comfort levels of the Avatars (A&C) that are in the direct path of the wind, going in and out of the building, are lower than the others but Avatar C has high PMV values on the eastern side of the body in the case of 8:00 o'clock.

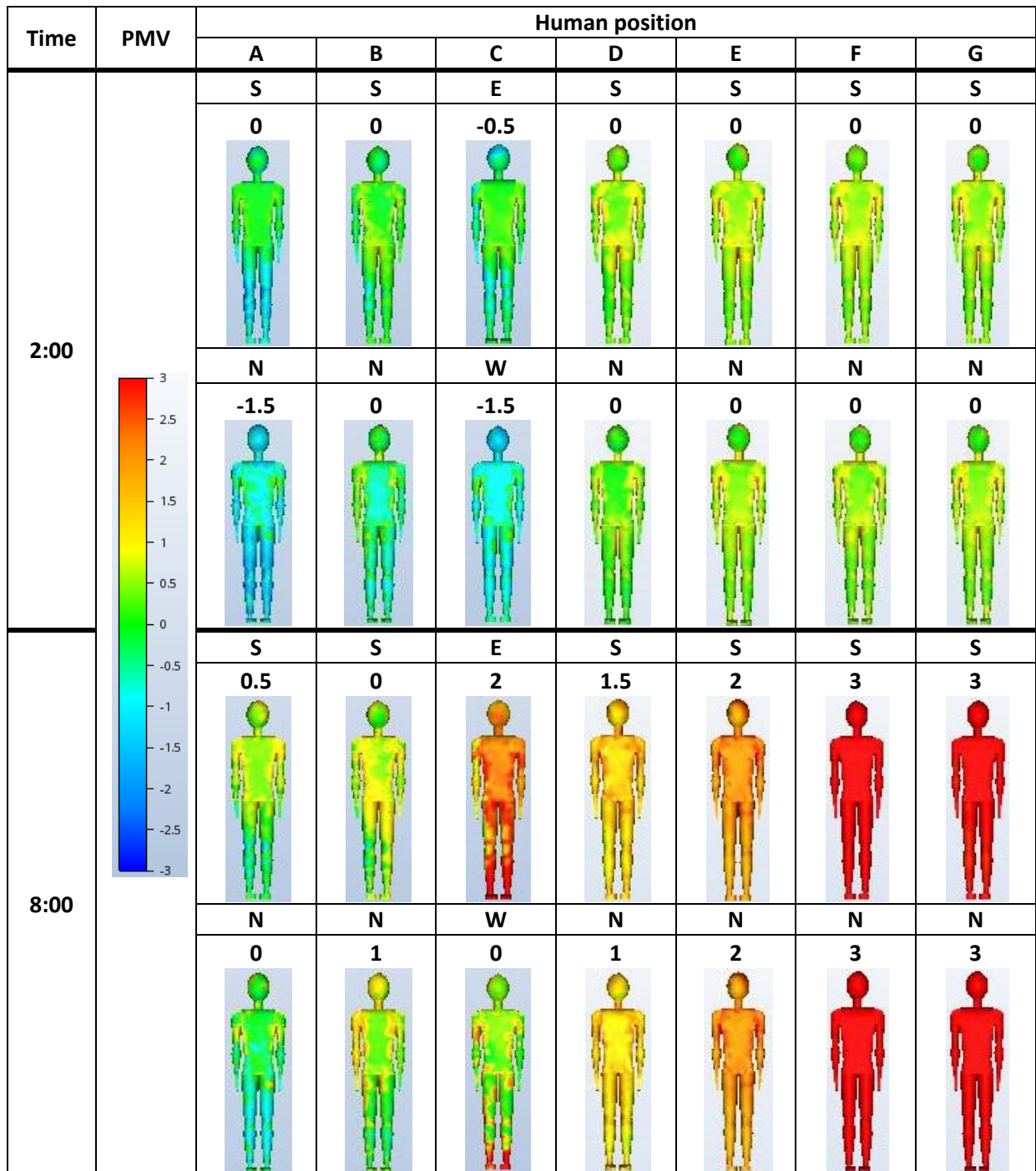


Figure 5.12 Detailed PMV results of the Avatars inside the building (A-G: position, S-E-N-W: orientation)

In the first case (2:00 o'clock, **Figure 5.12**) the PMV values of the Avatars A and C, that are in the direct wind path, are moving in the cold zone, while the other Avatars are in the comfort zone. In the second case (8:00 o'clock, **Figure 5.12**) we observe that the Avatar C has different values on each side of the body. On the east side where there is direct sunlight at that time, the value is 2 and on the west side where the wind is coming from, the value is 0. On the west side we also observe that there is higher PMV value on the feet, which could be caused from lack or very low air movement. Avatar A and B are in the comfort zone with the first one presenting negative values (cold zone) on the legs. Avatar D has lower value on the northern side of the body where the air is moving.

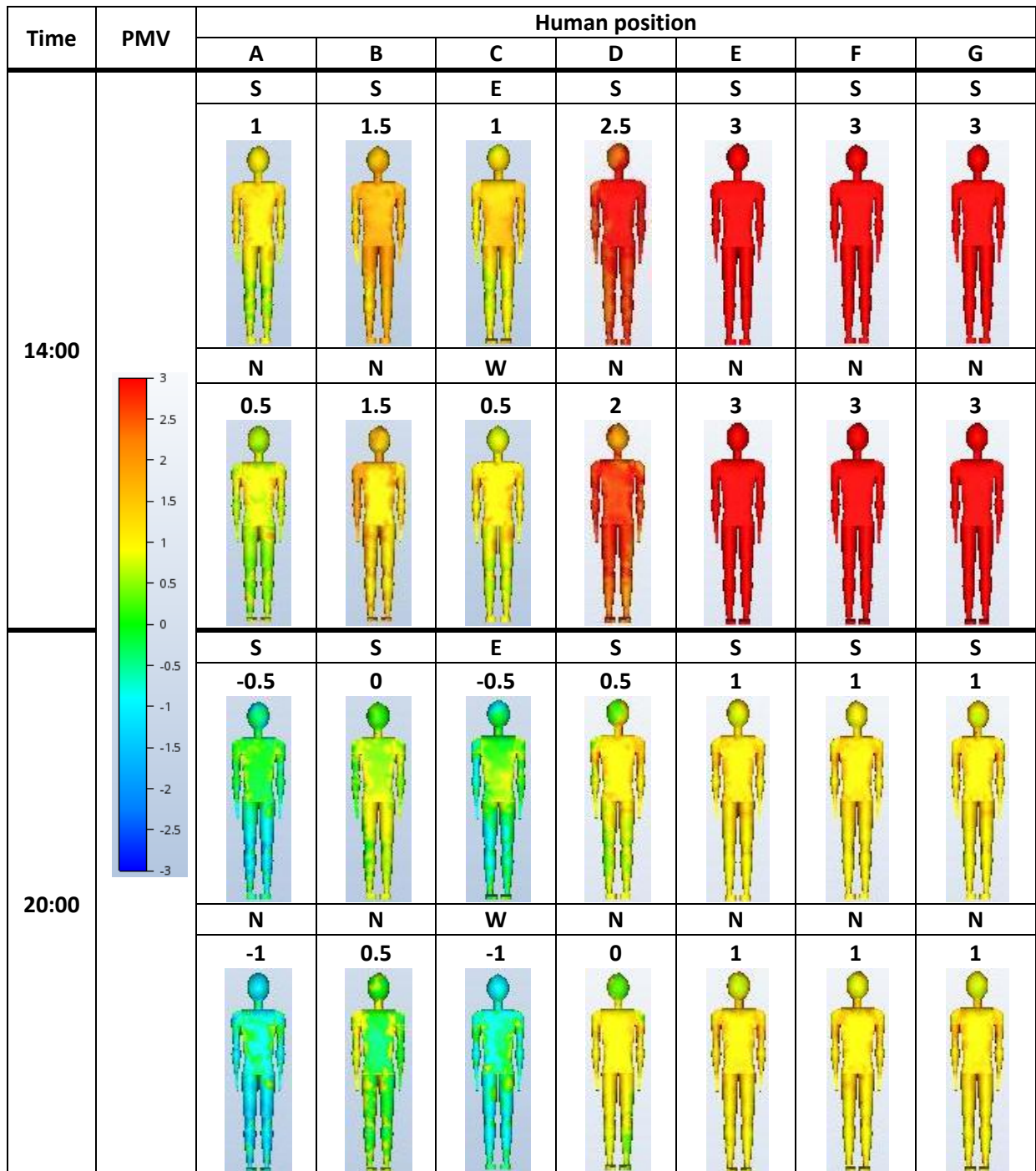


Figure 5.13 Detailed PMV results of the Avatars inside the building (A-G: position, S-E-N-W: orientation)

In the 14:00 o'clock case (Figure 5.13) the Avatars A and C recorded the lowest PMV values (0.75) and the Avatar B is following with value of 1.5. At 20:00 o'clock (Figure 5.13) the Avatars A and C are moving just outside of the comfort zone with value of -0.75.

In all the cases of this Scenario, the low airflow that appears in the dining area is able to reduce the high PMV values of Avatar B or keep it in the comfort zone. Avatars E, F and G are in spaces that the air cannot reach, therefore they do not record any difference in the PMV values in any case of this Scenario.

5.4. Scenario 3: openings in the kitchen and living room

In this Scenario the tested openings are the northern kitchen glass door (inlet) and the southern glass door of the living room (outlet). The air is going through the kitchen and living room with high speed and creates some vorticity in the dining room and the first floor of the open space in the living room (Figure 5.14).

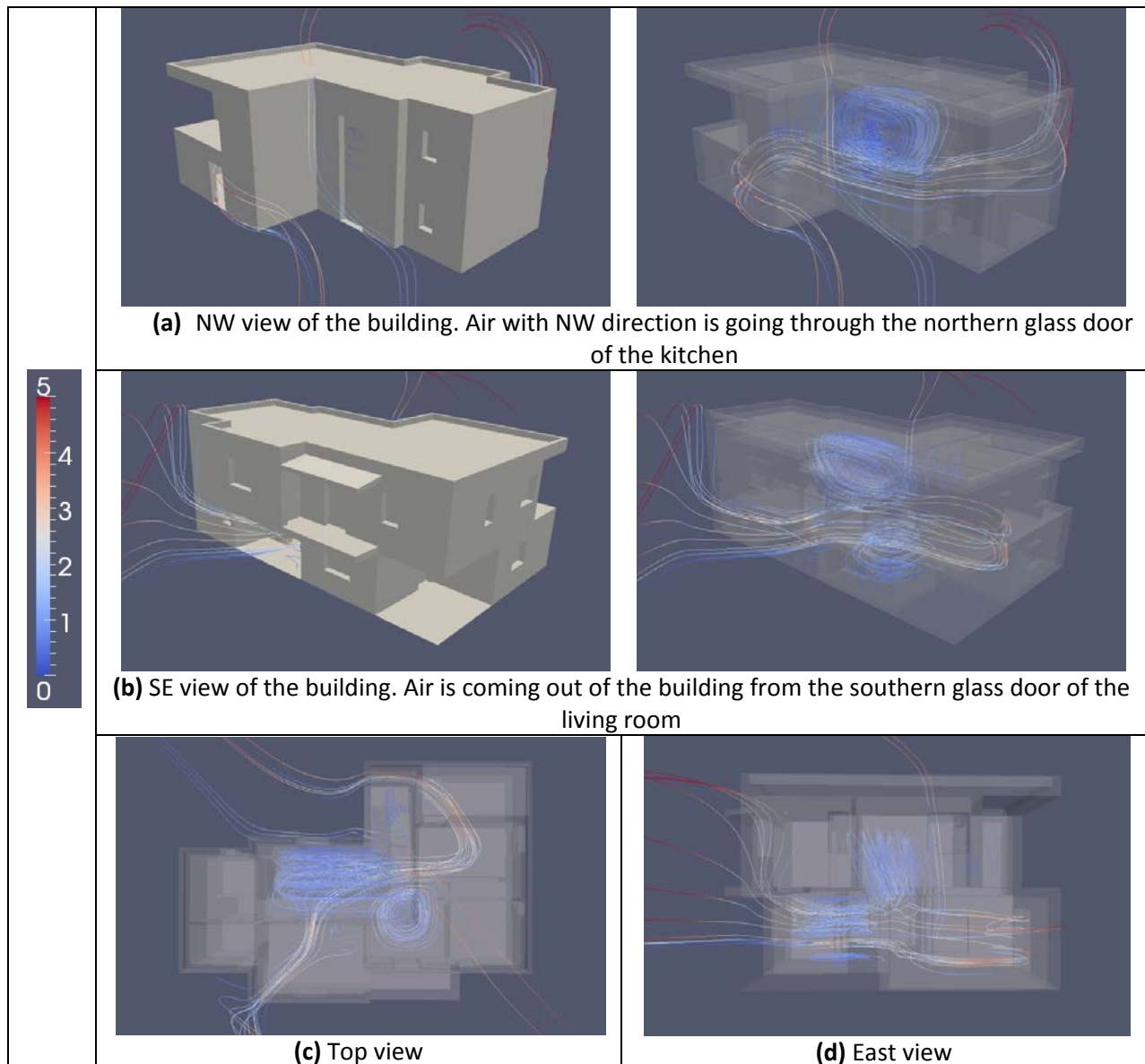
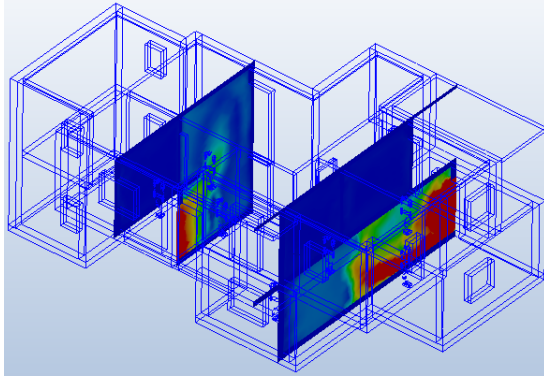


Figure 5.14 Airflow movement inside the building

Figure 5.15 shows of the measurement planes a (inlet) and b (outlet). In all the cases we observe higher air speed in the openings and in the kitchen area where the wind is coming through. In the two last cases the air movement in the first floor of the open space in the living room is more clear and the speed is recorded around 1m/s. For the cases of 2:00 and 8:00 o'clock the maximum speed is around 2m/s and for the 14:00 and 20:00 o'clock around 3m/s.



Position of the measurement planes, SE view

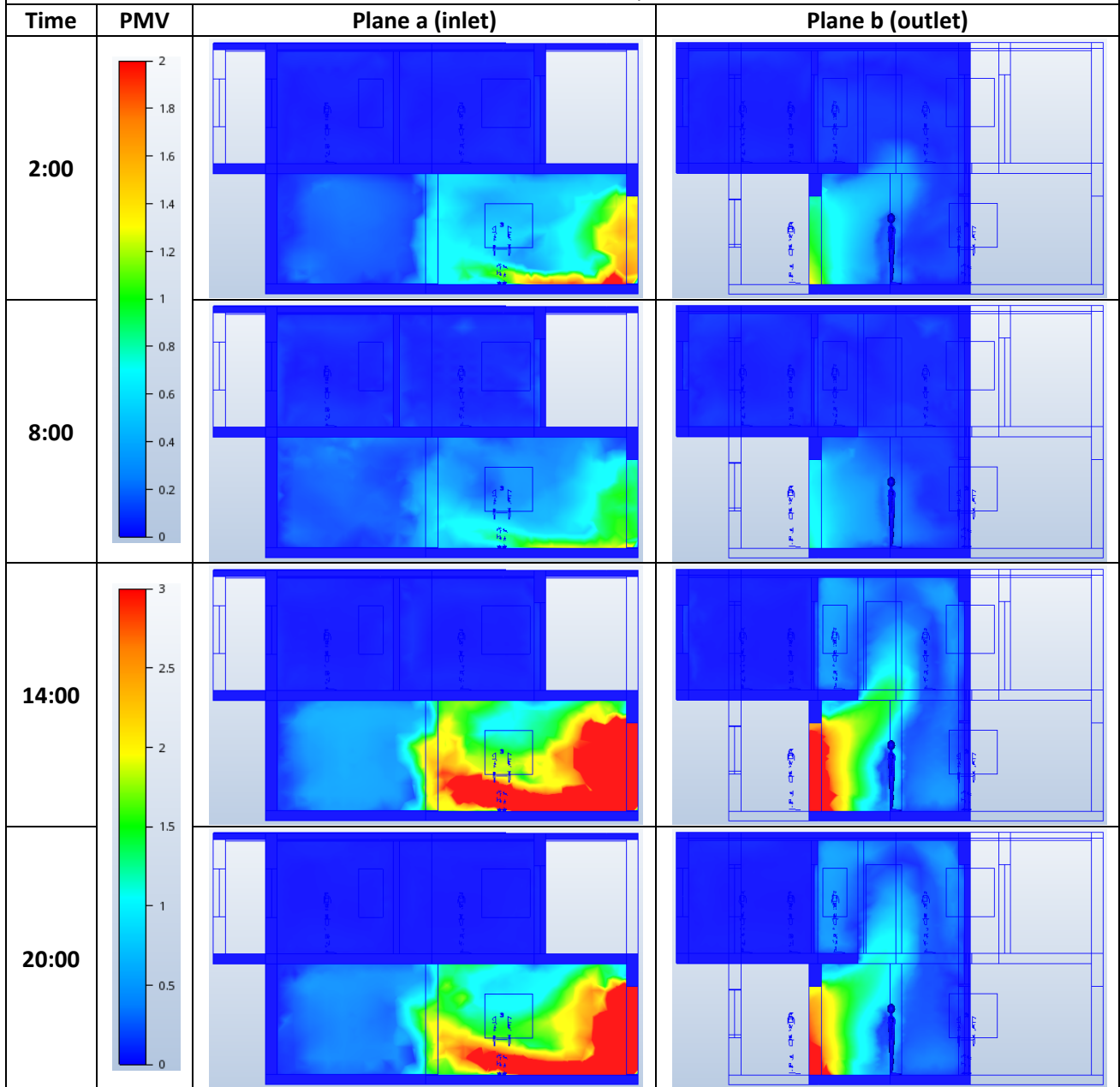


Figure 5.15 Velocity results for the four examined hours of the day

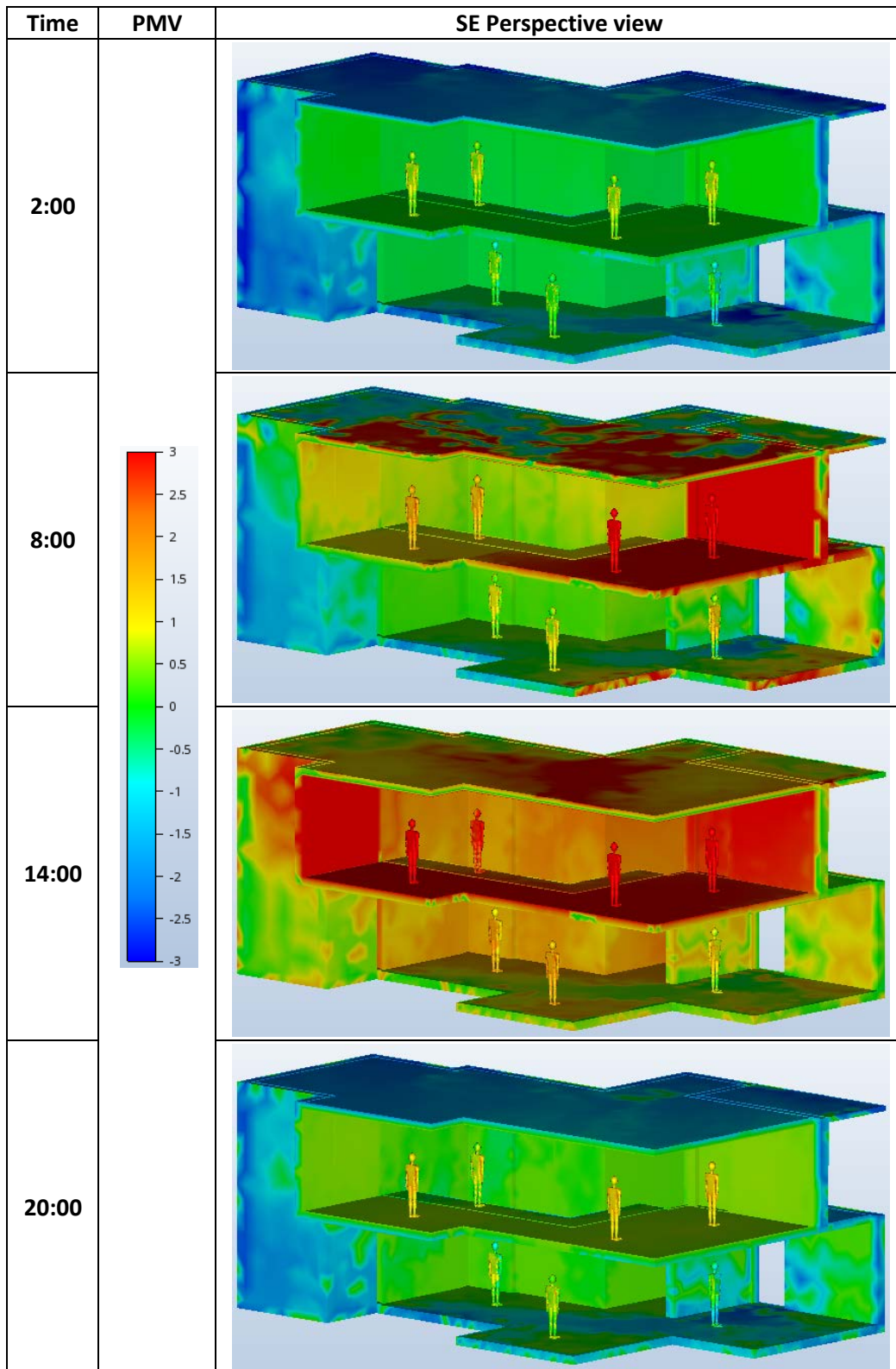


Figure 5.16 PMV results for the four examined hours of the day

From the perspective view in **Figure 5.16** the Avatar C seems to be more affected from the airflow that is created from the selected openings.

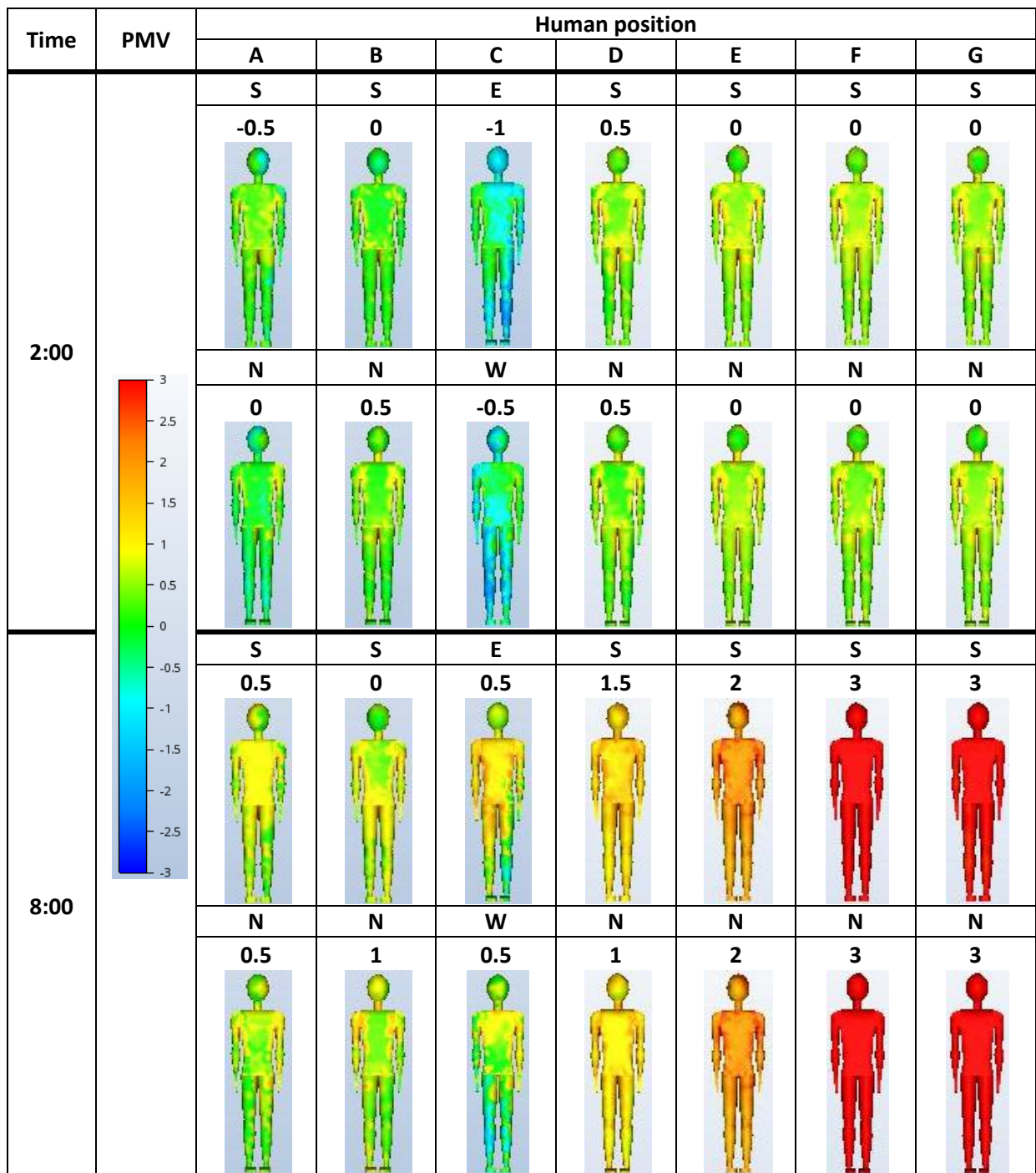


Figure 5.17 Detailed PMV results of the Avatars inside the building (A-G: position, S-E-N-W: orientation)

In the first case (2 o'clock, **Figure 5.17**) the PMV of Avatar C is moving just outside of the comfort zone (-0.75) while in the other Avatars is inside the comfort zone. In the next case (8 o'clock, **Figure 5.17**), Avatar C presents a value of 0.5 (inside the comfort zone range) but we notice negative values on the legs, especially on the west side because of its location regarding the open glass door. Avatar D is slightly affected on the northern side of the body by the low airflow movement in the first floor level of the open space. The PMV of the Avatars A and B is moving inside the comfort zone with value of 0.5.

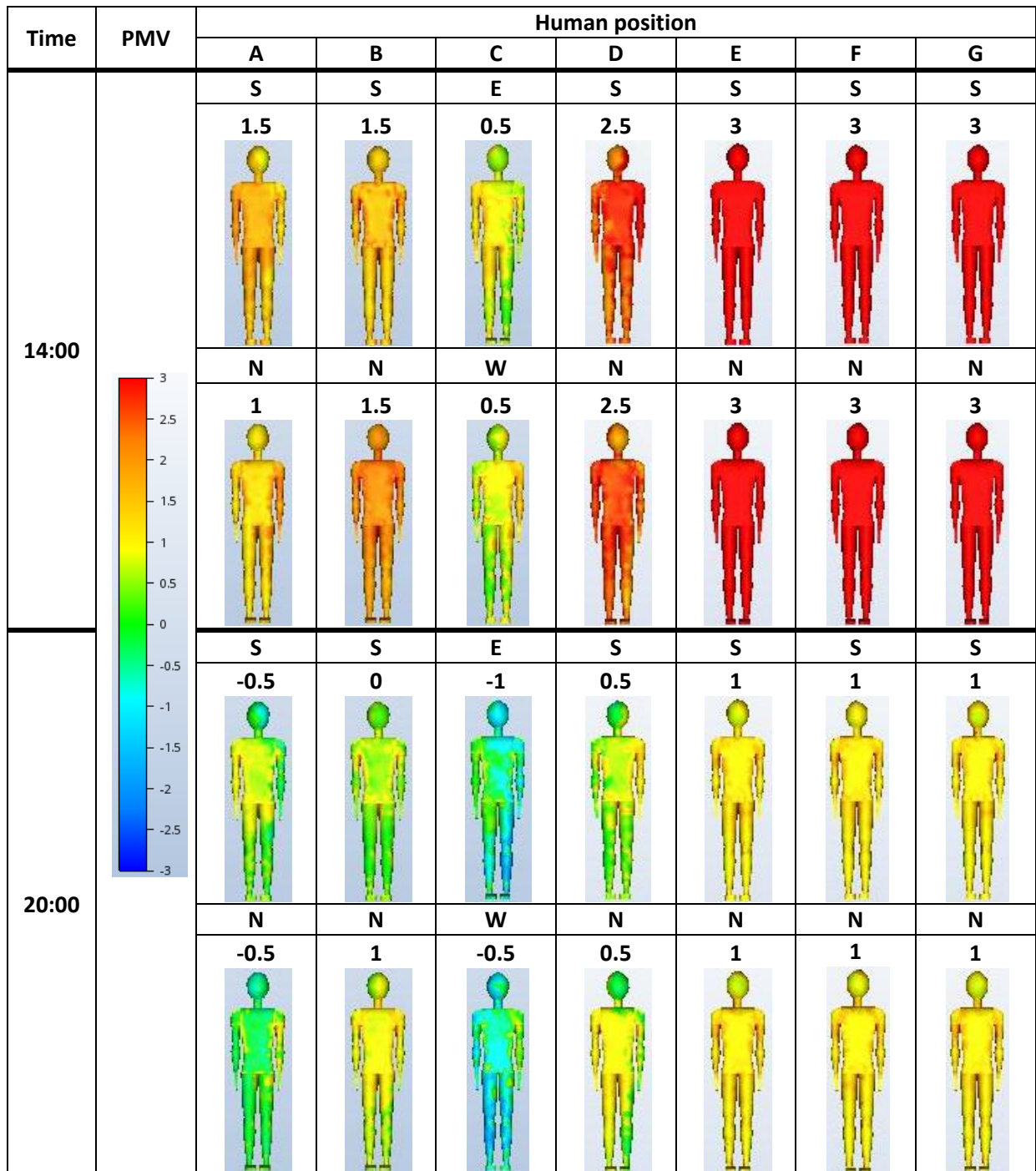


Figure 5.18 Detailed PMV results of the Avatars inside the building (A-G: position, S-E-N-W: orientation)

Avatar C, in the case of 14:00 o'clock (Figure 5.18), because of its position and the created airflow, has a significantly drop in the PMV values that fall in the comfort zone. For the Avatars A and B on the other hand, the air movement is not enough for them to reach comfort conditions. In the last case (Figure 5.18), the PMV of Avatar C is moving in the cold zone with a value of -0.75 and of Avatars A, B and D inside the comfort zone.

Avatars E, F and G are in spaces that the air cannot reach, therefore they do not record any difference in the PMV values in any case of this Scenario.

5.5. Scenario 4: openings in the living room and bedroom

In Scenario 4 the northern glass door of the living room (inlet) and the southern window of bedroom 1 (outlet) are open. The air is moving mostly in the living room, less in the dining room and kitchen, and goes outside through the bedroom with high speed without staying in the space (Figure 5.19).

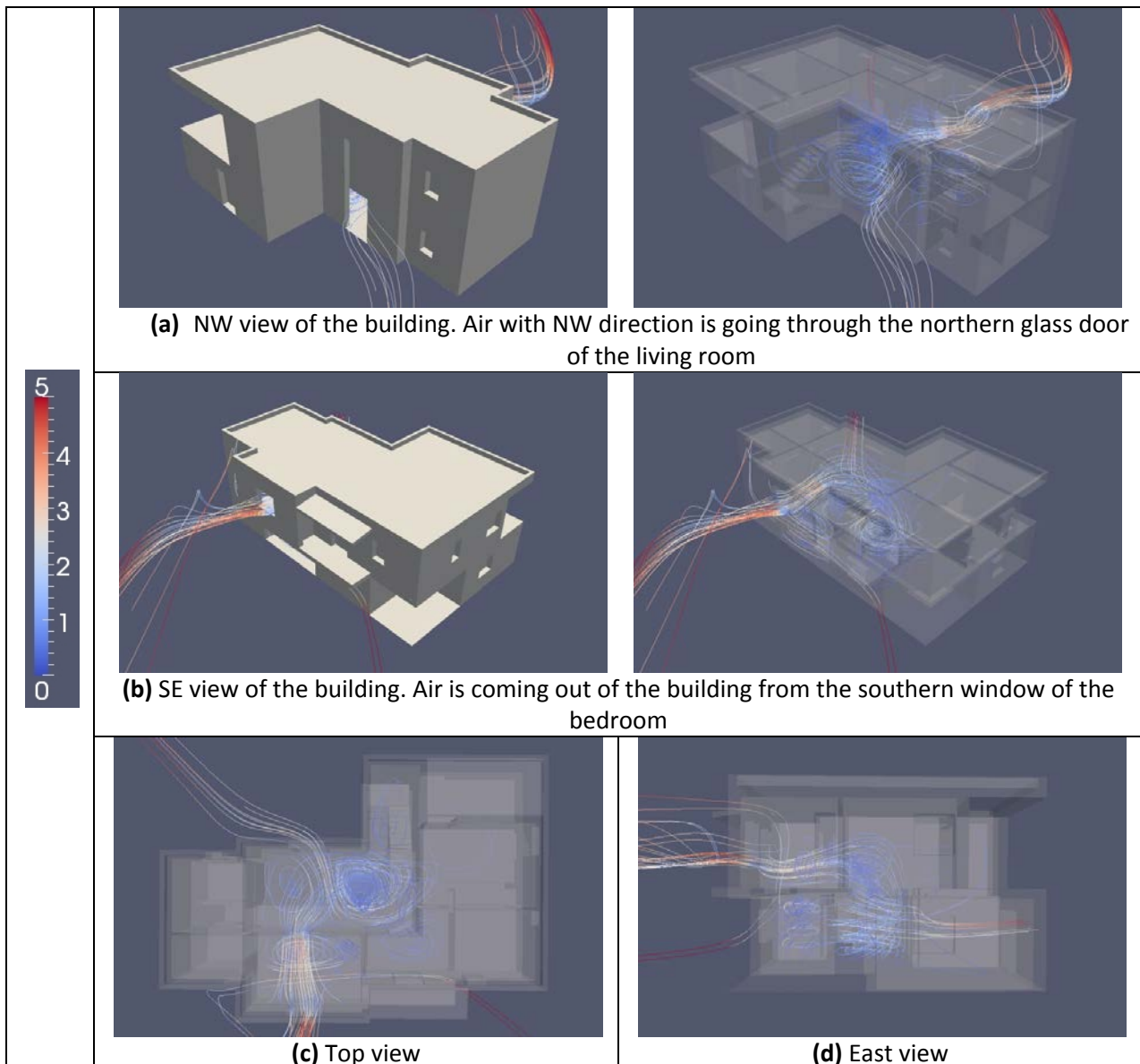
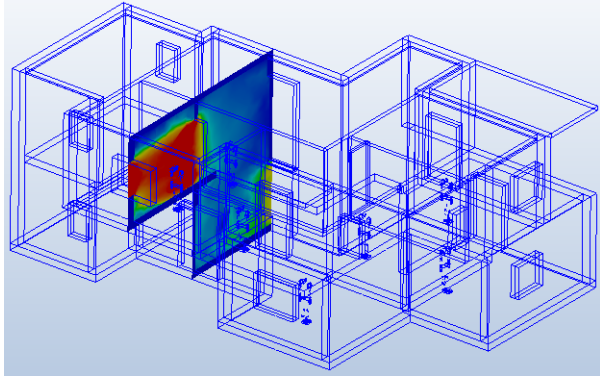


Figure 5.19 Airflow movement inside the building

The measurement plane a (inlet and outlet) is shown in the Figure 5.20 below. In all the cases higher air speed is recorded in the bedroom 1 and then at the glass door from where the wind is entering the building. For the cases of 2:00 and 8:00 o'clock the maximum speed is recorded around 1m/s and for the 14:00 and 20:00 o'clock around 5m/s.



Position of the measurement plane, SE view

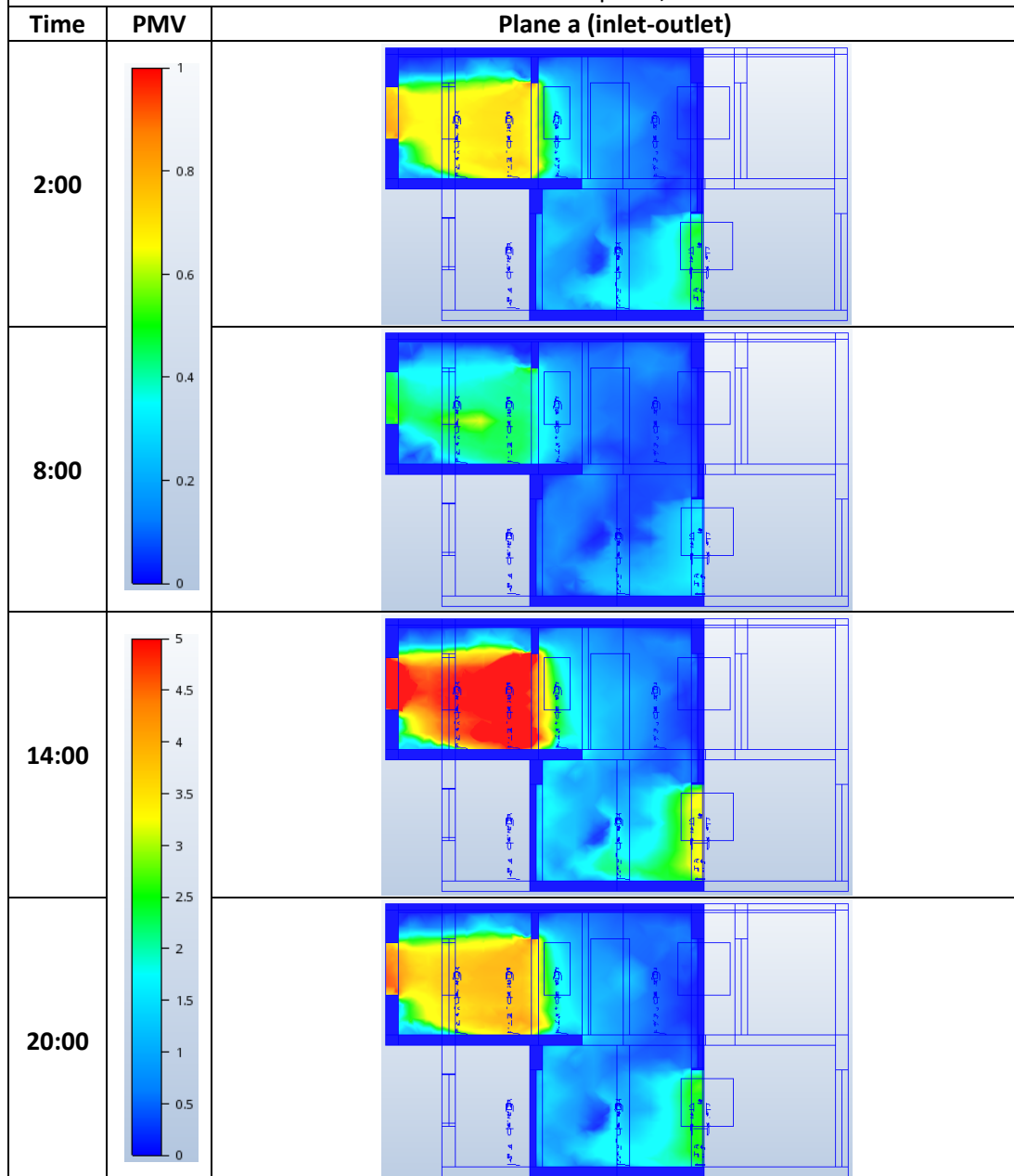


Figure 5.20 Velocity results for the four examined hours of the day

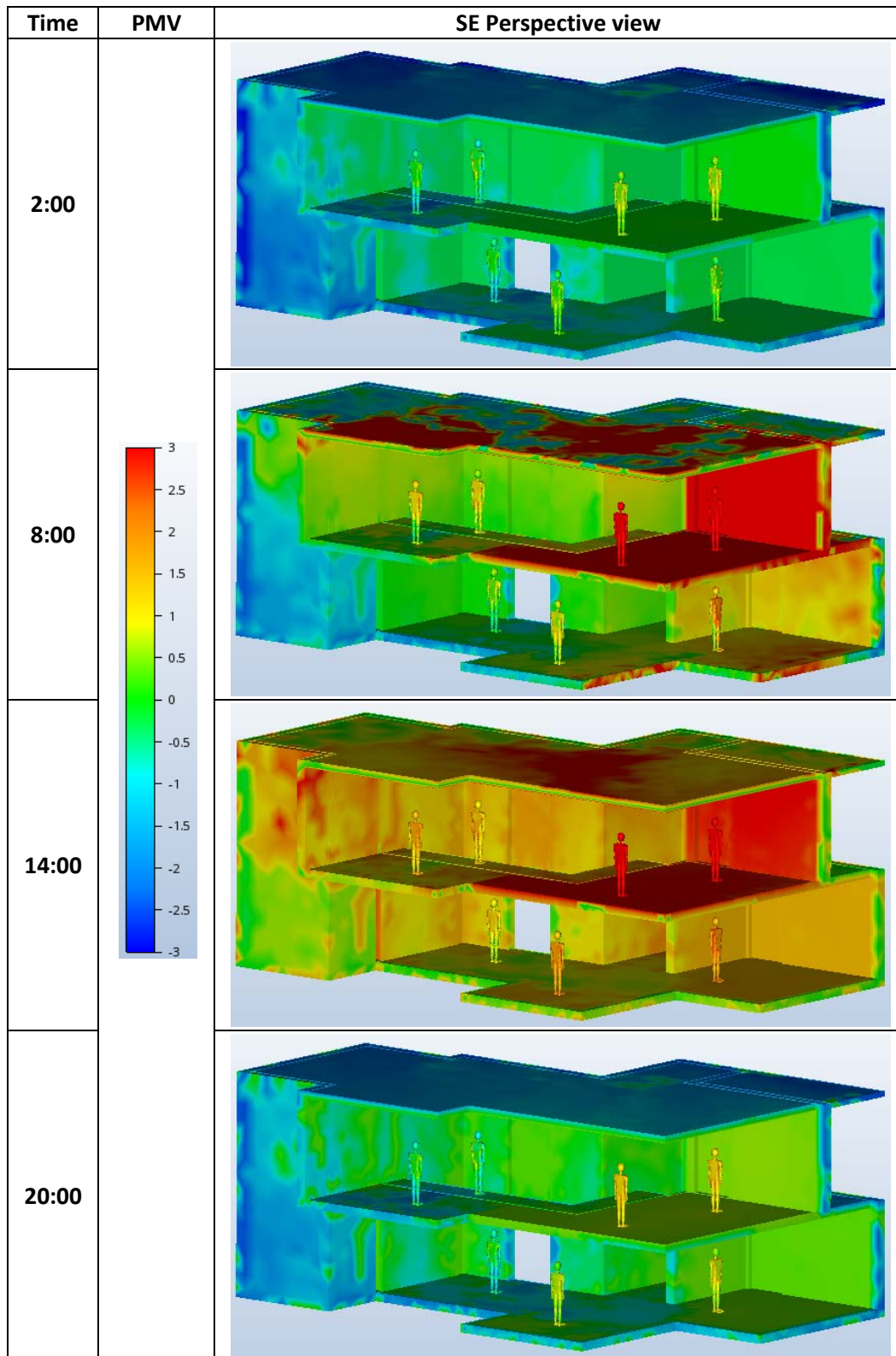


Figure 5.21 PMV results for the four examined hours of the day

From the perspective view (Figure 5.21) we notice that Avatars A, D and E are mostly affected from the created airflow.

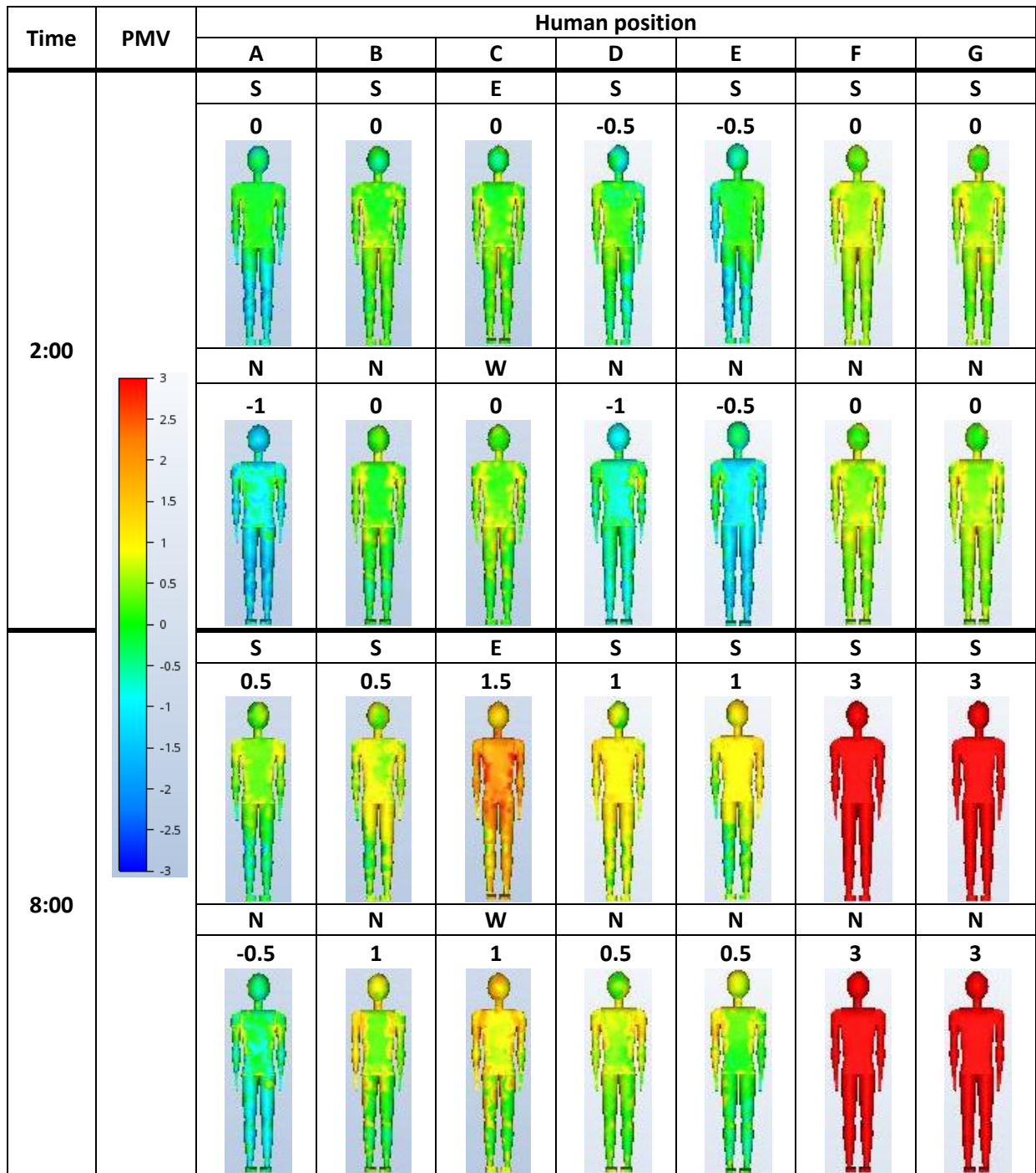


Figure 5.22 Detailed PMV results of the Avatars inside the building (A-G: position, S-E-N-W: orientation)

In the 2:00 o'clock case (Figure 5.22), the PMV of the Avatars A, D and E resides around the low end of the comfort zone. In the 2nd case (Figure 5.22) Avatar C presents lower values on the western side of the body (especially on the legs) which means that the airflow and the lack of direct sunlight helped to decrease the PMV values. Different values are also recorded in Avatar A and they are moving from -1, on the legs of the northern side, to 0.5 on the southern side of the body.

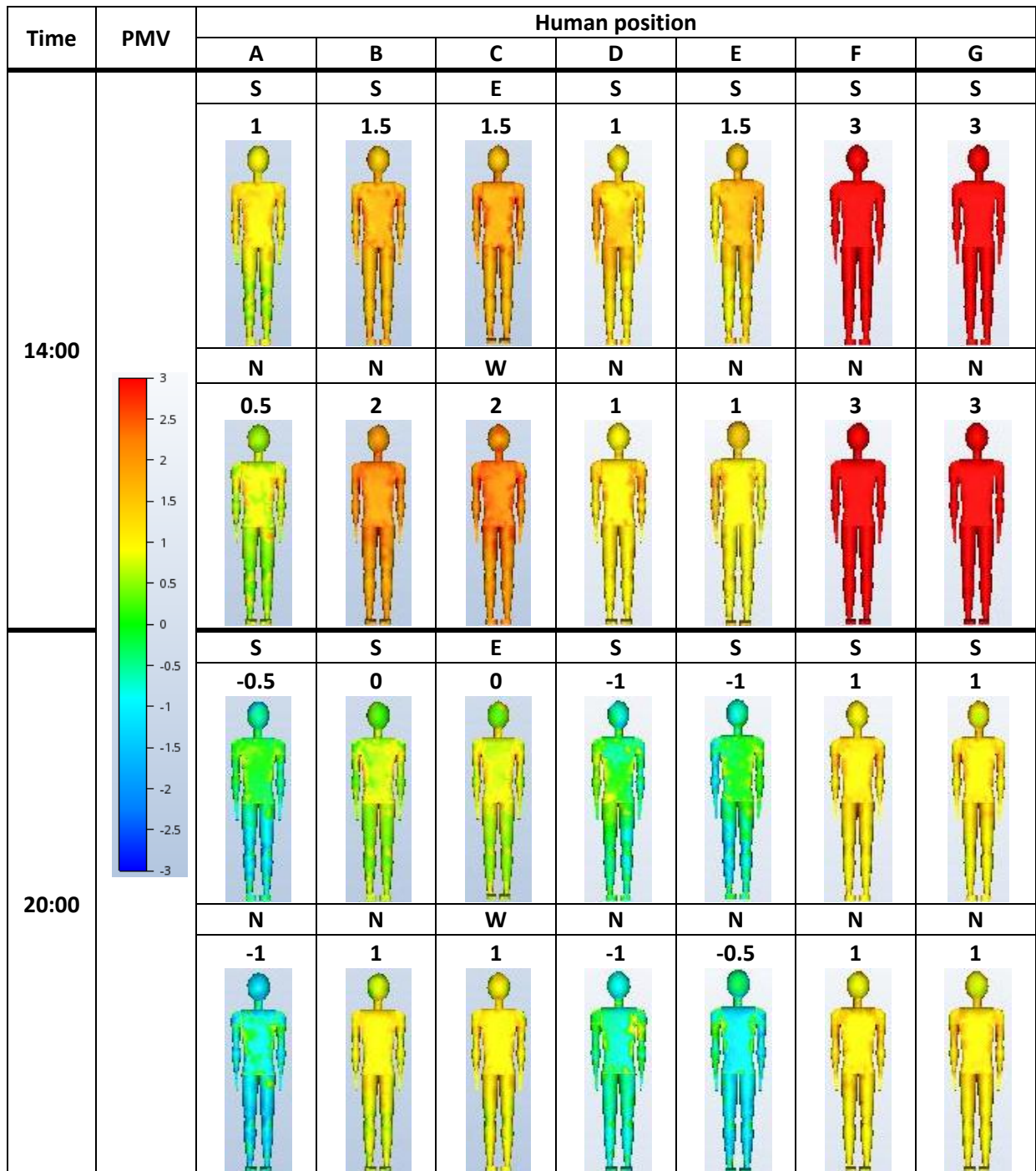


Figure 5.23 Detailed PMV results of the Avatars inside the building (A-G: position, S-E-N-W: orientation)

In the case of 14:00 o'clock (Figure 5.23) the Avatar A seems to have been more affected from the air movement; however the new indoor conditions are not able to make the PMV values of any Avatar fall in the comfort zone. At 20:00 (Figure 5.23), the PMV of the Avatars A, D and E is moving around the low values of the cold zone, probably because they are located in the direct wind path.

Avatars F and G are in spaces that the air cannot reach, therefore they do not record any difference in the PMV values in any case of this Scenario.

5.6. Scenario 5: openings in the kitchen and bedroom

In Scenario 5 the northern glass door of the kitchen (inlet) and the northern window of bedroom 1 (outlet) are open (**Figure 5.24**). The air is moving fast through the kitchen and the bedroom but stays in the dining and living room exploiting the height of the open space.

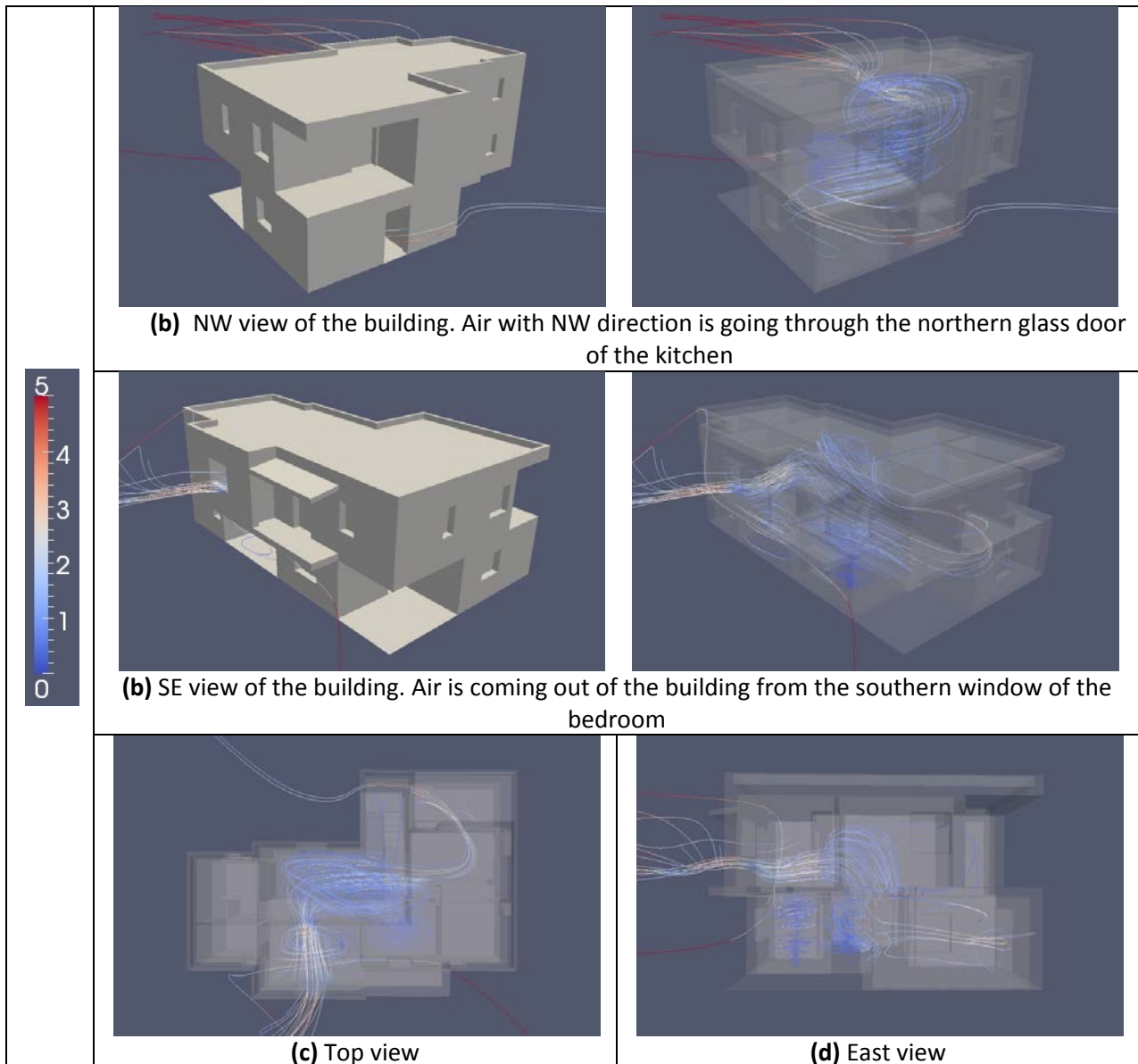
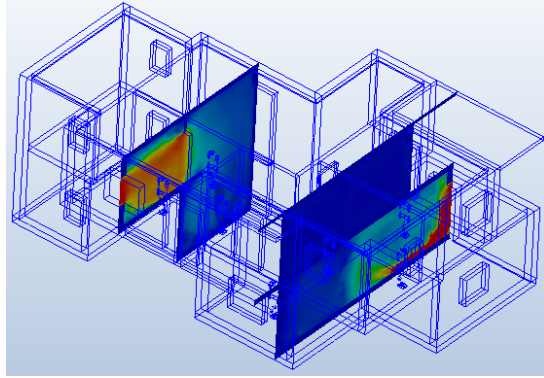


Figure 5.24 Airflow movement inside the building

In the **Figure 5.25** below the measurement planes a (inlet) and b (outlet) are presented. The highest velocity is recorded close to the inlet kitchen opening and in the bedroom space. The air that is moving in the two storey open space reaches 2m/s velocity at 14:00 and 20:00 o'clock. For the cases of 2:00 and 8:00 o'clock the maximum air speed is around 2m/s and for the 14:00 and 20:00 o'clock around 5m/s.



Position of the measurement planes, SE view

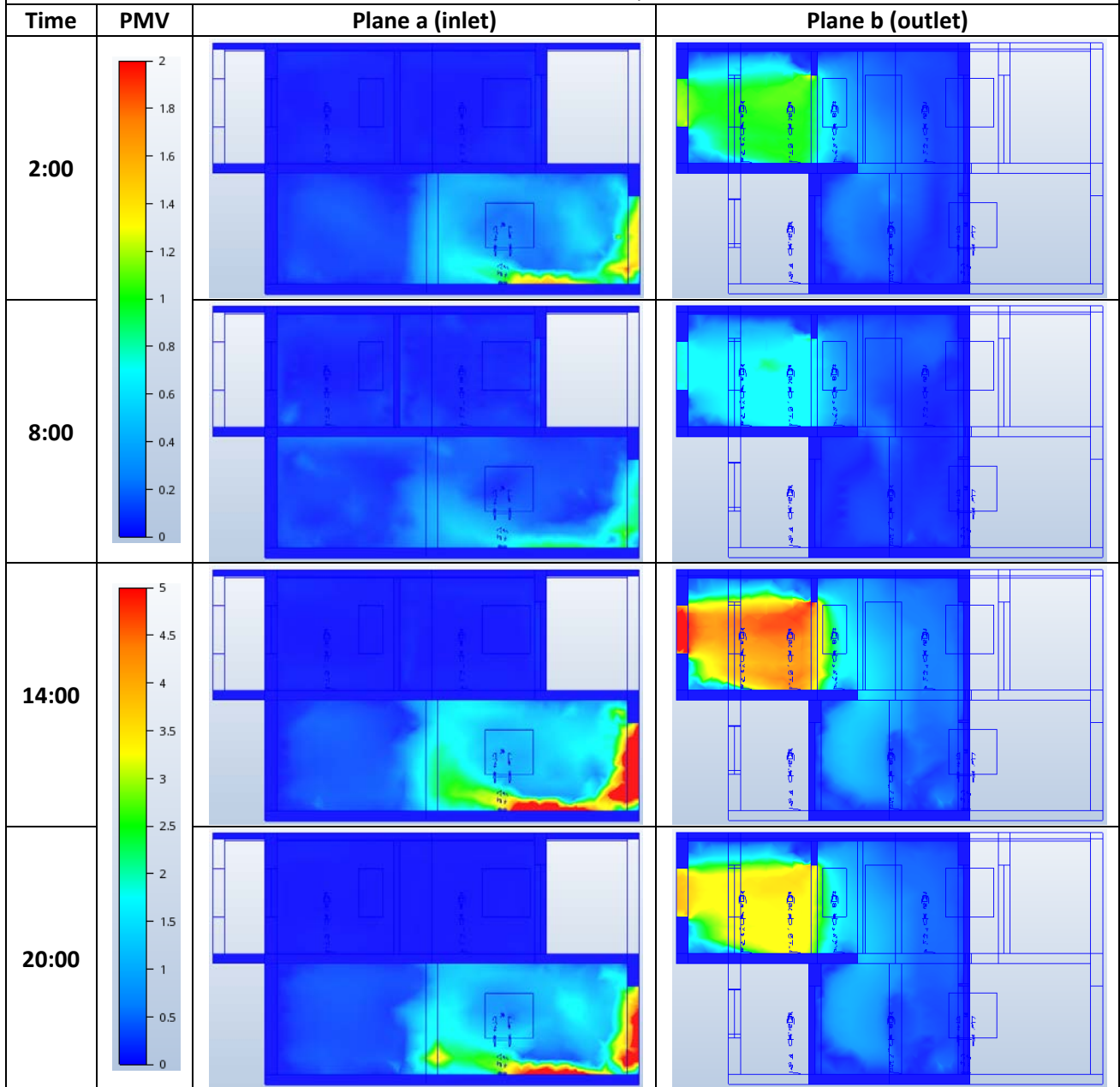


Figure 5.25 Velocity results for the four examined hours of the day

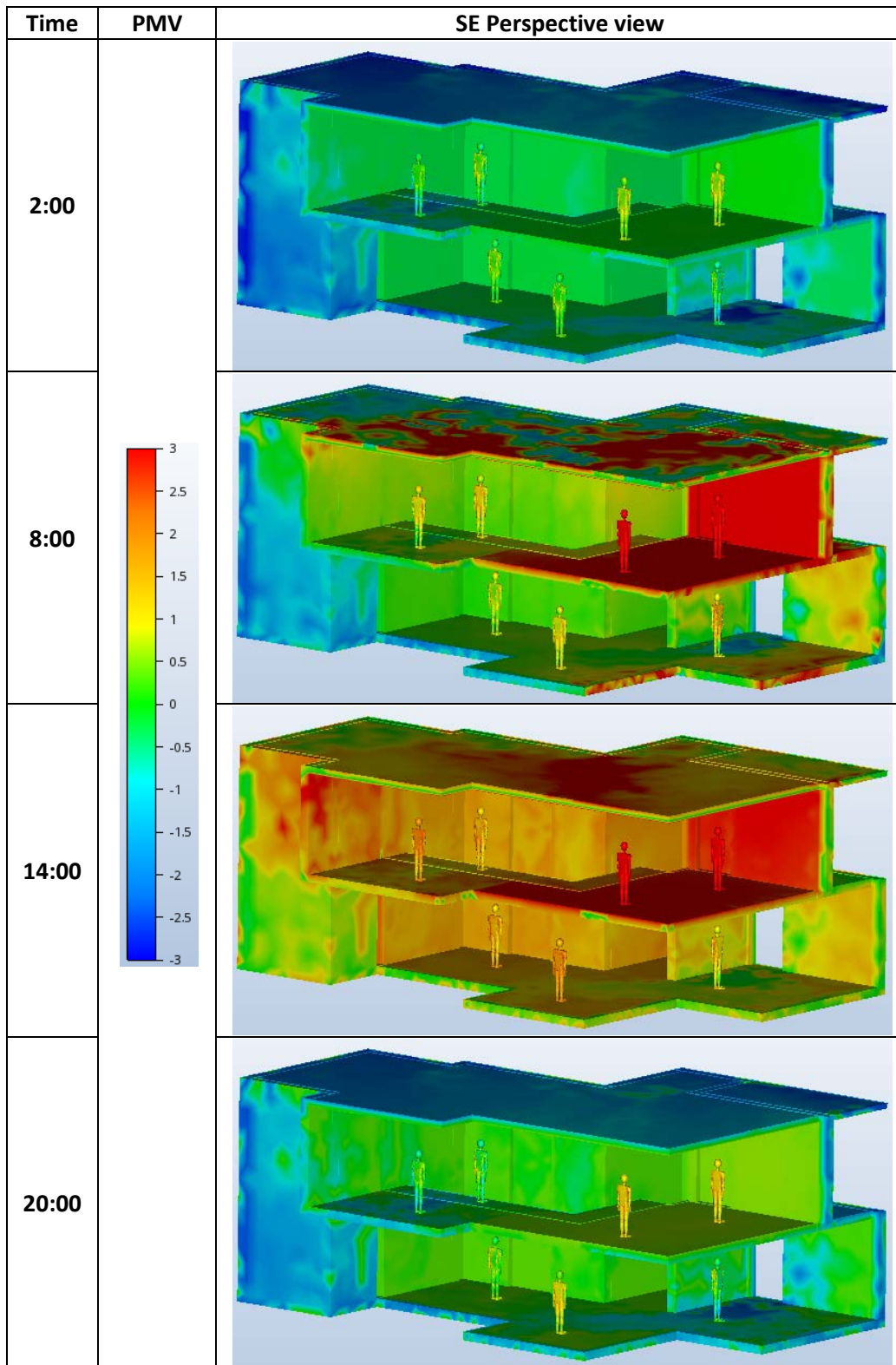


Figure 5.26 PMV results for the four examined hours of the day

From **Figure 5.26** we observe that the Avatars C, D and E present bigger decrease of their PMV values in all the cases.

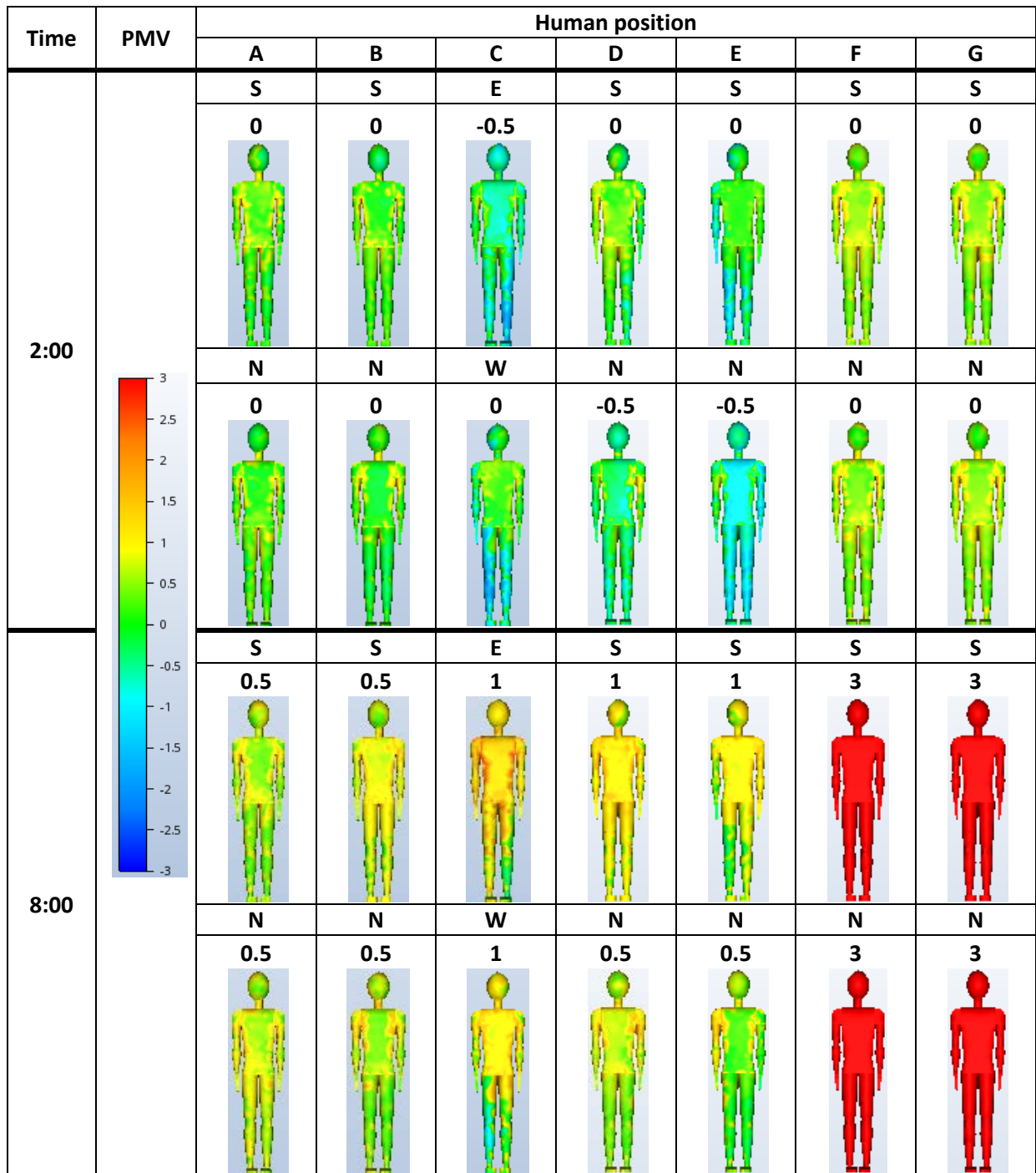


Figure 5.27 Detailed PMV results of the Avatars inside the building (A-G: position, S-E-N-W: orientation)

In the **Figure 5.27** above at 2:00 o'clock, Avatars C, D and E present a decrease of their PMV values but they remain in the comfort zone. Avatar C records high negative values on the legs, where the air is moving with high speed, and Avatar E on the northern side of the body where the air is coming from. In the case of 8:00 o'clock (**Figure 5.27**) the PMV of the Avatars A and B is in the comfort zone, while the values of the Avatars C, D and E are moving around the high end of the comfort zone.

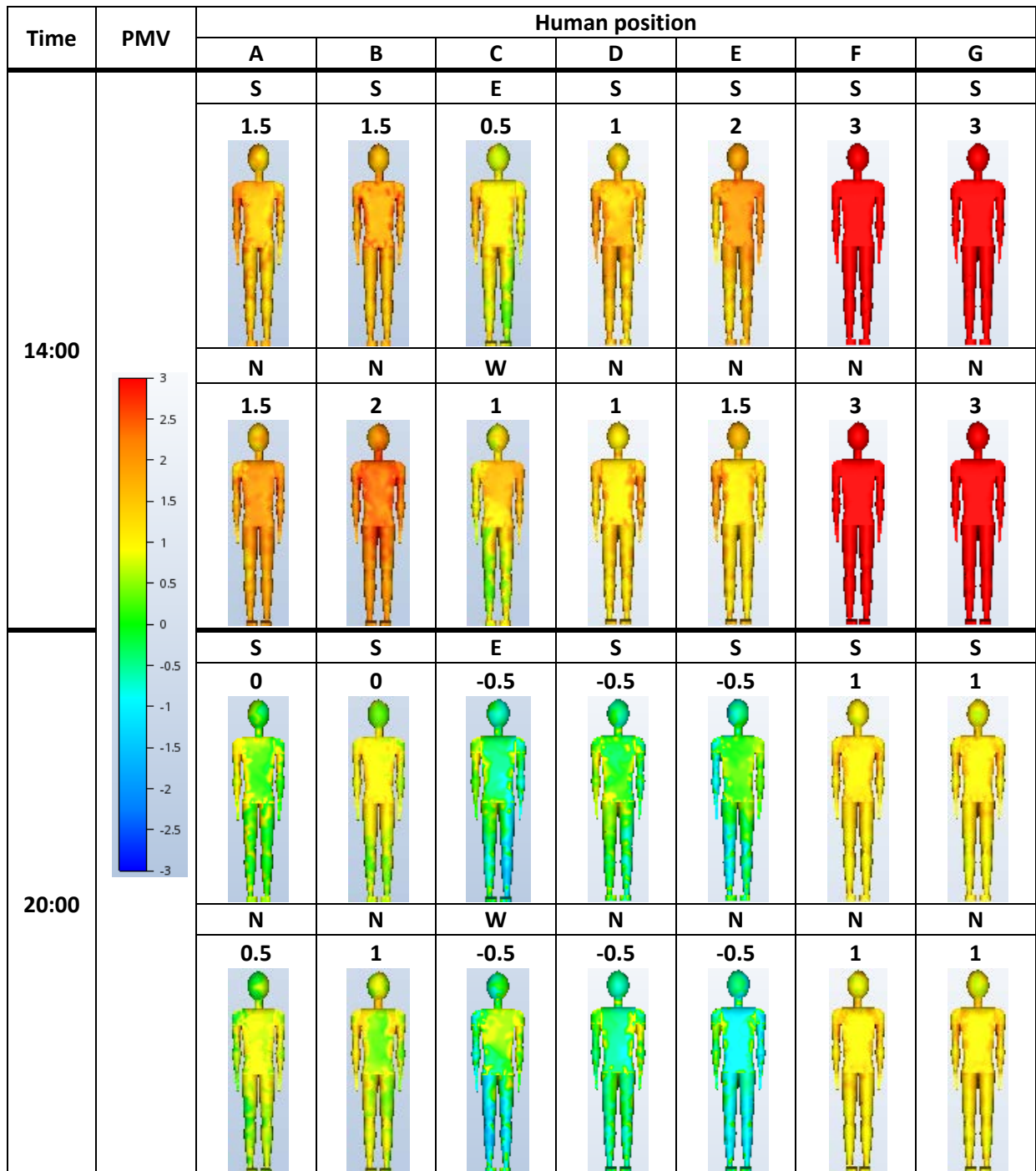


Figure 5.28 Detailed PMV results of the Avatars inside the building (A-G: position, S-E-N-W: orientation)

In the 14:00 o'clock case (Figure 5.28) none of the Avatars present PMV values in the comfort zone but Avatar C is close with a value of 0.75. At 20:00 o'clock (Figure 5.28) the PMV of the Avatars C, D and E is located in the low end of the comfort zone but higher negative values are observed on their legs.

Avatars F and G are in spaces that the air cannot reach, therefore they do not record any difference in the PMV values in any case of this Scenario.

5.7. Scenario 6: openings in the living room, kitchen and bedroom

In Scenario 6 the northern glass door of the living room (inlet), the eastern window of the kitchen (outlet) and the southern window in bedroom 1 (outlet) are open. Higher air speed is recorded in the living room, kitchen and bedroom and vorticities are created in the living and dining room (Figure 5.29).

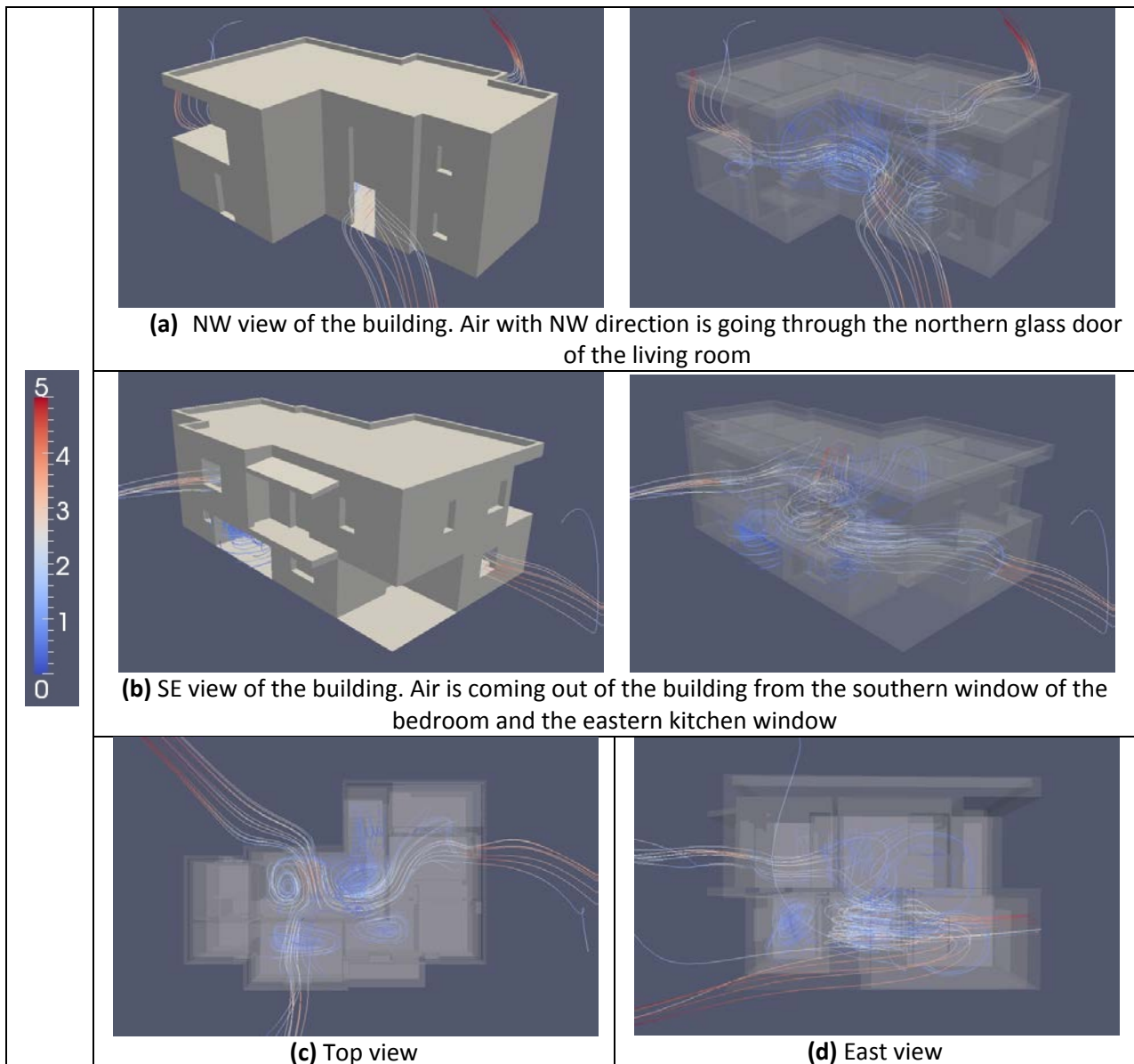
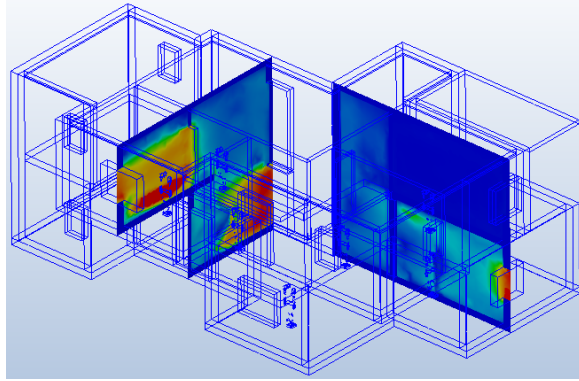


Figure 5.29 Airflow movement inside the building

In Figure 5.30 below, the measurement planes a (inlet-outlet) and b (outlet) are presented. From the planes higher air speed is recorded in the living room and bedroom space while in the kitchen the speed is reduced. Air movement is located in the two-storey open space of the living room that in some cases (14:00 and 20:00 o'clock) reaches 2m/s. For the cases of 2:00 and 8:00 o'clock the maximum speed is around 2m/s and for the 14:00 and 20:00 o'clock around 5m/s.



Position of the measurement planes, SE view

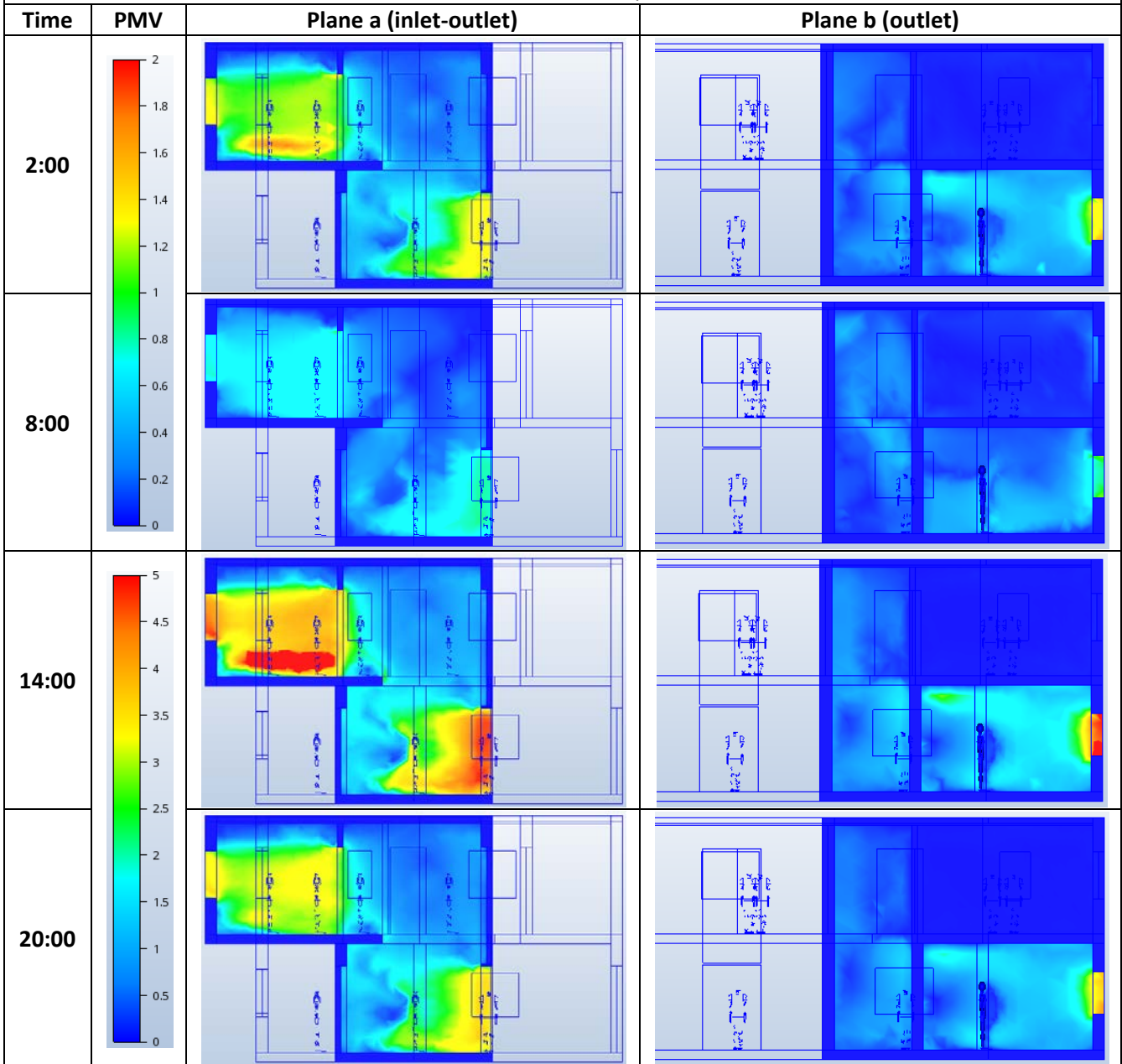


Figure 5.30 Velocity results for the four examined hours of the day

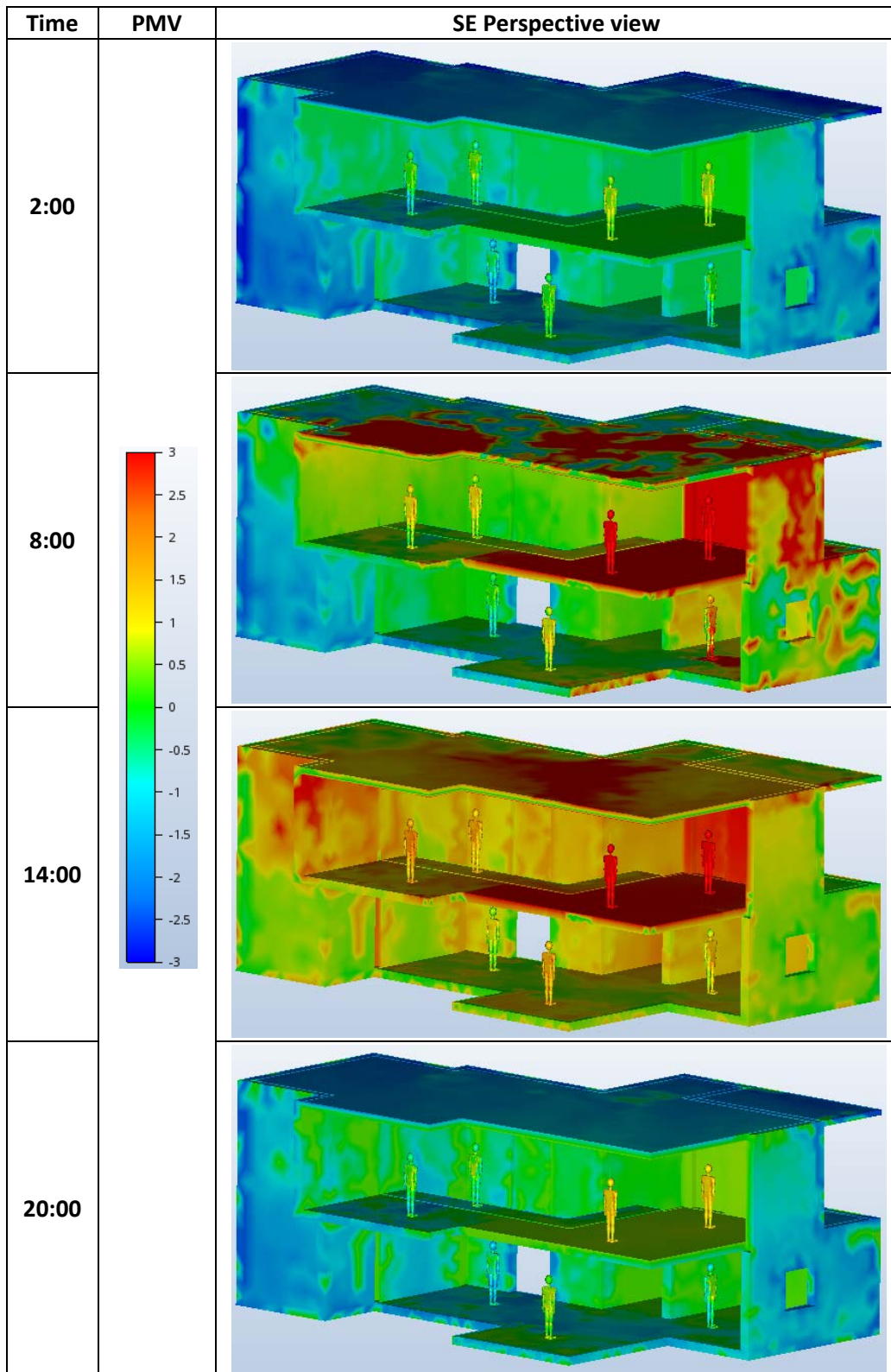


Figure 5.31 PMV results for the four examined hours of the day

From **Figure 5.31** from the NE perspective, we observe many changes in the PMV values of Avatars A and C.

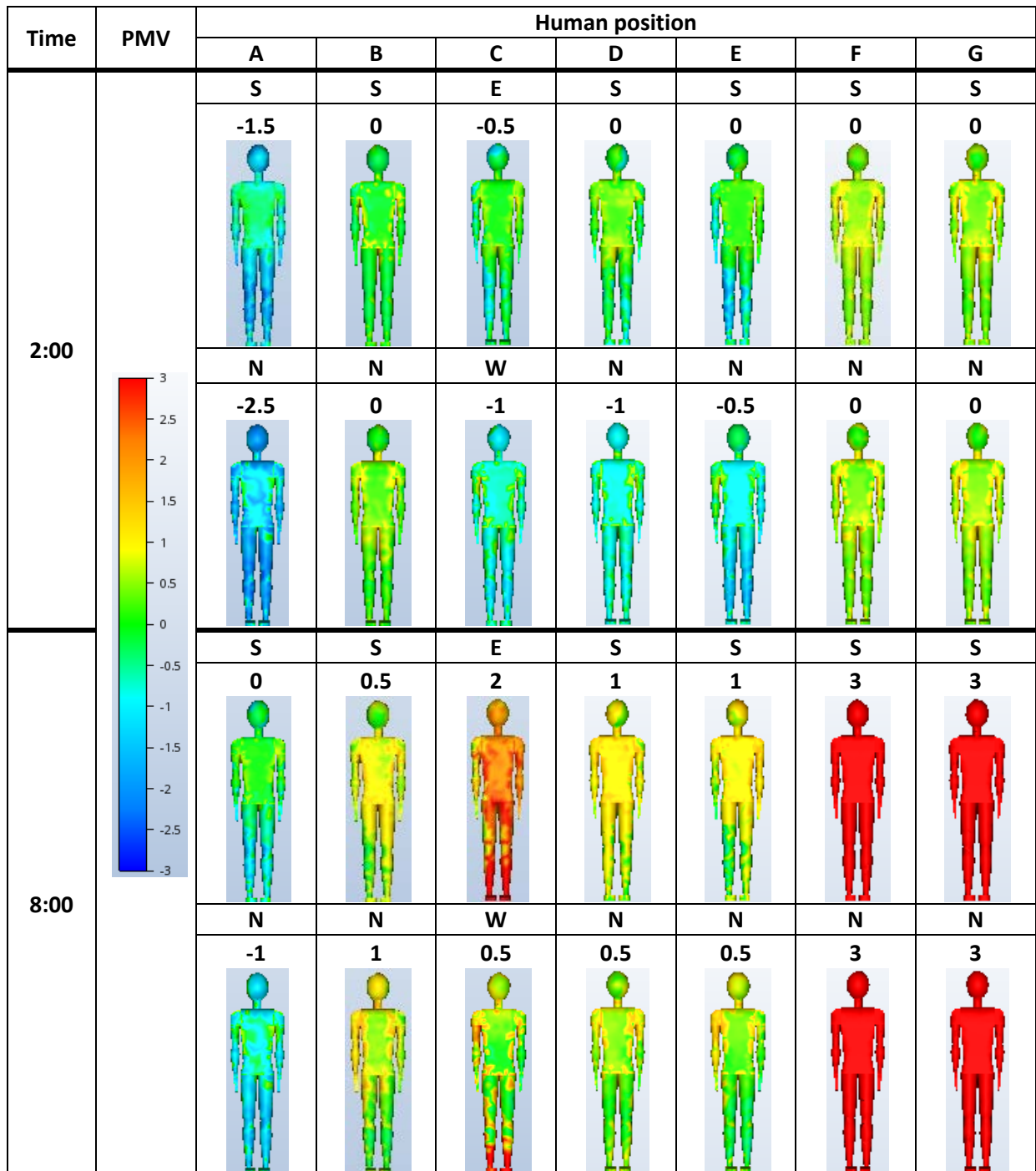


Figure 5.32 Detailed PMV results of the Avatars inside the building (A-G: position, S-E-N-W: orientation)

At 2:00 o'clock (Figure 5.32), the PMV of Avatar A is moving in the cold zone with mean value of -2 while the PMV of Avatars C, D and E is moving in the low end of the comfort zone. In the case of 8:00 o'clock (Figure 5.32), the PMV of Avatar A has negative values on the northern side of the body but the mean value of the head is -0.5, inside the comfort zone. The PMV of Avatar C has high values on the eastern side of the body and lower (inside the comfort zone) on the western side, except on its feet, but the mean value of the head is 1.25 (warm zone). For these Avatars we observe that the lower PMV values are recorded on the side where the air is coming from. The Avatars B, D and E have a 0.75 value, close to the comfort zone.

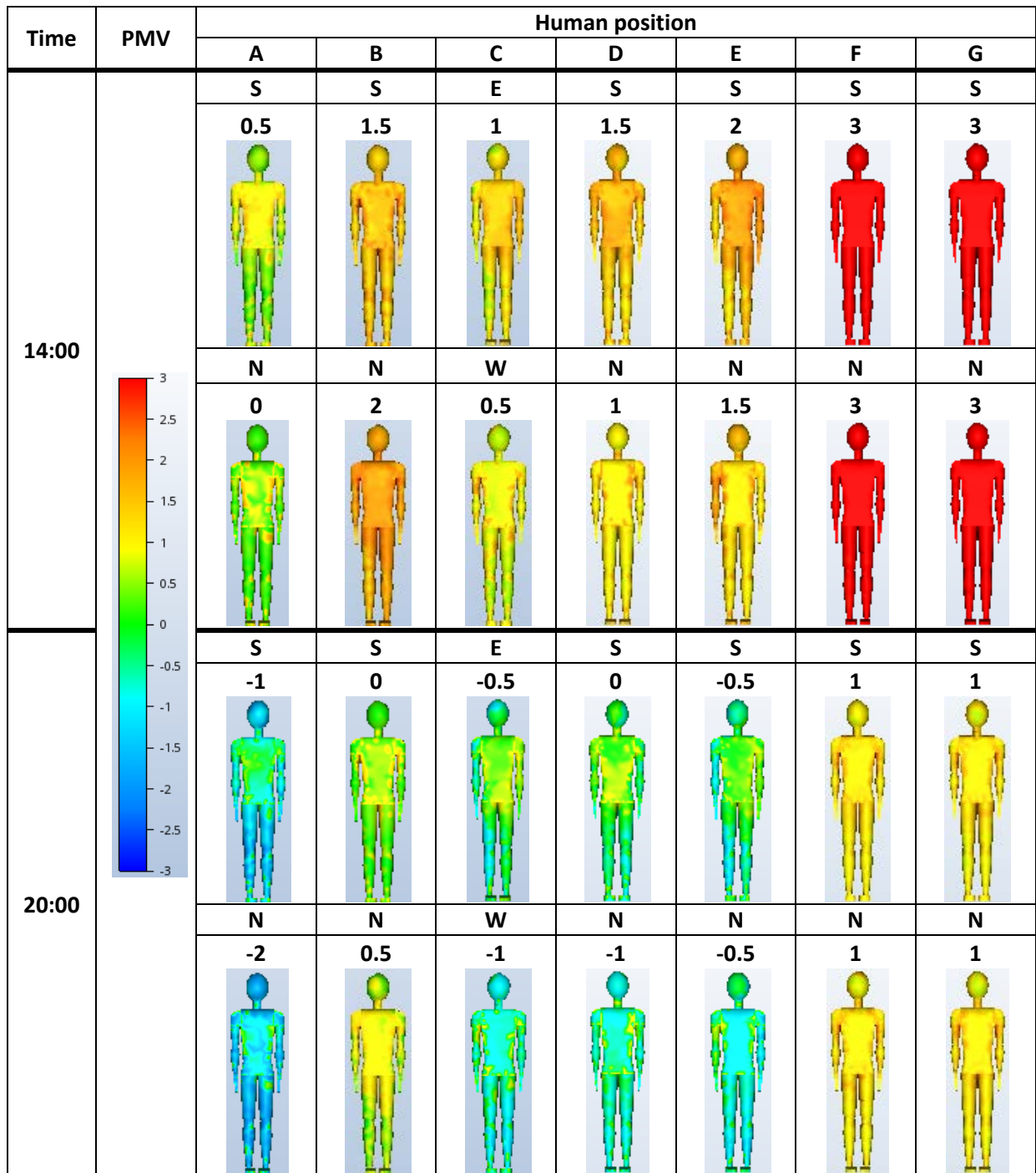


Figure 5.33 Detailed PMV results of the Avatars inside the building (A-G: position, S-E-N-W: orientation)

At 14:00 o'clock (Figure 5.33), the PMV of Avatar A is the only one that is recorded inside the comfort zone. In the last case (20:00 o'clock, Figure 5.33) the PMV of Avatar A has negative values in almost the whole body, Avatars B, D and E are inside the comfort zone and Avatar C is moving in the low end.

Avatars F and G are in spaces that the air cannot reach, therefore they do not record any difference in the PMV values in any case of this Scenario.

5.8. Scenario 7: openings in the office and living room

In Scenario 7 the building is simulated with the northern glass door of the office (inlet) and the southern glass door of the living room (outlet) open. The air is moving through all the available areas of the building with low velocity (**Figure 5.34**).

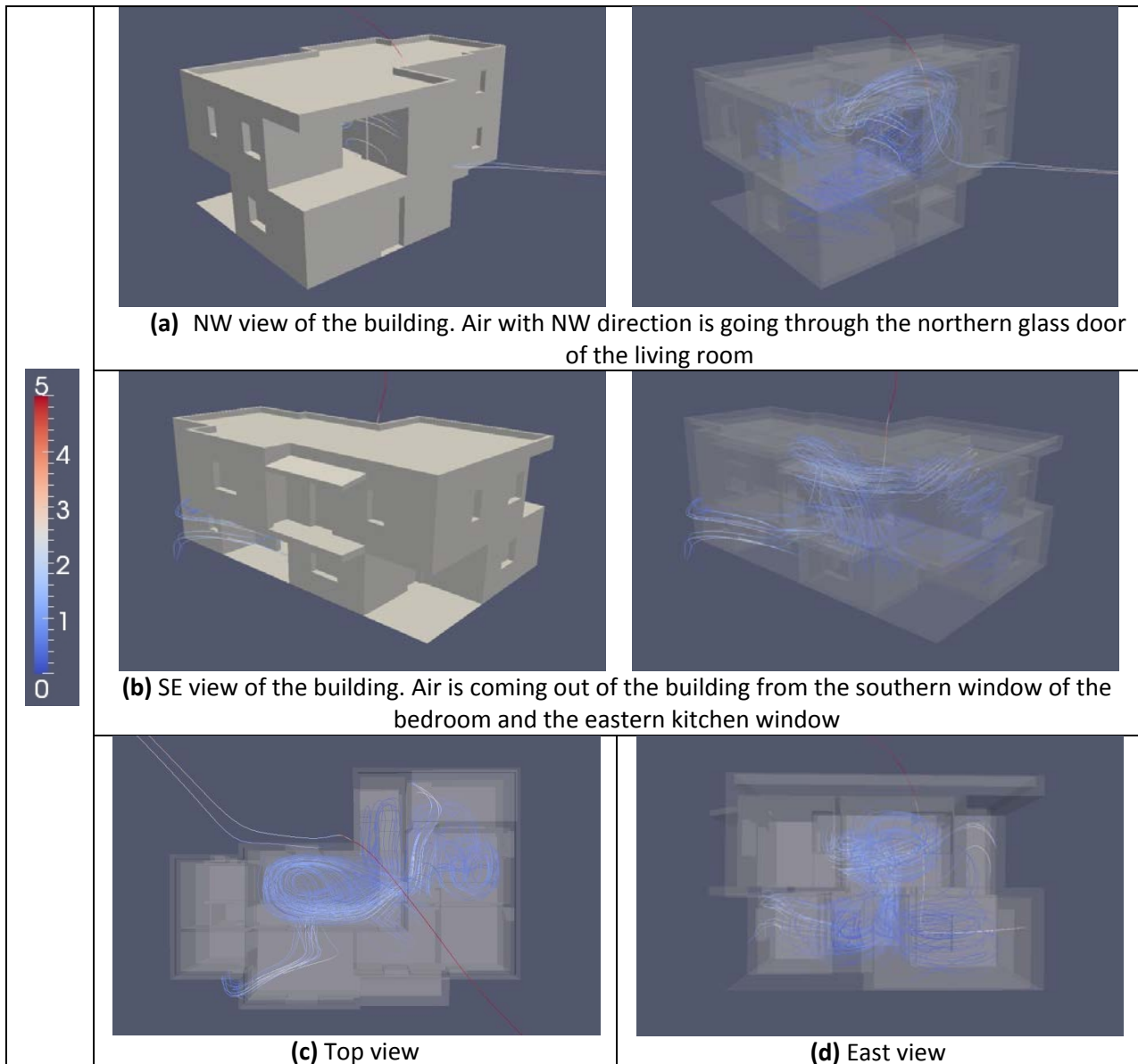
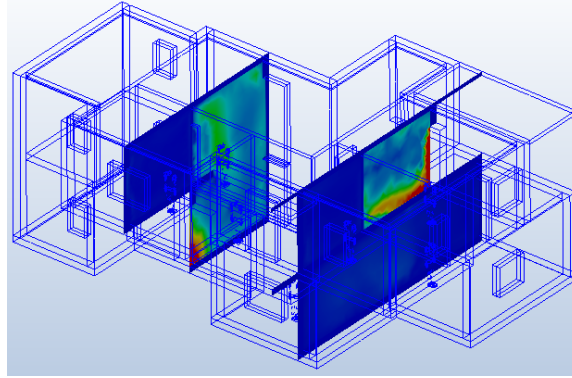


Figure 5.34 Airflow movement inside the building

The measurement planes a (inlet) and b (outlet) are shown in the **Figure 5.35** below. In all the cases higher speed is recorded close to the openings and the airflow appears to be more in the spaces of the office and living room (in all its height). For the cases of 2:00 and 8:00 o'clock the maximum air speed is noted around 1m/s and for the 14:00 and 20:00 o'clock around 3m/s.



Position of the measurement planes, SE view

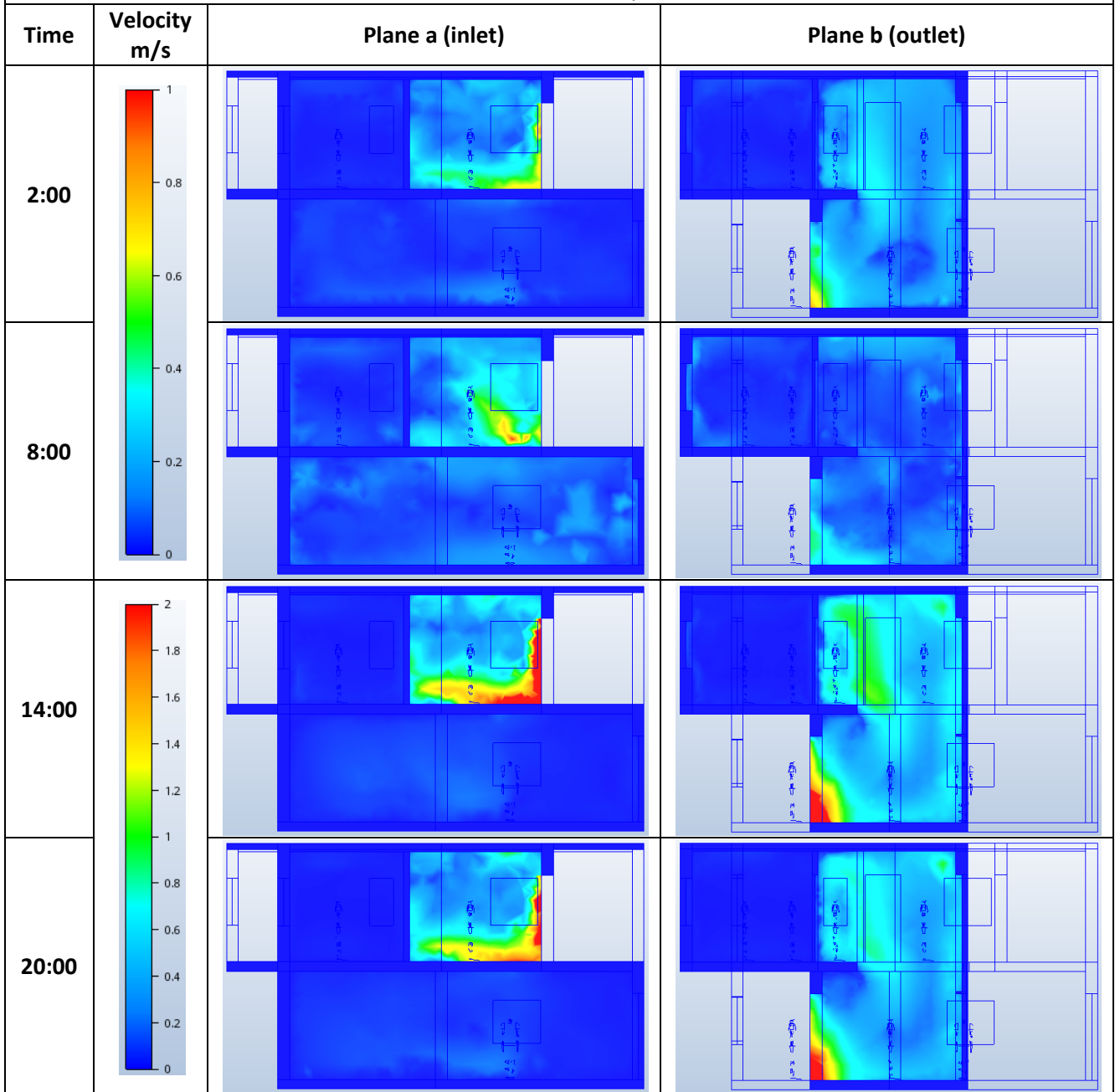


Figure 5.35 Velocity results for the four examined hours of the day

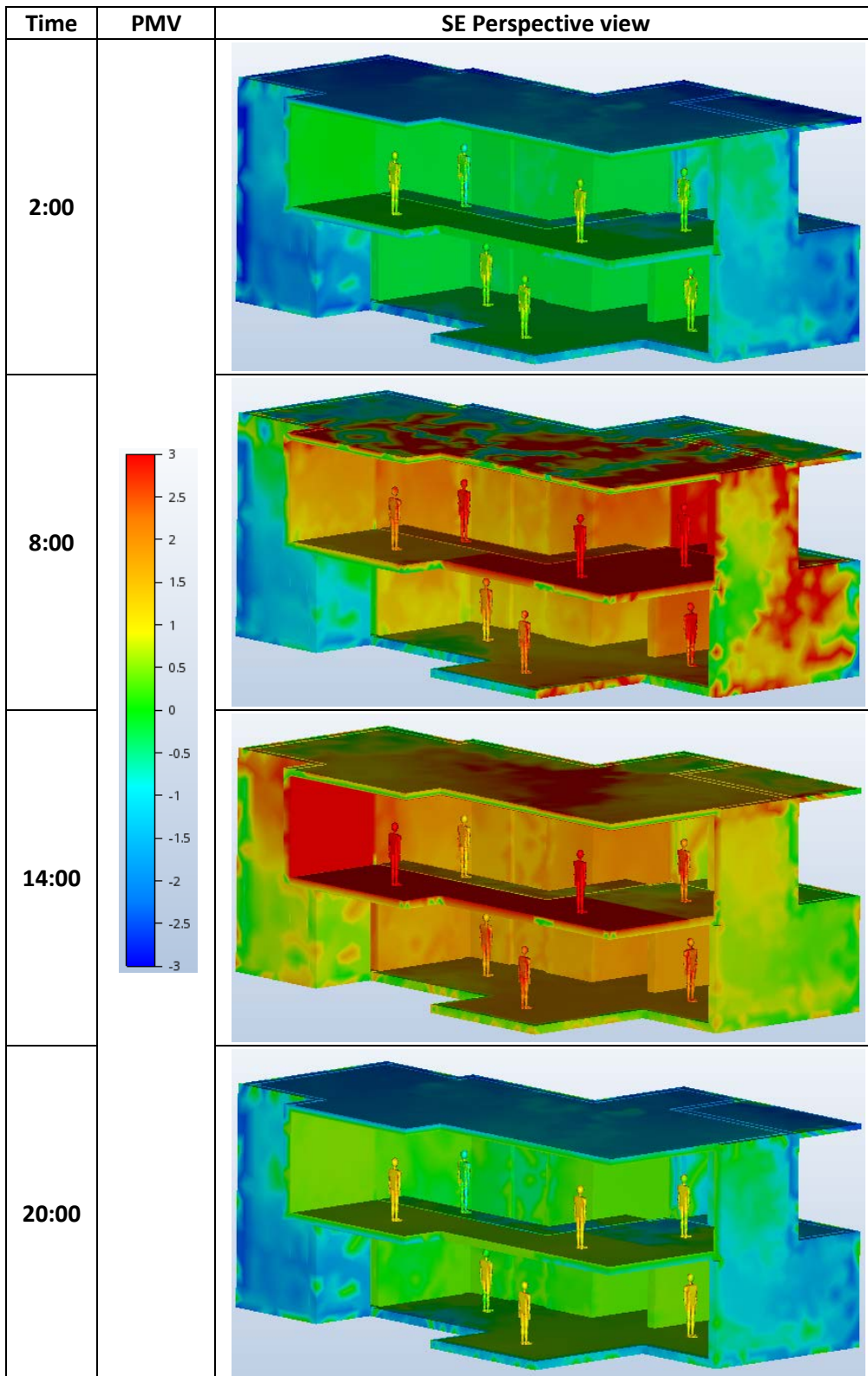


Figure 5.36 PMV results for the four examined hours of the day

From the perspective view (Figure 5.36) we notice that the PMV of Avatar D presents more changes in its values in most of the cases.

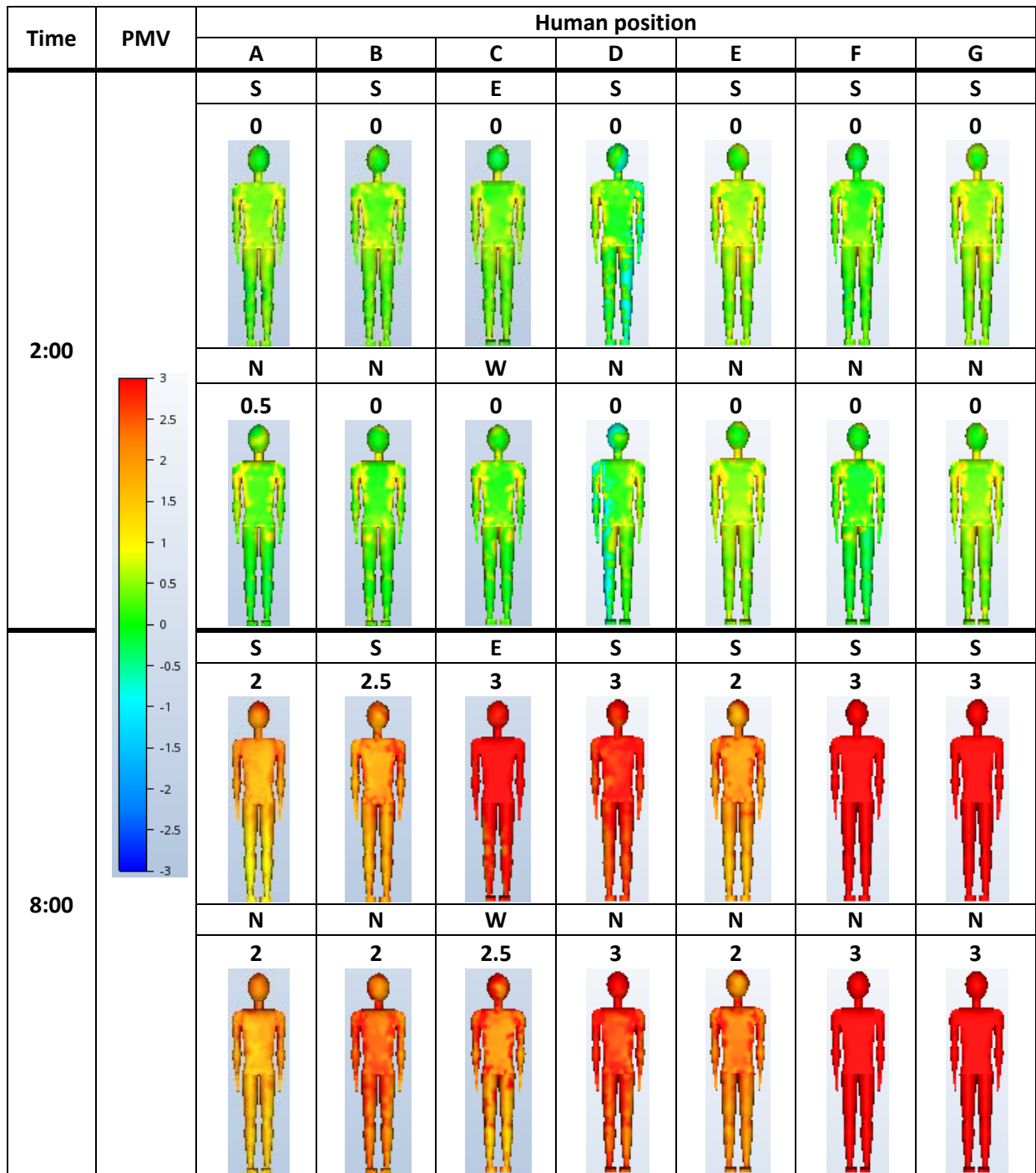


Figure 5.37 Detailed PMV results of the Avatars inside the building (A-G: position, S-E-N-W: orientation)

At 2:00 o'clock (Figure 5.37), the PMV of all the Avatars is inside the comfort zone. For the case of 8:00 o'clock (Figure 5.37), the PMV of all the Avatars is very high, where the lower value is 2 and appears on the Avatars A and E. The high values appear due to the heat transfer that occurs when the air is entering a very warm space of the building and moves to a cooler space.

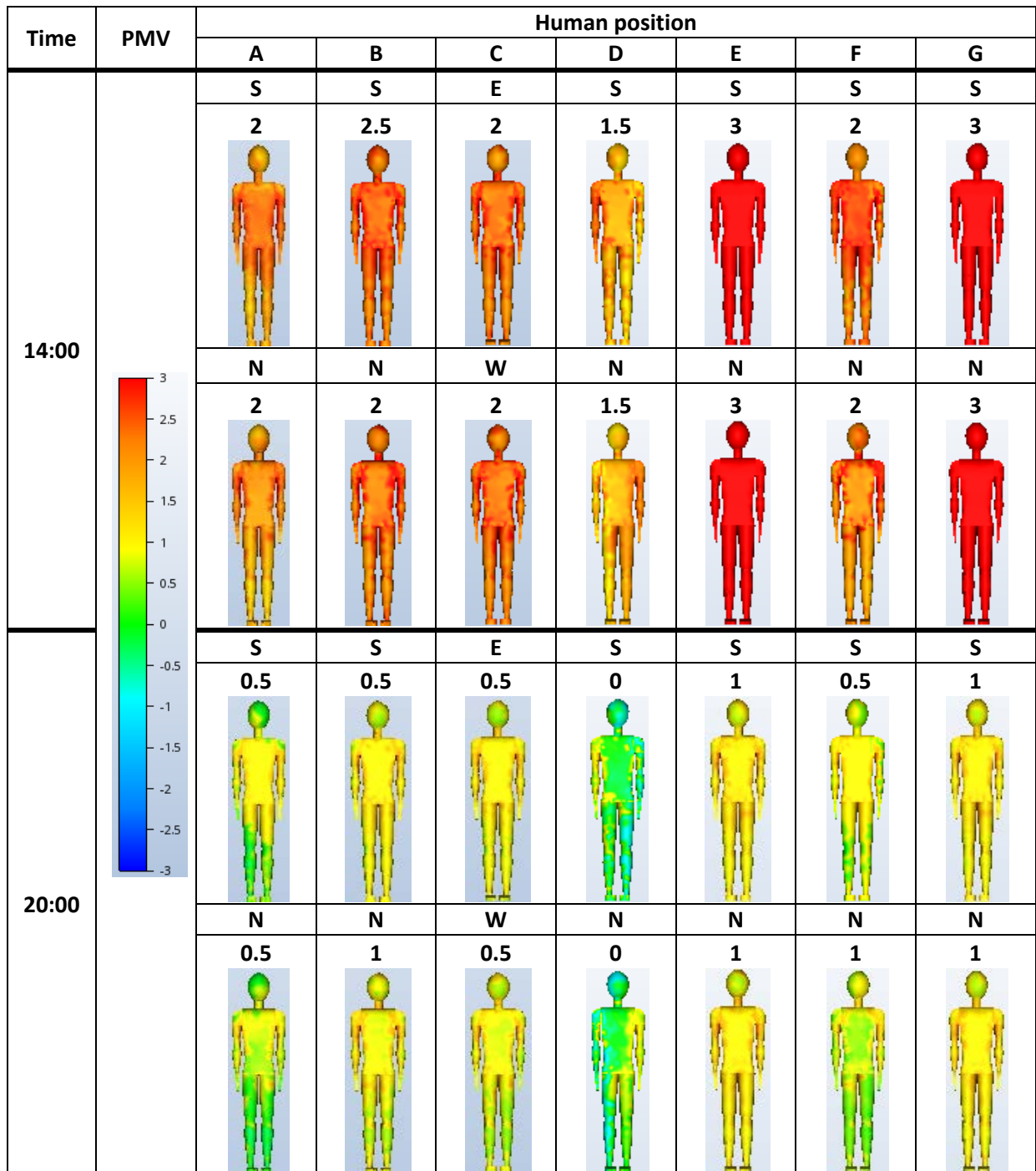


Figure 5.38 Detailed PMV results of the Avatars inside the building (A-G: position, S-E-N-W: orientation)

At 14:00 (Figure 5.38), the PMV of all the Avatars has high values with the lowest recorded at 1.5 on Avatar D. In the last case of 20:00 o'clock (Figure 5.38), the PMV values of all the Avatars are moving closer to the comfort zone. On Avatar D we observe different values on the body caused by the direction of the airflow. Cooler values appear on the eastern side of the body, where the air is coming from, neutral in the middle and warmer on the western side.

Avatars E and G are in spaces that the air cannot reach, therefore they do not record any difference in the PMV values in any case of this Scenario.

5.9. Scenario 8: openings in the living room and office

In this Scenario the northern glass door of the living room (inlet) and the eastern window of the office (outlet) are open. The wind is going through the living room and the office with high speed but stays in the kitchen and dining room. The direct wind path is preventing a better air movement in the two-storey open space but a vorticity is created in the area of the living room and the stairs (Figure 5.39).

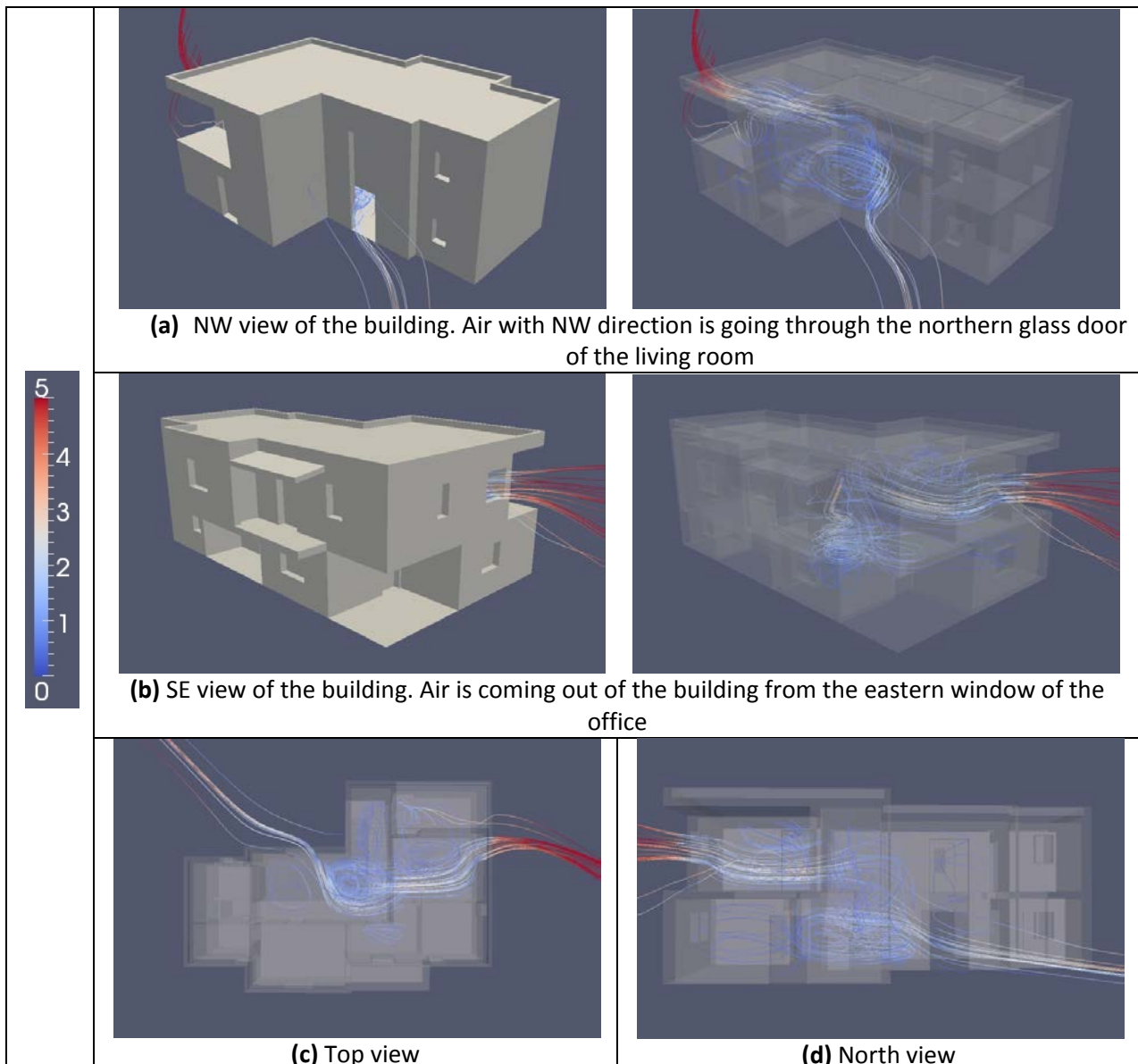
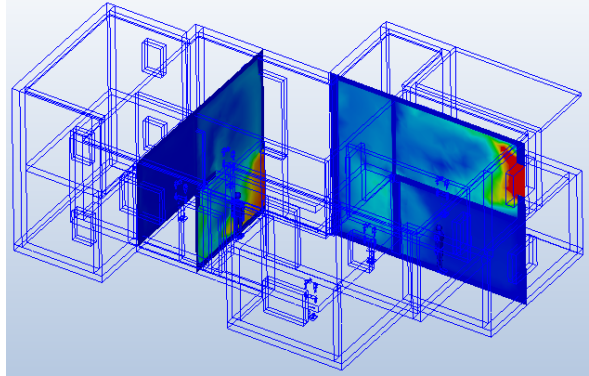


Figure 5.39 Airflow movement inside the building

The following Figure 5.40 presents the measurement planes a (inlet) and b (outlet). From the planes we observe that higher speed is recorded close to the openings and low air movement in the kitchen and in the first floor level of the open space of the living room. For the cases of 2:00 and 8:00 o'clock the maximum air speed is around 1m/s and for the 14:00 and 20:00 o'clock around 3m/s.



Position of the measurement planes, SE view

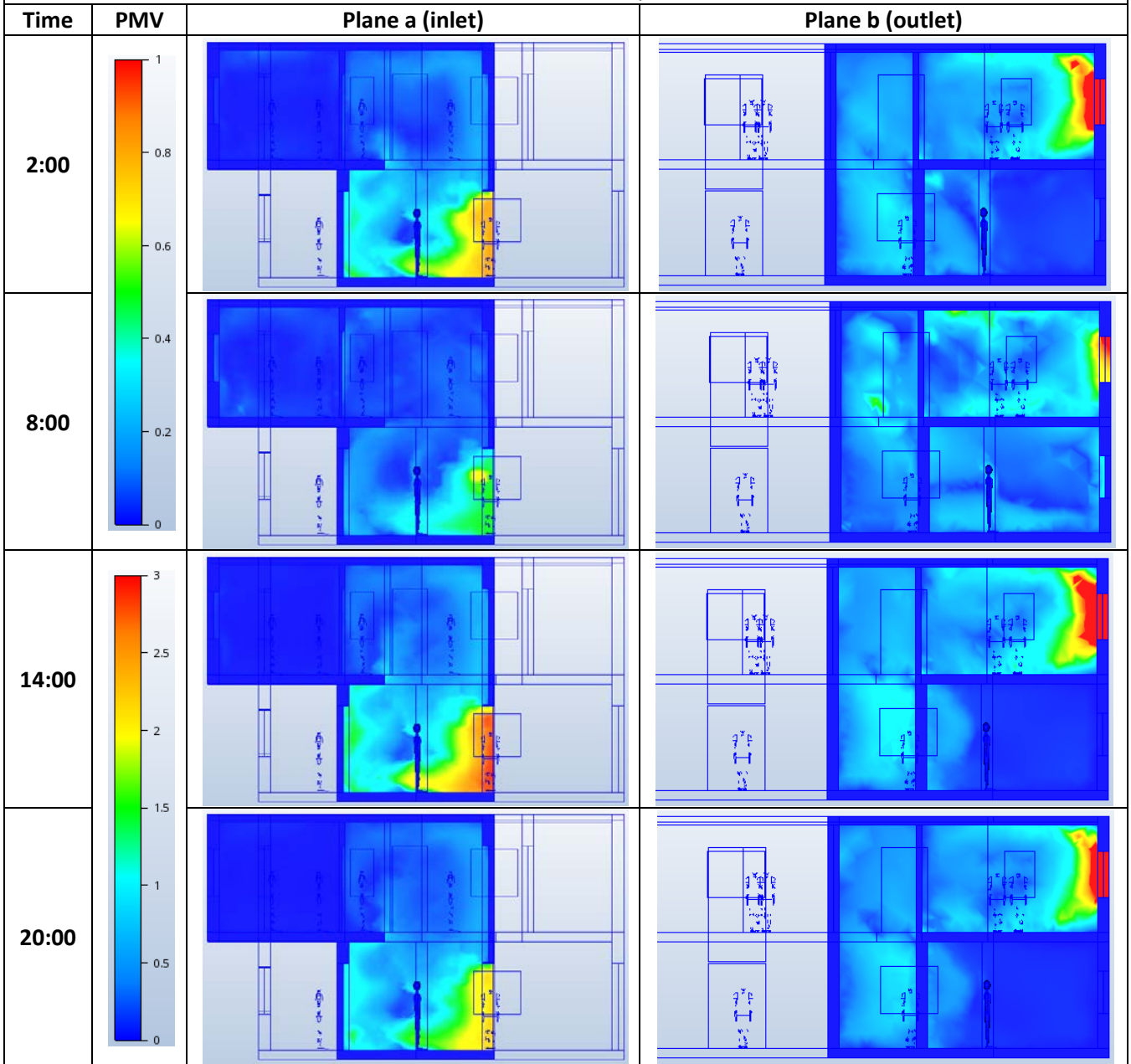


Figure 5.40 Velocity results for the four examined hours of the day

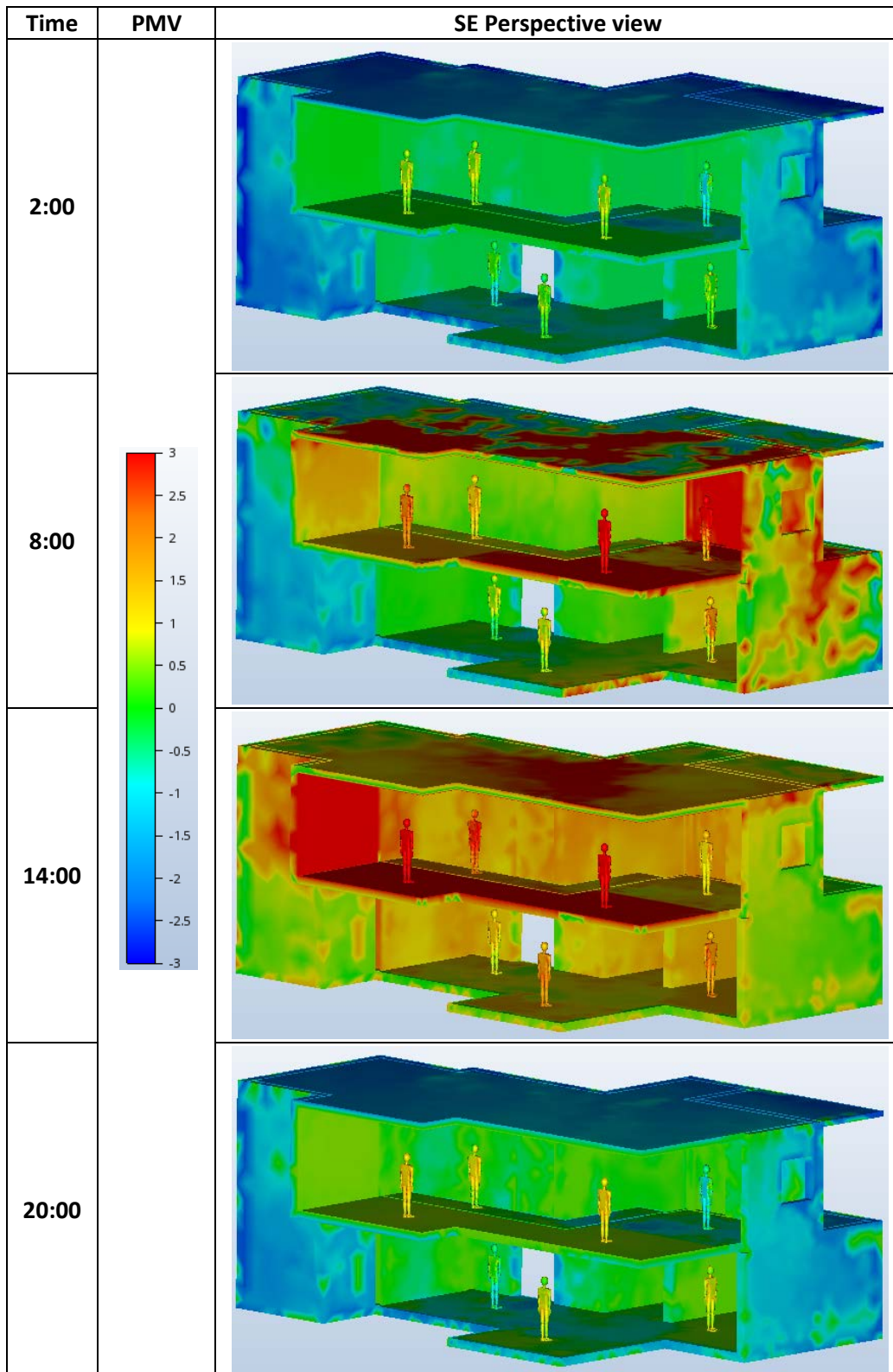


Figure 5.41 PMV results for the four examined hours of the day

From **Figure 5.41** the PMV values of the Avatars A and F seem to be more affected from the created airflow of the selected openings. At 8:00 o'clock we observe that the airflow is not able to improve the indoor conditions of the office and the Avatar F shows high PMV values on its upper body.

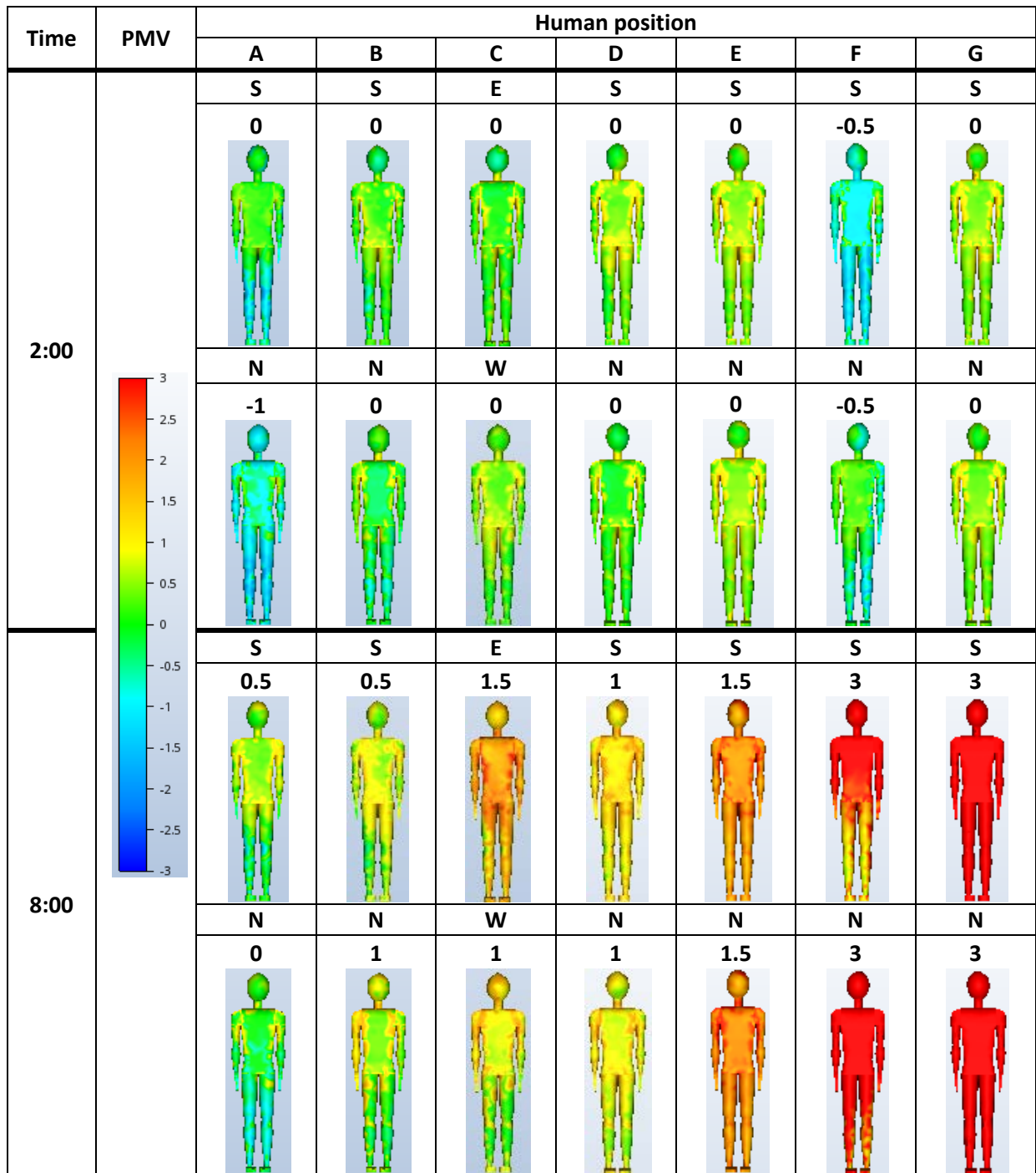


Figure 5.42 Detailed PMV results of the Avatars inside the building (A-G: position, S-E-N-W: orientation)

At 2:00 o'clock (Figure 5.42) the northern side of Avatar A and the southern side of Avatar F present negative values on the whole body and is caused from their position and the direction of the incoming air in the spaces they are located (living room and office respectively). In the second case (8:00 o'clock, Figure 5.42), Avatar A presents negative values on the legs (northern side) where the air is entering the building. The PMV of Avatar C on the eastern side of the body has values that indicate the level of thermal sensation as warm but values of comfort are recorded on its western side where the air has bigger movement.

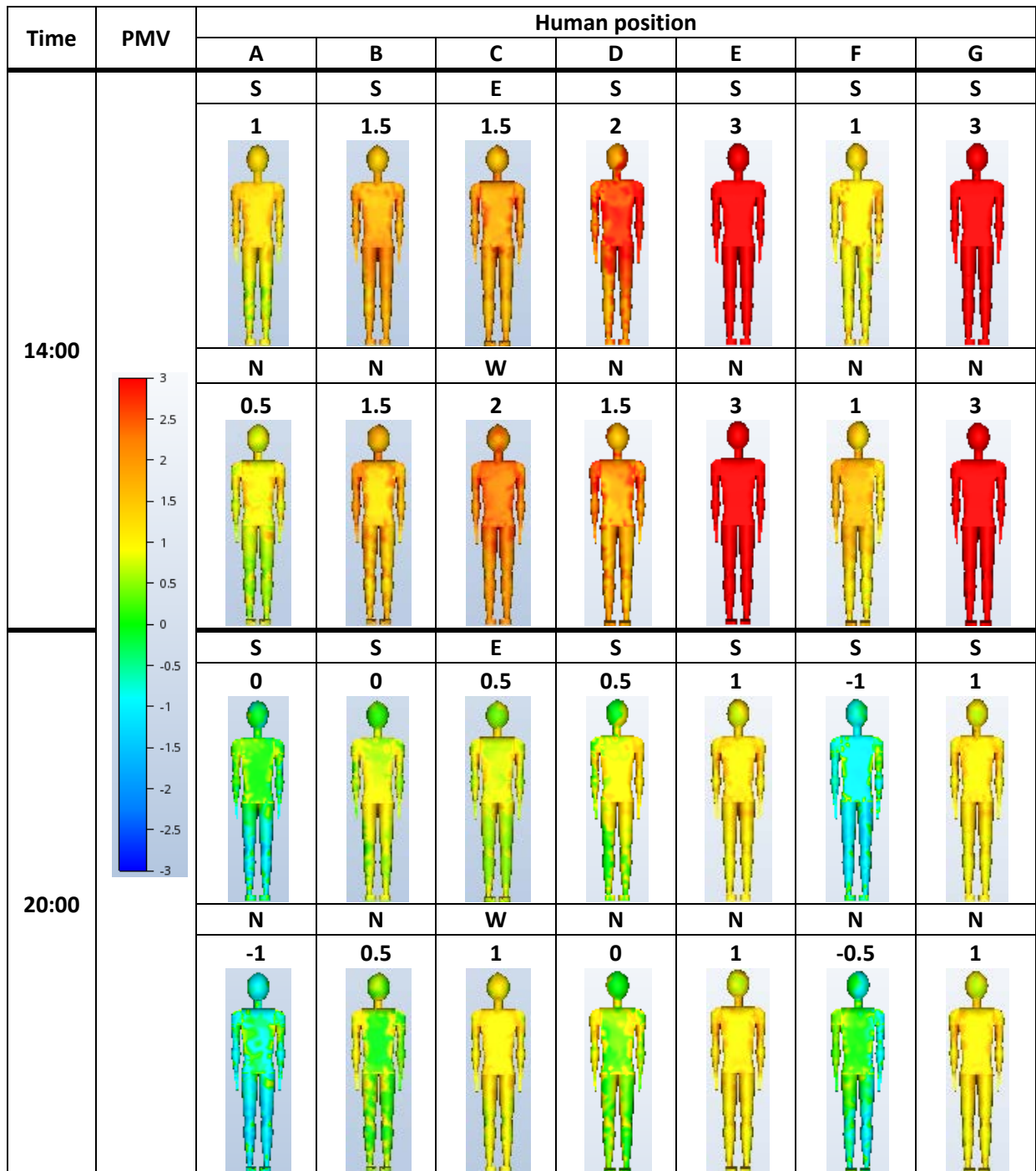


Figure 5.43 Detailed PMV results of the Avatars inside the building (A-G: position, S-E-N-W: orientation)

In the case of 14:00 o'clock (Figure 5.43), only the northern side of Avatar A presents some PMV values of thermal comfort sensation while in all the other Avatars the values are in the warm or hot zone (from 1 to 3). At 20:00 o'clock (Figure 5.43), Avatar A and F show similar results with the case of 8:00 o'clock, negative values on the side and parts of their body where the air is moving.

Avatars E and G are in spaces that the air cannot reach, therefore they do not record any difference in the PMV values in any case of this Scenario.

5.10. Scenario 9: openings in the office, living room and kitchen

In Scenario 9 the building is simulated with the northern glass door of the office (inlet), the southern glass door of the living room (outlet) and the eastern window of the kitchen (outlet) open. The air is moving in all the available spaces (not so much in the dining area) with low velocity (Figure 5.44).

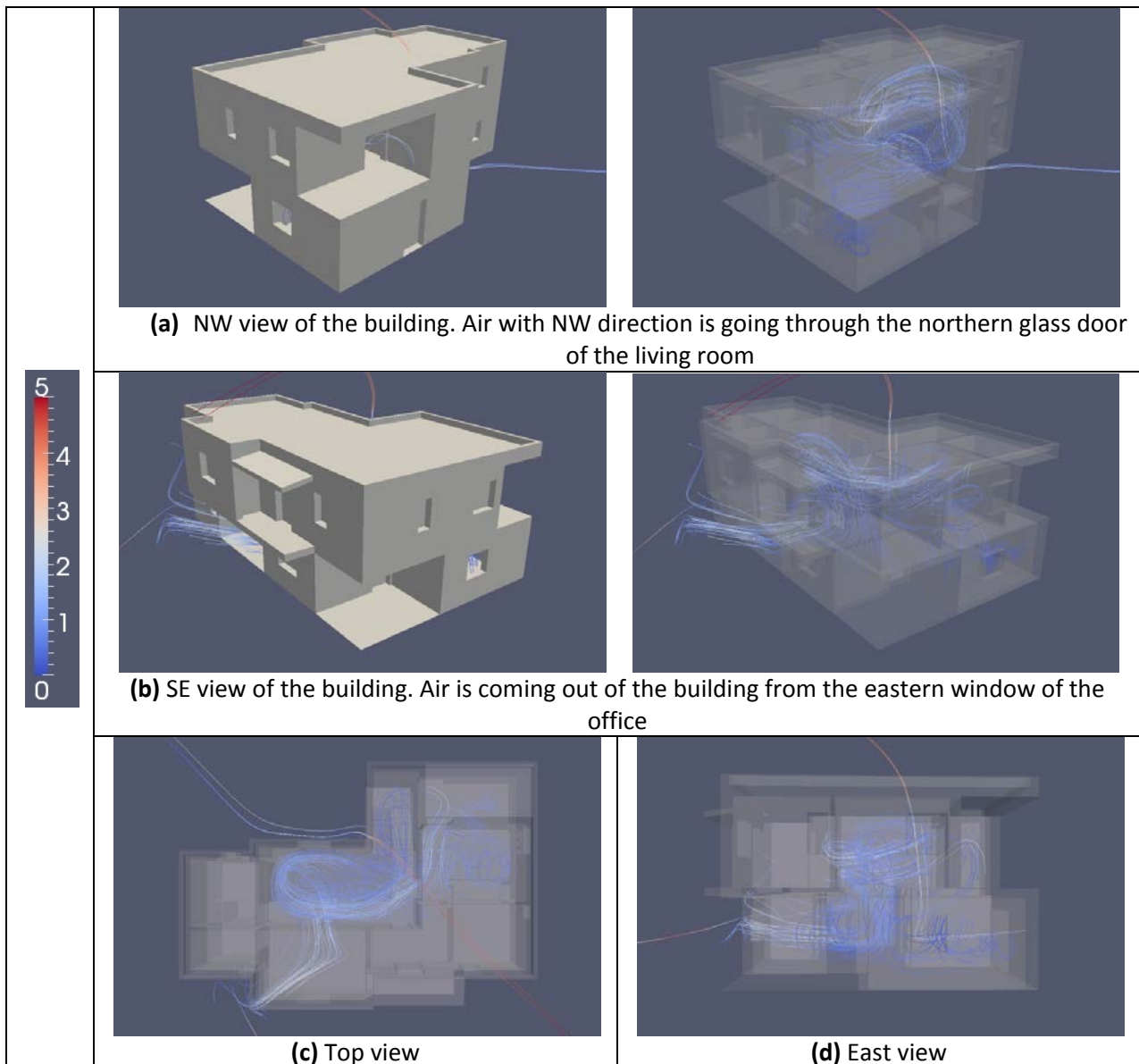
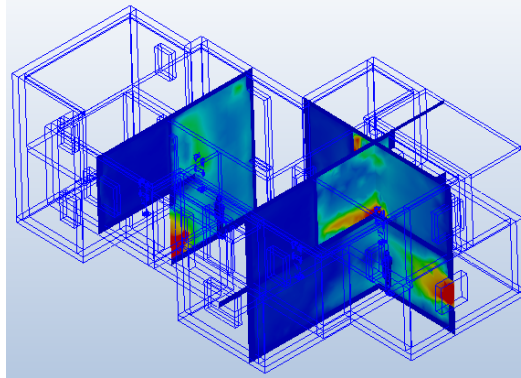


Figure 5.44 Airflow movement inside the building

Figure 5.45 shows the measurement planes a (inlet), b (outlet) and c (outlet). Higher velocities are observed from the planes near the openings and the air speed in the other space is not higher than 1 m/s. For the cases of 2:00 and 8:00 o'clock the maximum air speed is recorded around 1 m/s and for the 14:00 and 20:00 o'clock around 2m/s.



Position of the measurement planes, SE view

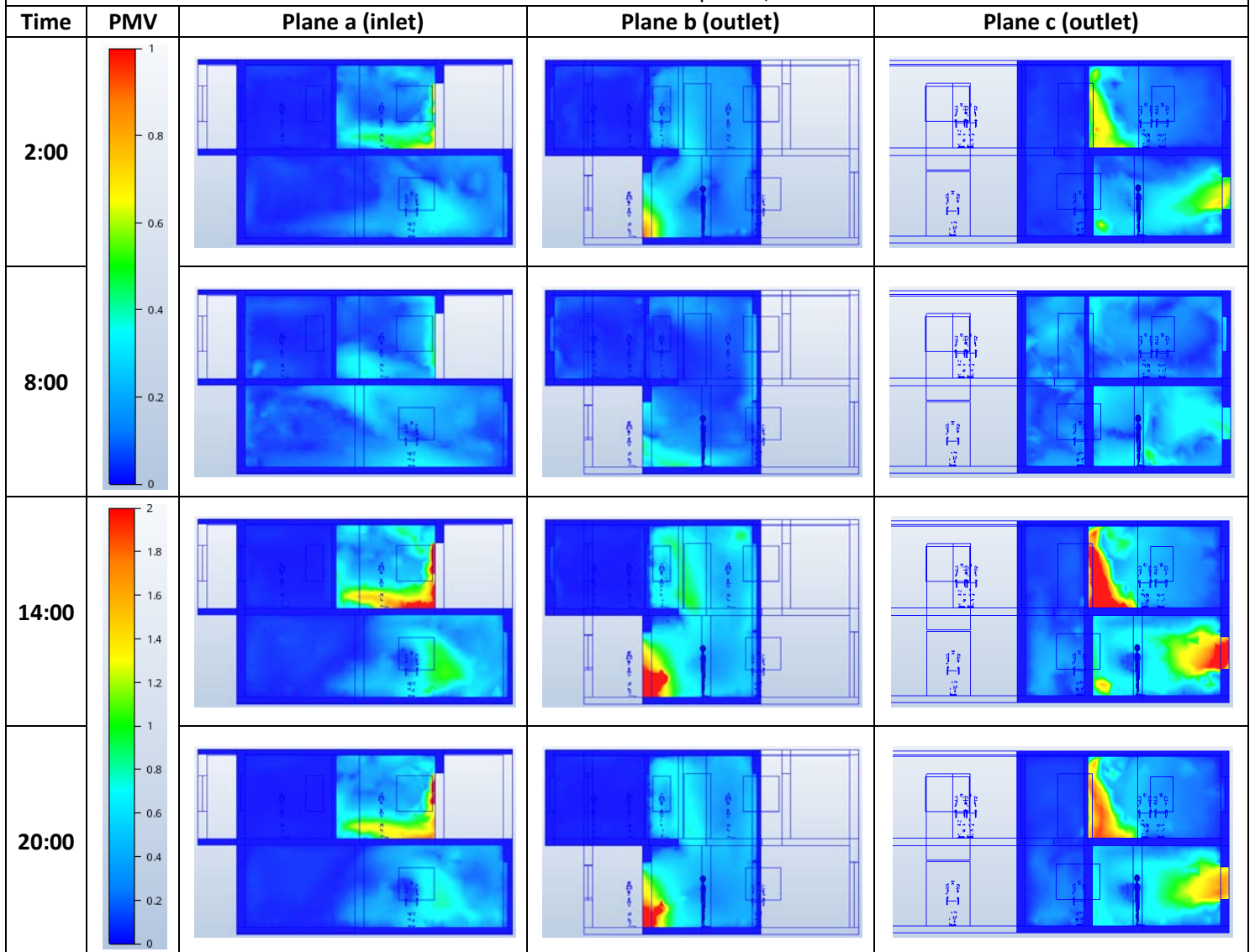


Figure 5.45 Velocity results for the four examined hours of the day

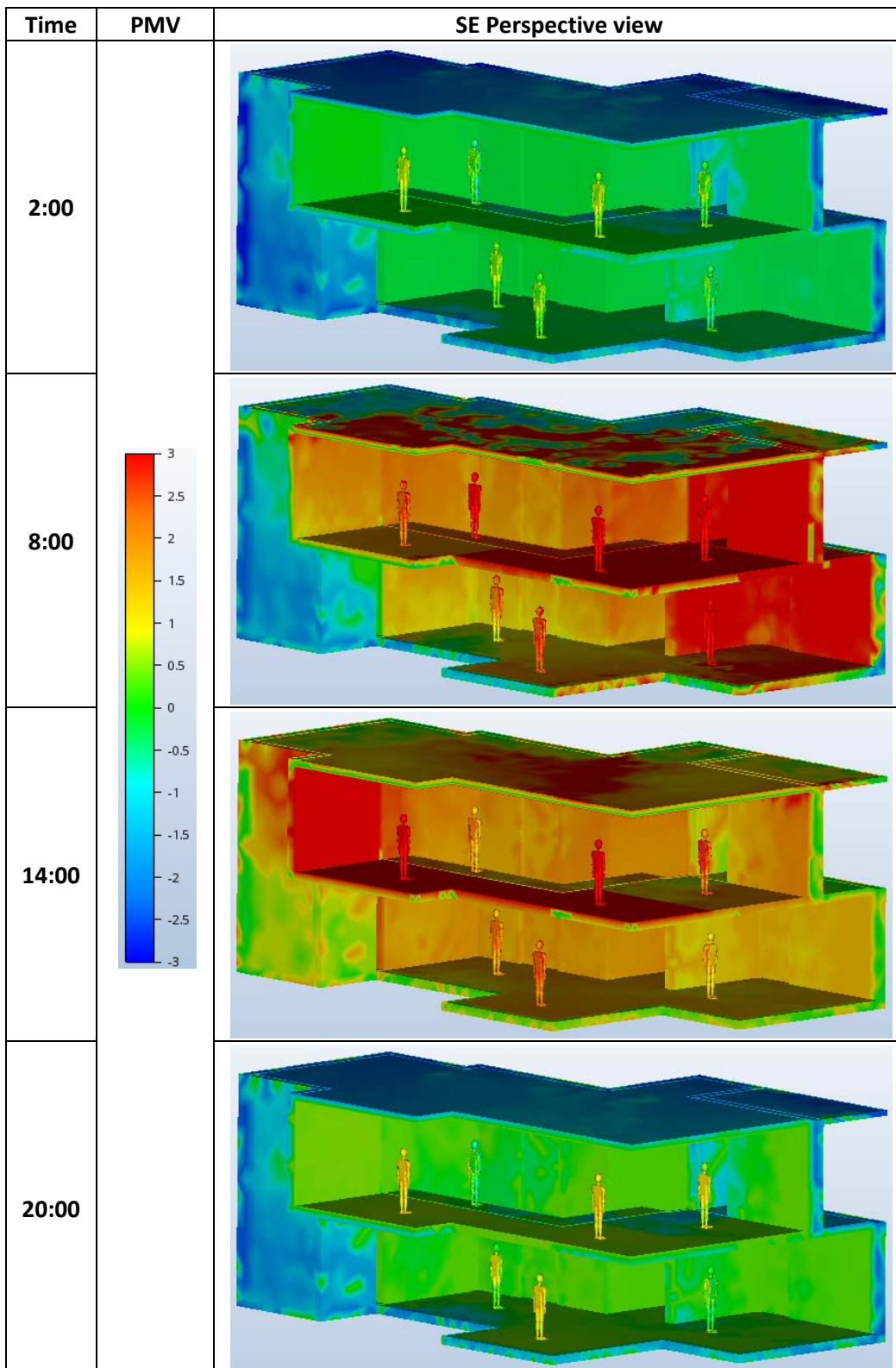


Figure 5.46 PMV results for the four examined hours of the day

From the above **Figure 5.46** we observe that the created airflow, from the selected openings, is not able to make the PMV values of Avatar F reach the comfort zone (except at 2:00 o'clock where the indoor conditions are comfortable from the base Scenario).

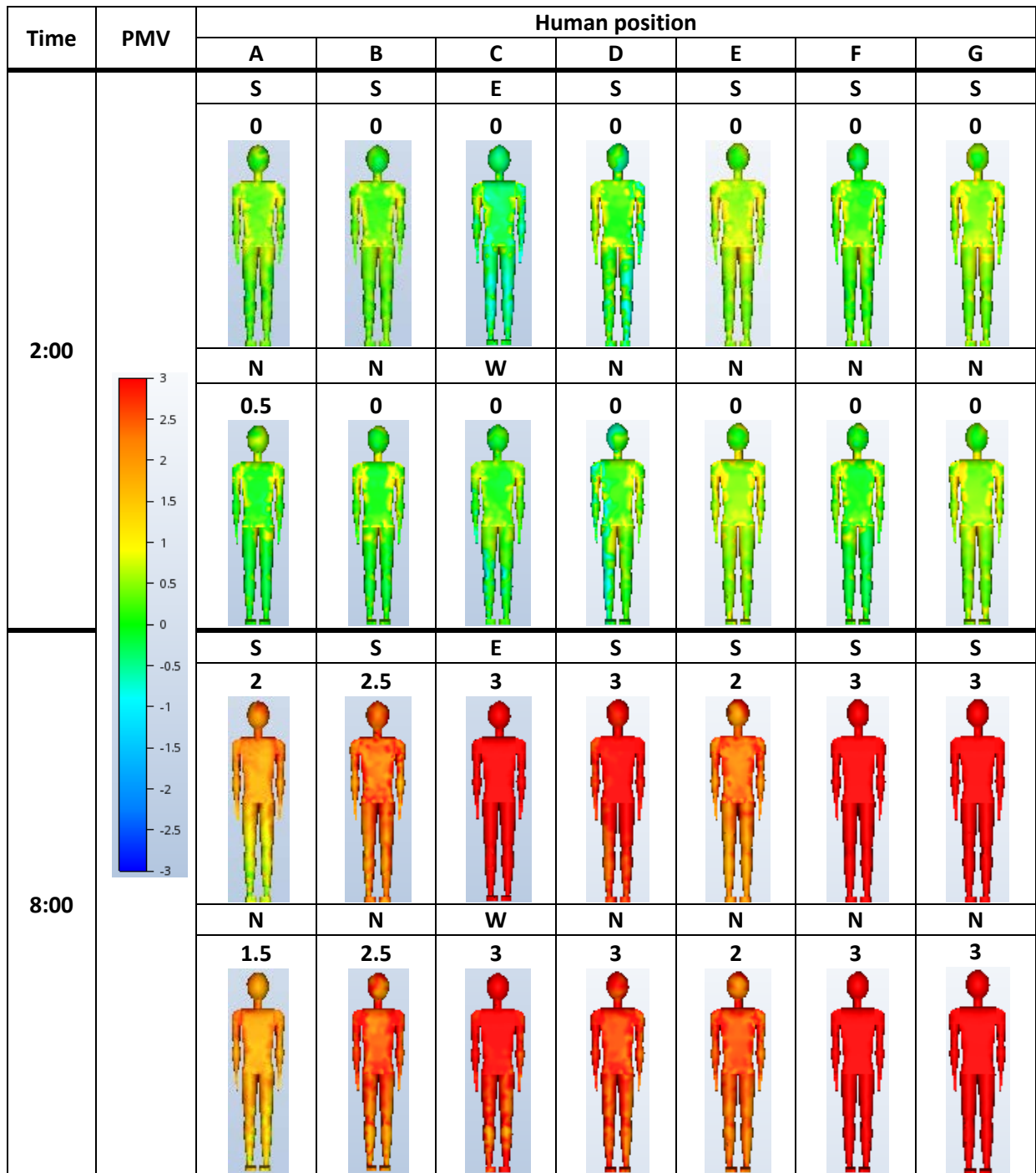


Figure 5.47 Detailed PMV results of the Avatars inside the building (A-G: position, S-E-N-W: orientation)

In the first case of 2:00 o'clock (**Figure 5.47**), the PMV of all the Avatars is recorded inside the comfort zone. From the created airflow some negative values appear on some parts of the body of Avatars C and D. At 8:00 o'clock (**Figure 5.47**), the PMV values are very high but values of thermal comfort appear on the legs of Avatar A. Even though some windows are open, the high values appear due to the heat transfer that occurs when the air is entering a very warm space of the building and moves to a cooler space.

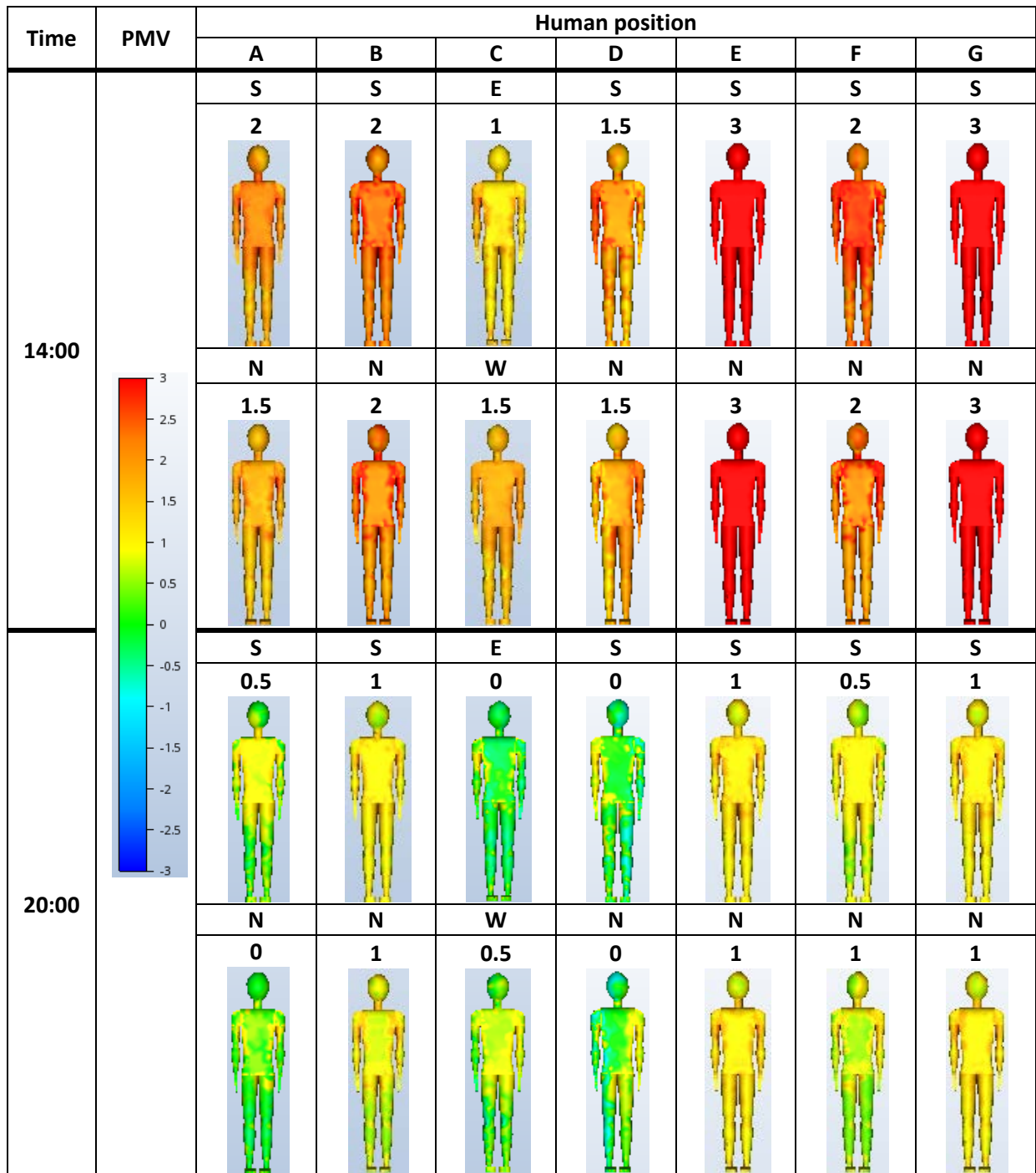


Figure 5.48 Detailed PMV results of the Avatars inside the building (A-G: position, S-E-N-W: orientation)

At 14:00 o'clock (Figure 5.48), high values, but generally lower than the 8:00 o'clock case, of PMV are recorded. In the last case (20:00 o'clock, Figure 5.48), the values are moving close to the comfort zone. On Avatar D we observe cooler values on the eastern side of the body, where the air is coming from, neutral in the middle and warmer on the western side.

Avatars E and G are in spaces that the air cannot reach, therefore they do not record any difference in the PMV values in any case of this Scenario.

5.11. Comparison between all Scenarios

From the results above, we observe in all the Scenarios air movement in the two-storey open space of the living room area and stairs. The air movement there appears in all the Scenarios regardless the windows/doors that are open and usually has low speed.

In the first 3 Scenarios we notice that the air is moving in the first storey level without any windows/doors open in that floor. This is probably caused by the geometry of the building and the stack effect, where the different pressures that exist that moment inside and around the building make the air move upwards and in other areas. Higher speed is recorded near the openings and on the direct path of the airflow from the inlet opening to the outlet opening. In Scenarios 2 and 3 the air is following the direct path through the kitchen and does not mix in that area. The same is happening in Scenario 1 in the dining area and there is not any air movement in the kitchen.

In the next 3 Scenarios the combination of open windows and doors between the bedroom 1 in the 1st floor and the ground floor is simulated. In Scenario 4 we observe low air movement in the kitchen and dining area. The position of the selected openings, the direct path of the airflow going in and out, does not allow a better movement in the two-storey open space and the air does not reach the roof. In Scenario 5, the air moves quickly from the kitchen and the bedroom but there is better movement in the living room and dining area than in the previous Scenario. Scenario 6 presents a combination of the results from the previous Scenarios. The air is moving in all the available areas of the residence but because of the selected openings (2 in the ground floor and 1 in the bedroom) the direct path that is created might cause uncomfortable conditions for the users.

In the last 3 Scenarios the combination of openings between the office in the 1st floor and the ground floor is simulated. The airflow pattern in Scenario 7 seems to cover all the available areas of the residence with small velocity, except the dining area where the movement is very low. In Scenario 8 the airflow does not cover the whole living room area because of the direct path that is created and restricts the air movement. The air goes through the office with higher velocity but a small circulation movement is created. Scenario 9 shows similar airflow pattern as Scenario 7 even though it has one more window open in the kitchen.

In some Scenarios we notice that air that is going fast through a space might not be able to decrease the PMV values inside the comfort zone. In these cases different PMV values on the Avatars' body are observed (i.e. Scenarios 6, 8). The values on the head could fall in the hot zone or comfort zone while there are negative values on their legs or some other part of the body, or values of the hot, comfort and cold zone can be recorded on different parts of the body. In these cases the indoor conditions cannot reach the comfort level and the fast movement of the air most possibly creates uncomfortable conditions.

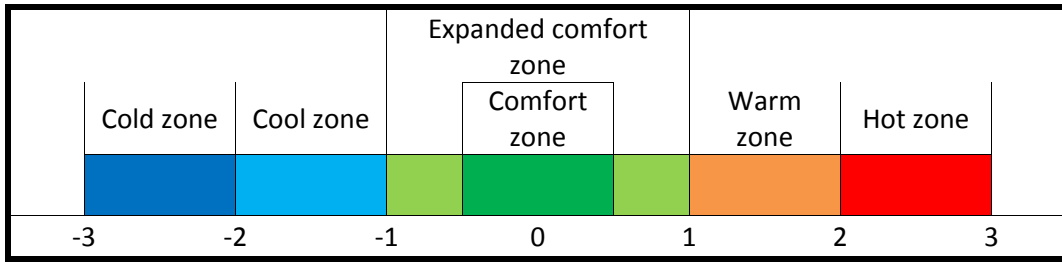


Table 6.1 Legend of the PMV range

2:00	Human position						
	A	B	C	D	E	F	G
Base	0	0	0	0.25	0	0	0
S1	-0.75	-1.25	0	0	0	0	0
S2	-0.75	0	-1	0	0	0	0
S3	-0.25	0.25	-0.75	0.5	0	0	0
S4	-0.5	0	0	-0.75	-0.5	0	0
S5	0	0	-0.25	-0.25	-0.25	0	0
S6	-2	0	-0.75	-0.5	-0.25	0	0
S7	0.25	0	0	0	0	0	0
S8	-0.5	0	0	0	0	-0.5	0
S9	0.25	0	0	0	0	0	0

Table 6.2 PMV results of the Avatars at 2:00 o'clock of all the Scenarios

8:00	Human position						
	A	B	C	D	E	F	G
Base	1.25	2	2.5	2.25	2	3	3
S1	0.25	0.25	1.5	1.25	2	3	3
S2	0.25	0.5	1	1.25	2	3	3
S3	0.5	0.5	0.5	1.25	2	3	3
S4	0	0.75	1.25	0.75	0.75	3	3
S5	0.5	0.5	1	0.75	0.75	3	3
S6	-0.5	0.75	1.75	0.75	0.75	3	3
S7	2	2.25	2.75	3	2	3	3
S8	0.25	0.75	1.75	1	1.5	3	3
S9	1.75	2.5	3	3	2	3	3

Table 6.3 PMV results of the Avatars at 8:00 o'clock of all the Scenarios

14:00	Human position						
	A	B	C	D	E	F	G
Base	2.5	2.5	2.25	3	3	3	3
S1	0.5	0.75	2	2.25	3	3	3
S2	0.75	1.5	0.75	2.25	3	3	3
S3	1.25	1.5	0.5	2.5	3	3	3
S4	0.75	1.75	1.75	1	1.25	3	3
S5	1.5	1.75	0.75	1	1.75	3	3
S6	0.25	1.75	0.75	1.25	1.75	3	3
S7	2	2.25	2	1.5	3	2	3
S8	0.75	1.5	1.75	1.75	3	1	3
S9	1.75	2	1.25	1.5	3	2	3

Table 6.4 PMV results of the Avatars at 14:00 o'clock of all the Scenarios

20:00	Human position						
	A	B	C	D	E	F	G
Base	1	1	0.75	1	1	1	1
S1	-1.25	-1	0.5	0.5	1	1	1
S2	-0.75	0.25	-0.75	0.25	1	1	1
S3	-0.5	0.5	-0.75	0.5	1	1	1
S4	-0.75	0.5	0.5	-1	-0.75	1	1
S5	0.25	0.5	-0.5	-0.5	-0.5	1	1
S6	-1.5	0.25	-0.75	-0.5	-0.5	1	1
S7	0.5	0.75	0.5	0	1	0.75	1
S8	-0.5	0.25	0.75	0.25	1	-0.75	1
S9	0.25	1	0.25	0	1	0.75	1

Table 6.5 PMV results of the Avatars at 20:00 o'clock of all the Scenarios

From the **Table 6.2** (2:00 o'clock) we observe that the PMV of all the Scenarios is inside the comfort or the expanded comfort zone except of the PMV of Avatars B in Scenario 1, which is in the cool zone and the PMV of Avatar A in the Scenario 6, which is in the cold zone. Generally all the Scenarios at 2:00 o'clock are able to keep the indoor conditions in a comfort level.

At 8:00 o'clock (**Table 6.3**), there is a decrease of the PMV values almost in all the Scenarios. Scenarios 7 and 9 present an increase of the values because the air is entering a very warm space of the building and is moving to cooler spaces, transferring in that way the heat and making the existent conditions hotter. This is also a result from a steady state situation where the simulation stops when the selected conditions met. A transient state, where the time is taken into account, would show how the natural ventilation affects the indoor conditions and the levels of comfort sensation regarding a period of time.

At 14:00 o'clock (**Table 6.4**), we observe a decrease of the PMV values of all the Avatars that are located in the available spaces (for the airflow movement) of each Scenario. The decrease can even reach the 2 points (inside the comfort or expanded comfort zone) but the PMV is moving mostly to the warm zone. In Scenario 1, 7 and 9 the decrease of the values is very small on a few Avatars and they are located in the warm and hot zone.

In **Table 6.5**, at 20:00 o'clock, the PMV values in all the Scenarios are moving in the comfort or expanded comfort zone, except for the Avatar A in Scenarios 1&6 that is located in the cool zone. The incoming air is causing a decrease in the values and in the most Scenarios the PMV of the Avatars in the available spaces is dropping in the comfort zone.

From the airflow analysis of the examined Scenarios we observe that the indoor airflow pattern is affected by:

- the geometry of the building,
- the position of the selected inlet openings in the geometry of the building, and
- the relative position and orientation of the outlet openings in respect to the inlet openings.

The impact of the incoming velocity between the selections of different position of the inlet openings can be observed from the Scenarios 7 and 8. In the first Scenario, the inlet opening is the northern glass door of the office, where that wall has a retreat on that side of the building and the volume of the stairwell is frontmost of the office. The air is entering the building with low velocity and is moving in all the available spaces. In the second Scenario, the inlet opening is the northern glass door of the living room, where the air is directly entering the building, without meeting any obstacle, with higher speed but the air does not move in all the available spaces.

It must be noticed that, even though the airflow pattern in a Scenario seems efficient, the velocity might not be enough in some areas for the indoor thermal conditions to reach a comfort level. The wind speed and other factors (such as temperature, humidity, etc) affect the sensation levels.

From the analysis of the thermal comfort results of the examined Scenarios and their conditions, we observe that:

- even at 14:00 o'clock, one of the hottest times of the day, the use of natural ventilation for cooling purposes can be effective.
- for night cooling, even a breeze (air with very low velocity) inside the building can make the comfort sensation of the humans move in the cold zone of comfort (Scenarios 1 and 6).
- the conditions of the space where the air is entering the building are important factors for the indoor conditions that will be created when the windows/doors will open.

6. Conclusions and Future work

6.1. Conclusions

In the presented study the impact of natural cross-ventilation of sustainable residential buildings on thermal comfort levels is evaluated. A residence with bioclimatic parameters is designed in Chania, Crete, and its energy consumption is assessed. Afterwards, the building is modelled for the study of the indoor airflow pattern created by natural wind-driven cross-ventilation from the different selection of the openings. Nine Scenarios of the previous study are chosen for the assessment of indoor thermal comfort. In all the simulations the building is isolated modelled.

A two storey open space between the floors seems to be significant for the air movement and cooling of all the possible areas of the building, even if there are no open windows on the upper floor. The impact of the floors' layout on the indoor airflow needs to be studied and taken into account from the early stages of the architectural design. The geometry of the building, as well as the position of the selected openings affect the conditions of the incoming air. The position and orientation of the outlet opening regarding the inlet opening must be cautiously selected so the architectural design and environmental conditions can be best exploited. The asymmetric position of the selected openings is suggested for a better movement of the air inside the building.

Naturally wind-driven ventilation appears to be an effective way of cooling the building in many cases during the day. In the majority of the cases the thermal comfort levels drop 1 thermal zone and in many cases two thermal zones. Night ventilation is able to provide comfortable indoor conditions, but in a few cases it can drop the thermal comfort levels in the cool zone of comfort and thus creating uncomfortable conditions. The selected openings must be chosen regarding the environmental conditions, indoor conditions and the spaces that need cooling.

From this research it is also concluded that for the study of natural indoor ventilation and thermal comfort levels on a complex building geometry the followed methodology can be applied. Natural ventilation has a significant impact on the quality of living standards and energy consumption and needs to be acknowledged both from the architects and the occupants. CFD simulations can be effectively used for the study of natural ventilation and the provided information can be used in the early stage of architectural design. Software packages prove to be a useful tool for the architects and other professionals and are frequently used for similar studies for the purpose of understanding and designing of appropriate actions.

6.2. Future work

A further assessment of the PMV results can be made regarding the newly formed indoor air temperature from the natural ventilation.

Further research can be made in a transient state where the impact of natural ventilation on thermal comfort levels will be assessed regarding the time factor.

In this work the PMV index is used for the evaluation of thermal comfort levels. This index is the most common method and the selected program is using it for the thermal comfort evaluation. Some studies have reported that it might not be appropriate for thermal comfort assessment in naturally ventilated buildings. Another method or program could be used for the study of thermal comfort levels from natural ventilation in the designed building and a comparison of the results can be made.

During the process of architectural designing, the need for shading systems was perceived. A further study for their implementation and impact assessment on indoor airflow and thermal comfort levels can be made.

The described building is used for the development of a control system for the openings of the Scenarios that were tested. The maquette of the building was built and the system was implemented and tested on the openings (**Figure 6.1**). Further work is needed for the improvement of the model and the conduction of the experimental measurements.



Figure 6.1 The physical model of the residence with the implementation of the control system

7. References

- [1] T. Ayata and O. Yildiz, "Investigating the potential use of natural ventilation in new building designs in Turkey," vol. 38, pp. 959–963, 2006.
- [2] T. Schulze and U. Eicker, "Controlled natural ventilation for energy efficient buildings," *Energy Build.*, vol. 56, pp. 221–232, 2013.
- [3] M. Santamouris and D. Kolokotsa, "Passive cooling dissipation techniques for buildings and other structures : The state of the art," *Energy Build.*, vol. 57, pp. 74–94, 2013.
- [4] G. M. Stavrakakis, M. K. Koukou, M. G. Vrachopoulos, and N. C. Markatos, "Natural cross-ventilation in buildings : Building-scale experiments , numerical simulation and thermal comfort evaluation," vol. 40, pp. 1666–1681, 2008.
- [5] G. Evola and V. Popov, "Computational analysis of wind driven natural ventilation in buildings," vol. 38, pp. 491–501, 2006.
- [6] X. Su, X. Zhang, and J. Gao, "Evaluation method of natural ventilation system based on thermal comfort in China," vol. 41, pp. 67–70, 2009.
- [7] N. H. Wong, H. Feriadi, P. Y. Lim, K. W. Tham, C. Sekhar, and K. W. Cheong, "Thermal comfort evaluation of naturally ventilated public housing in Singapore," vol. 37, pp. 1267–1277, 2002.
- [8] S. Cui, P. Stabat, and D. Marchio, "Numerical simulation of wind-driven natural ventilation : Effects of loggia and facade porosity on air change rate," *Build. Environ.*, vol. 106, pp. 131–142, 2016.
- [9] C. Chu, Y. Chiu, Y. Tsai, and S. Wu, "Wind-driven natural ventilation for buildings with two openings on the same external wall," *Energy Build.*, vol. 108, pp. 365–372, 2015.
- [10] P. Karava, T. Stathopoulos, and A. K. Athienitis, "Airflow assessment in cross-ventilated buildings with operable façade elements," vol. 46, pp. 266–279, 2011.
- [11] K. Nikas, N. Nikolopoulos, and A. Nikolopoulos, "Numerical study of a naturally cross-ventilated building," *Energy Build.*, vol. 42, no. 4, pp. 422–434, 2010.
- [12] D. Kolokotsa, G. Saridakis, A. Pouliezios, and G. S. Stavrakakis, "Design and installation of an advanced EIB (TM) fuzzy indoor comfort controller using Matlab (TM)," no. October 2015, 2006.
- [13] A. L. Pisello, V. L. Castaldo, J. E. Taylor, and F. Cotana, "The impact of natural ventilation on building energy requirement at inter-building scale," *Energy Build.*, vol. 127, pp. 870–883, 2016.
- [14] J. Good, A. Frisque, and D. Phillips, "The role of wind in natural ventilation simulations using airflow network models," 2008.
- [15] O. Kinnane, D. Sinnott, and W. J. N. Turner, "Evaluation of passive ventilation provision in domestic housing retrofit," *Build. Environ.*, vol. 106, pp. 205–218, 2016.
- [16] J. A. Castillo and G. Huelsz, "A methodology to evaluate the indoor natural ventilation in hot climates: Heat Balance Index," *Build. Environ.*, vol. 114, pp. 366–373, 2016.

- [17] M. A. Menchaca-Brandan, F. A. Dominguez Espinosa, and L. R. Glicksman, "The influence of radiation heat transfer on the prediction of air flows in rooms under natural ventilation," *Energy Build.*, vol. 138, pp. 530–538, 2017.
- [18] A. Bastide, P. Lauret, and H. Boyer, "Building energy efficiency and thermal comfort in tropical climates Presentation of a numerical approach for predicting the percentage of well-ventilated living spaces in buildings using natural ventilation," vol. 38, pp. 1093–1103, 2006.
- [19] E. Prianto and P. Depecker, "Characteristic of airflow as the effect of balcony , opening design and internal division on indoor velocity A case study of traditional dwelling in urban living quarter in tropical humid region," vol. 34, pp. 401–409, 2002.
- [20] W. Liping and W. N. Hien, "The impacts of ventilation strategies and facade on indoor thermal environment for naturally ventilated residential buildings in Singapore," vol. 42, pp. 4006–4015, 2007.
- [21] O. A. R. Mohamad Mohd Faizal, Hagishima Aya, Tanimoto Jun, Ikegaya Naoki, "Wind-induced natural ventilation in typical single storey terraced houses in Malaysia," pp. 587–593, 2013.
- [22] S. Gilani, H. Montazeri, and B. Blocken, "CFD simulation of stratified indoor environment in displacement ventilation : Validation and sensitivity analysis," *Build. Environ.*, vol. 95, pp. 299–313, 2016.
- [23] T. Van Hooff, B. C. C. Leite, and B. Blocken, "CFD analysis of cross-ventilation of a generic isolated building with asymmetric opening positions : Impact of roof angle and opening location," vol. 85, 2015.
- [24] A. Baghaei Daemei, A. Khalatbari Limaki, and H. Safari, "Opening Performance Simulation in Natural Ventilation using Design Builder (Case Study: A Residential Home in Rasht)," vol. 100, pp. 412–422, 2016.
- [25] T. Van Hooff, B. C. C. Leite, and B. Blocken, "CFD simulation of wind-driven upward cross ventilation and its enhancement in long buildings : Impact of single-span versus double-span leeward sawtooth roof and opening ratio," vol. 96, pp. 142–156, 2016.
- [26] T. Van Hooff, B. Blocken, and Y. Tominaga, "On the accuracy of CFD simulations of cross-ventilation flows for a generic isolated building: Comparison of RANS , LES and experiments," *Build. Environ.*, vol. 114, pp. 148–165, 2017.
- [27] S. Hawendi and S. Gao, "Impact of an external boundary wall on indoor flow field and natural cross-ventilation in an isolated family house using numerical simulations," *J. Build. Eng.*, vol. 10, no. December 2016, pp. 109–123, 2017.
- [28] P. O. Fanger, *Thermal Analysis and Applications in Environmental Engineering*. New York: McGraw-Hill, 1970.
- [29] B. W. Olesen and K. C. Parsons, "Introduction to thermal comfort standards and to the proposed new version of EN ISO 7730," vol. 34, 2002.
- [30] R. De Dear, G. Brager, and D. Cooper, "Developing an Adaptive Model of Thermal Comfort and Preference," no. March, 1997.

- [31] R. J. De Dear and G. S. Brager, "Thermal comfort in naturally ventilated buildings : revisions to ASHRAE Standard 55," vol. 34, pp. 549–561, 2002.
- [32] P. Fanger, "Assessment of man's thermal comfort practice," pp. 313–324, 1973.
- [33] A. Pitts, J. Saleh, and S. Sharples, "Paper No : 591 Building Transition Spaces , Comfort and Energy Use," no. October, 2008.
- [34] Z. Luo, J. Zhao, J. Gao, and L. He, "Estimating natural-ventilation potential considering both thermal comfort and IAQ issues," vol. 42, pp. 2289–2298, 2007.
- [35] S. J. Emmerich, B. Polidoro, and J. W. Axley, "Impact of adaptive thermal comfort on climatic suitability of natural ventilation in office buildings," *Energy Build.*, vol. 43, no. 9, pp. 2101–2107, 2011.
- [36] N. Papamanolis, "Natural ventilation as a design factor in buildings in Greece," *Archit. Sci. Rev.*, vol. 43, no. 4, pp. 175–182, 2000.
- [37] C. Karkanias, S. N. Boemi, A. M. Papadopoulos, T. D. Tsoutsos, and A. Karagiannidis, "Energy efficiency in the Hellenic building sector: An assessment of the restrictions and perspectives of the market," *Energy Policy*, vol. 38, no. 6, pp. 2776–2784, 2010.
- [38] E. Andreadaki (2006), *Βιοκλιματικός Σχεδιασμός-Περιβάλλον και Βιωσιμότητα [Bioclimatic Design-Environment and Sustainability]*. University Studio Press, 2006.
- [39] "Google Maps." [Online]. Available: <https://www.google.gr/maps>. [Accessed: 27-Apr-2017].
- [40] "Τεχνική Οδηγία Τεχνικού Επιμελητηρίου Ελλάδας 20701_2 1η έκδοση [Technical Guidelines of Technical Chamber of Greece 20701_2 1st edition]," 2010.
- [41] T. C. C. 156 "Ventilation for Buildings", "Indoor environmental input parameters for design and assessment of energy performance of buildings addressing indoor air quality, thermal environment, lighting and acoustics," no. August. 2007.
- [42] "Τεχνική Οδηγία Τεχνικού Επιμελητηρίου Ελλάδας 20701_1 3η έκδοση [Technical Guidelines of Technical Chamber of Greece 20701_1 3rd edition]," vol. 2014, 2014.
- [43] "Πιστοποιητικά Ενεργειακής Απόδοσης Κτιρίων: Στατιστική Ανάλυση για το έτος 2015 [Building Energy Efficiency Certification Statistical: Analysis for year 2015]." pp. 1–18, 2016.
- [44] "Γεωγραφία (Ε Δημοτικού): Ηλεκτρονικό Βιβλίο [Geography ebook]." [Online]. Available: <http://ebooks.edu.gr/modules/ebook/show.php/DSDIM-E100/692/4594,20786/>. [Accessed: 09-May-2017].
- [45] E. A. Mccullough and D. Ph, "A Comprehensive Data Base for Estimating Clothing Insulation," vol. 2888, no. 2888, pp. 29–47.
- [46] F. Haghighat, "Thermal Comfort in Housing and Thermal Environments," vol. I.
- [47] "Autodesk Knowledge Network." [Online]. Available: <https://knowledge.autodesk.com/>. [Accessed: 28-Apr-2017].

